Impact of Increased Allowable Truck Loads on Pavement Life

June 2024

BEB11

Task 6 Deliverable
Draft Final Report

Prepared for:
Florida Department of Transportation

Prepared by:
Zafrul H. Khan, Ph.D.
zkhan@ara.com

Hyung S. Lee, Ph.D., P.E.
hslee@ara.com

Ahmad Alhasan, Ph.D.
aalhasan@ara.com

Hadi Nabizadeh, Ph.D., P.E.

Applied Research Associates Inc. (ARA Inc.)

DISCLAIMER

The opinions, findings, and conclusions expressed in this publication are those of the authors and not necessarily those of the Florida Department of Transportation.

TECHNICAL REPORT DOCUMENTATION PAGE

1. Report No.	2. Government Accession No.	3. Recipient's Catalog No.
4. Title and Subtitle Impact of Increased Allowable Truck Loads on Pavement Life		**5. Report Date** June 2024
		6. Performing Organization Code
7. Author(s) Zafrul H. Khan, Ph.D., Hyung S. Lee, Ph.D., P.E., Ahmad Alhasan, Ph.D., Hadi Nabizadeh, Ph.D., P.E.		**8. Performing Organization Report No.**
9. Performing Organization Name and Address Applied Research Associates Inc. (ARA Inc.) 100 Trade Center Dr., Suite# 200, Champaign, IL 61820		**10. Work Unit No. (TRAIS)**
		11. Contract or Grant No. BEB11
12. Sponsoring Agency Name and Address Florida Department of Transportation 605 Suwannee Street, MS 30 Tallahassee, FL 32399		**13. Type of Report and Period Covered**
		14. Sponsoring Agency Code
15. Supplementary Notes 		

16. Abstract

Current truck size and weight standards are a blend of federal and state regulations. Typically, state highway agencies limit the movement of superheavy loads and overweight vehicles because they can cause excessive damage to the pavement. Weigh-in-motion data from different sites across Florida were analyzed to study the trends of overweight vehicles. Based on the analysis, it is recommended that the Florida Department of Transportation consider updating the equivalent axle load factor values used for the design of non-limited highway pavements. Furthermore, the report also outlines the necessary steps to assess the impact of superheavy load (SHL) movement on pavement life without any iterative approach.

17. Key Word Weigh-in-motion, EALF, Thickness, Legal weight truck, Overweight truck		18. Distribution Statement No restrictions.	
19. Security Classif. (of this report) Unclassified	**20. Security Classif. (of this page)** Unclassified	**21. No. of Pages** 128	**22. Price** N/A

Form DOT F 1700.7 (8-72) Reproduction of completed page authorized

EXECUTIVE SUMMARY

Current truck size and weight standards are a blend of federal and state regulations and laws. According to Section 127 of Title 23, United States Code (USC), the maximum axle(s) weight limitations for vehicles operating on Interstate highways are 20,000 pounds on a single axle, 34,000 pounds on a tandem axle, or the maximum allowed by the Federal Bridge Formula (FBF). Section 127 also states that the gross vehicle weight (GVW) may not exceed 80,000 pounds, except for those vehicles and loads that cannot be easily dismantled or divided, and therefore, they require specific permits in accordance with applicable state laws. Congress enacted the FBF in 1975 to limit the weight-to-length ratio of a vehicle crossing highway bridges. This is accomplished either by spreading weight over additional axles or by increasing the distance between axles. State highway agencies (SHAs), including FDOT, authorize a single trip permit for the operation of a vehicle or combination of vehicles with GVW exceeding a specified load limit (e.g., 350,000 pounds). Such heavy vehicles, referred to as super-heavy load (SHL) or overweight (OW) vehicles, require extensive damage analysis and load-carrying capacity investigation.

The movement of OW vehicles with increased axle and tire loads imposes premature damages on highway pavements that may lead to a faster deterioration of the highway system. As such, in order for SHAs to effectively manage their pavement system and consider alternative rehabilitation or design strategies with respect to OW vehicle movement, the impact of such vehicles on pavement and the extent of pavement damage must be assessed. Evaluating and quantifying pavement damage due to the movement of the OW vehicles requires consideration of several factors that are specific to each move. For example, GVW, axle and tire loads and configurations, properties of existing pavement layers, pavement condition at the time of the move, traveling speed, and pavement temperature (for asphalt surfaces) are some of the critical factors for the analysis of damage caused by OW vehicles.

In this report, Weigh-in-motion (WIM) data from different regions across Florida were analyzed to study the trends in the movement of the OW vehicles. The analyzed data were categorized into four groups based on the functional class of pavement where the WIM stations are situated: limited rural, limited urban, non-limited rural, and non-limited urban. In addition, this study also evaluated the pavement design approach adopted by FDOT and compared it with the design based on the WIM data. A sensitivity analysis was conducted to measure the impact of OW vehicles on the design thickness of the surface course. Based on the analysis, it is recommended that FDOT consider updating the equivalent axle load factor (EALF) values used for the design of non-limited pavements. Furthermore, the report also outlines the necessary steps to assess the impact of SHL movement on pavement life.

Table of Contents

LIST OF FIGURES

LIST OF TABLES

1   INTRODUCTION

With the substantial growth of freight transportation, the need for the movement of large non-divisible shipments that exceed the legal gross vehicle weight (GVW) as well as axle and tire weight limits on the nation's highways have increased significantly. As such, requests for special overweight (OW) with GWV greater than 80,000 pounds and oversize (OS) vehicles permits have risen from 20% to 50% across the nation during the past two decades (CPCS et al., 2016). According to the Freight Facts and Figures data published by the Federal Highway Administration (FHWA), the total permits issued from 2006 to 2018 in the U.S. have increased by 30%. A previous study showed that since 2016, the average daily OW/OS permits issued by the Florida Department of Transportation (FDOT) exceed 400 while 45% of these permits were issued for OW operation. It is anticipated that the number of issued permits will reach more than 450 per day in 2025 (Ali et al., 2020).

The impact of OW vehicles on pavement and associated damage have been studied for a long time in many research studies. Evaluating and quantifying pavement damage due to the movement of OW vehicles require the consideration of several factors that are specific to each move. GVW, axle and tire loads and configurations, properties of existing pavement layers, pavement condition at the time of the move, traveling speed, and pavement temperature (for asphalt surfaces) are critical factors for the damage analysis of OW vehicles. Empirical, mechanistic-empirical (ME), or finite element (FE) methodologies along with the load equivalency concept have been used in previous studies to evaluate pavement damage from increased axle and vehicle loads.

Moving an OS/OW vehicle is complicated due to the combination of infrastructure constraints, regulatory restrictions, permitting processes, and timelines. OS/OW carriers must traverse constrained routes, which include bridges or roads with limited weight capacities, bridge and tunnel clearances, overhead wires, turning radii, and pavement dimensions. OS/OW carriers also face a long list of policy regulations and operational restrictions. In addition, the operation of OW vehicles, with their increased axle and tire loads, can cause premature damage to highway pavements. This can lead to fast deterioration of the highway pavement system. State highway agencies (SHAs) must assess the impact of OW vehicles on pavements and determine the extent of damages. This is essential for effective management of the pavement system and for the development of appropriate design and timely rehabilitation strategies to avoid costly reconstruction. Therefore, the primary objectives of this research study were:

1. Quantify the effect of increased truck loads on pavement service life.
2. Define corridors that are most likely to be impacted by future increased truck loads.
3. Strategies to account for increases in axle and vehicle loads in the pavement design process.
4. Provide guidance on pavement structural evaluation methodologies needed to assess the impact of single trip oversized loads.

To achieve these objectives, the Florida Department of Transportation (FDOT) had searched and provided the research team with several sources of data, including those from the weigh-in-motion (WIM) stations and the FDOT's OS/OW Permit Application System (PAS).

This report documents the research team's effort performed to achieve these objectives.

2   LITERATURE REVIEW

At present, truck size and weight standards are a blend of Federal and State regulations and laws. Section 127 of Title 23 of the United States Code (23 USC 127) establishes weight limitations for vehicles operating on the Interstate System. The maximum axle(s) weight is 20,000 pounds on a single axle; 34,000 pounds on a tandem axle; or the maximum allowed by the Federal Bridge Formula (FBF). Section 127 states that the gross vehicle weight (GVW) may not exceed 80,000 pounds, except for those vehicles and loads which cannot be easily dismantled or divided, and therefore they require specific permits in accordance with applicable State laws (FHWA, 2021).

Non-divisible load is defined as any load or vehicle exceeding applicable length or weight limits which, if separated into smaller loads or vehicles, would:

- Compromise the intended use of the vehicle, i.e., make it unable to perform the function for which it was intended (see Figure 2-1);
- Destroy the value of the load or vehicle, i.e., make it unusable for its intended purpose; or
- Require more than 8 work hours to dismantle using appropriate equipment. The applicant for a non-divisible load permit has the burden of proof as to the number of workhours required to dismantle the load.

Divisible loads (see Figure 2-2) are the vast majority of loads on the nation's highways. Designated divisible load permits may be issued by the State based upon historic State "grandfather" rights or Congressional authorization for a State-specific commodity or route movement at greater size or weight (FHWA, 2021).

Figure 2-1. Illustration of nondivisible load (Big Truck Guide, 2016).

Figure 2-2: Illustration of divisible load (Big Truck Guide, 2016)

Congress enacted the FBF in 1975 to limit the weight-to-length ratio of a vehicle crossing highway bridges. This is accomplished either by spreading weight over additional axles or by increasing the distance between axles. Compliance with FBF weight limits is determined using the following formula in Eq. (1):

$$W = 500 \left[\frac{LN}{N-1} + 12N + 36 \right] \tag{1}$$

where:

        W = overall gross weight on any group of two or more consecutive axles to the nearest 500 pounds
        L = distance in feet between the outer axles of any group of two or more consecutive axles
        N = the number of axles in the group under consideration

On non-interstate highways, states allow more weight limits than the limit specified by the FBF (FHWA, 2019). As shown in Figure 2-3, 100,001 to 110,000 pounds is the most common legal or allowable weight for five-axle semi-trailers. As shown in Figure 2-4, the most common allowable weight limit on a single and tandem axle ranges from 20,001 to 25,000 pounds and 45,001 to 50,000 pounds, respectively (Dunning et al., 2016).

A recently conducted review of current OW/OS vehicle permitting practices in the US reported that agencies have adopted different permit fee structures. While some agencies use a GVW and an axle weight-distance permit scheme, some others collect flat fees for single-trip permits. The single-trip permit fee ranged anywhere from 25 to 550 dollars, regardless of associated pavement damage or any traveled distance indicators (Papagiannakis, 2015). Table 2-1 summarizes the different OW vehicle permit fee structures for different state highway agencies in the US.

State highway agencies (SHAs), including FDOT, authorize a single trip permit for the operation of a vehicle or combination of vehicles with GVW exceeding a specified load limit (e.g., 199,000 pounds in Florida). Such heavy vehicles which are referred to as Superheavy Load (SHL) or Overload vehicles require extensive damage analysis as well as load-carrying capacity investigation. Based on a recent NCHRP study, as many as 14 SHAs received more than 1,000 SHL movement requests per year, while two counted more than 100,000 requests (Papagiannakis, 2015).
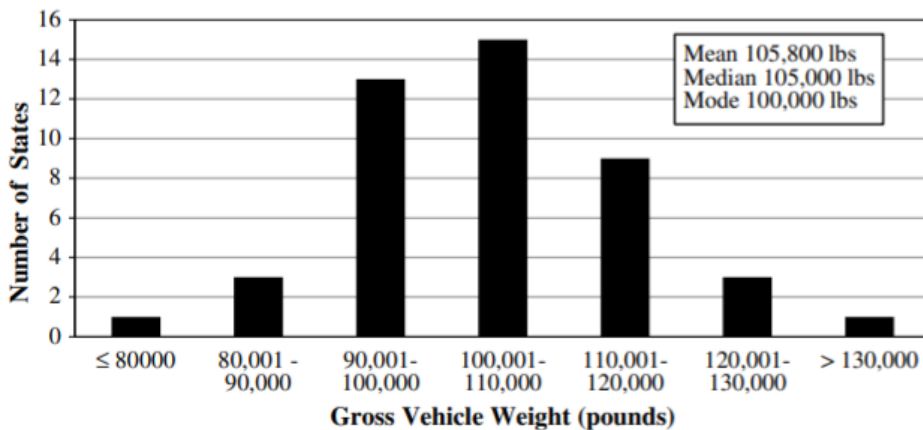
Figure 2-3. Allowable weight limits for five-axle semi-trailers (Dunning et al., 2016).
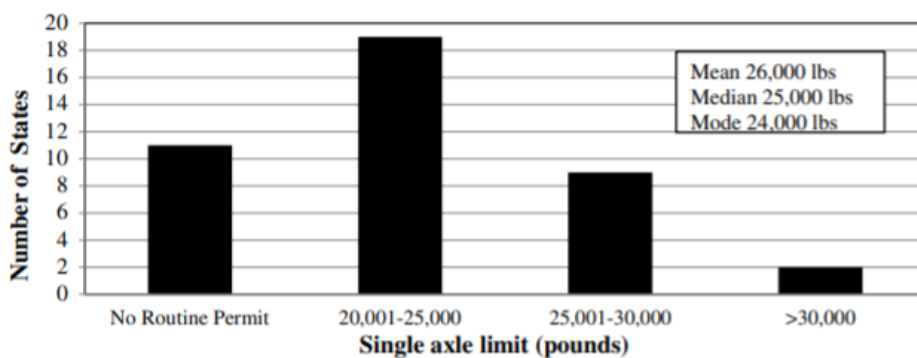
(a) Single Axle
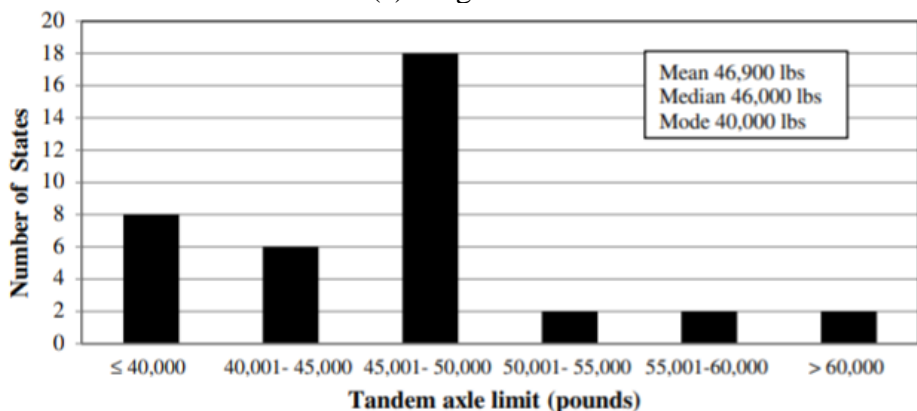
(b) Tandem Axle

Figure 2-4: Allowable weight limits on (Dunning et al., 2016)

Table 2-1: Summary of permit fee structures in the United States

Permit Structure Type	US States	Permit Fees Examples
Case by Case	Alabama, Nebraska, Iowa, Rhode Island, Michigan	At least $20
Weight Only	Colorado, North Carolina, South Carolina, Georgia, Kentucky, Delaware, Maryland, New Jersey, Massachusetts, Vermont, Maine	$10 per OW axle, $3 per 1,000 pound after 132,000 pound GVW
Weight – Distance	Washington, Oregon, Utah, New Mexico, Montana, Wyoming, North Dakota, South Dakota, Minnesota, Oklahoma, Missouri, Illinois, Louisiana, Mississippi, Tennessee, Indiana, Ohio, West Virginia, Virginia, Florida	$0.006 mile per ton $0.20 mile per ton $70 plus $3.5 per 5,000 pound per 25 mile $0.05 per mile per 1,000 pound $135 plus $0.04 per ton per mile after 120,000 pound GVW
Distance only	Arizona, Arkansas	$12 per trip < 50 miles < $48 per trip
Fixed Fee	Nevada, Idaho, Alaska, New Hampshire, Kansas	$25, $71, $20, $50
Damage Related	California, Kansas	Carrier pays damage fees
Other	Texas, New York	Fee per number of counties traversed

2.1 FDOT OW/OS Permitting Process

The laws governing truck size and weight in the State of Florida can be found in Florida Statutes §316-500 through §316-565 (Florida Statutes, 2020). The legal load limits enforced by Florida Statute 316.535 are similar to the Federal regulations. The GVW in regular operations (operating without a special permit) is governed by the FBF on interstate highways. However, several provisions allow trucks to exceed some elements of Federal limits on non-interstate highways which include: (1) up to 40,000 pounds on a tandem axle and (2) a 10 percent weight allowance for axle weight limits.

The FDOT Permit Office oversees OW/OS Permit issuance on all State-maintained highways and roadways. This includes permitting for commercial, public, and private motorists operating on the state system. The Permit Application System (PAS) can be used to self-issue trip permits for loads up to 16 feet wide, 18 feet high, 150 long, and 200,000 pounds (140,000 pounds for self-propelled equipment). This means that no interaction with the Permit Office is required. The type of permits available are:

- Blanket Permit – Allows unlimited trips on designated roads/highways and is not assigned to a specific vehicle. Blanket permits are valid for twelve months from the start date.
- Route Specific Blanket Permit – Reserved for loads that exceed the size or weight criteria for a regular blanket permit. This permit allows for unlimited trips on a specific route for a specific vehicle configuration. Additional permit restrictions such as law enforcement escorts may be required. Route-specific blanket permits are valid for 3 months.
- Trip Permit – Allows a single trip on a single route. A single trip is from a single point to a destination without any deliveries/pick up between the two points. Trip permits are valid for ten days from the start date.

- Vehicle Specific Blanket Permit – Same as a blanket permit except it is assigned to a specific vehicle. Vehicle-specific blanket permits are valid for twelve months from the start date.

According to Chapter 14-26: Safety Regulations and Permit Fees for Overweight and Overdimensional Vehicles regulated by the Florida Department of State, FDOT is responsible to evaluate the load-carrying capacity of the route (pavement, bridges, and other facilities). In addition, specific consideration is given to the moves when any axle exceeds 30,000 pounds, or when the GVW is 300,000 pounds or more. In such cases, a detailed description of vehicle configuration (e.g., longitudinal and transverse spacings, axle weights and dimensions, etc.) must be submitted by the hauler so that the department can conduct a comprehensive structural evaluation. The permit scheduling fee for operating overdimensional and overweight trucks in the State of Florida are represented in Table 2-2 and Table 2-3, respectively.

Table 2-2: Schedule of fees for overdimensional permits in the State of Florida

VEHICLE DESCRIPTION	TRIP PERMIT 10 Days	MULTI-TRIP PERMITS 12 Months	ROUTE SPECIFIC MULTI-TRIP PERMIT 3 Months
(a) Straight trucks and semi-truck-tractor-trailer.			
Up to 12 feet wide, or up to 13 feet 6 inches high or up to 85 feet long.	$5.00	$20.00	$5.00
Up to 14 feet wide or up to 14 feet 6 inches high or up to 95 feet long.	$15.00	$150.00	$38.00
Up to 14 feet wide or up to 18 feet high or up to 120 feet long.	$25.00	$250.00	$63.00
Over 14 feet wide or over 18 feet high or over 120 feet long.	$25.00	NOT ISSUED	$125.00
(b) Overlength semi-trailers of legal width, height, and weight, which exceed 53 feet In Length up to 57 feet 6 inches in length or overlength semi-trailer with kingpin setting greater than 41 feet.	$10.00	$30.00	NOT ISSUED
(c) Truck crane or earth handling equipment moving under own power, up to 12 feet wide or 14 feet 6 inches high.	$15.00	$150.00	$38.00
*(d) Trailers or equipment towed with ball or pintle.			
*Up to 10 feet wide or up to 13 feet 6 inches high or up to 80 feet long.	$5.00	$20.00	$5.00
*Up to 12 feet wide or up to 13 feet 6 inches high or up to 105 feet long.	$5.00	$330.00	$83.00
*Up to 14 feet wide or up to 14 feet 6 inches high or up to 105 feet long.	$15.00	$500.00	$125.00
Over 14 feet wide or over 14 feet 6 inches high or over 105 feet long.	$25.00	NOT ISSUED	$250.00
*Dimensions greater than 12 feet wide or 13 feet 6 inches high or 85 feet long will have an additonal dimension fee with a combined fee of not to exceed $500.00. NOTE: All permitted dimensions (length, height, width) must be within limits shown for permit fee.			

Table 2-3: Schedule of fees for overweight permits in the State of Florida

VEHICLE DESCRIPTION	TRIP PERMIT 10 Days	MULTI-TRIP PERMITS 12 Months	ROUTE SPECIFIC MULTI-TRIP PERMITS 3 months
*(a) Up to 95,000 pounds.	$0.27 Per Mile	**$240.00	$60.00
*(b) Up to 112,000 pounds.	$0.32 Per Mile	**$280.00	$70.00
*(c) Up to 122,000 pounds.	$0.36 Per Mile	**$310.00	$78.00
*(d) Up to 132,000 pounds.	$0.38 Per Mile	**$330.00	$83.00
*(e) Up to 142,000 pounds.	$0.42 Per Mile	**$360.00	$90.00
*(f) Up to 152,000 pounds.	$0.45 Per Mile	**$380.00	$95.00
*(g) Up to 162,000 pounds.	$0.47 Per Mile	**$400.00	$100.00
(h) Up to 199,000 pounds.	$0.003 Per 1,000 Pounds Per Mile	$500.00	$125.00
(i) Over 199,000 pounds.	$0.003 Per 1,000 Pounds Per Mile	NOT ISSUED	$250.00
(j) Containerized Cargo Unit.	$0.27 Per Mile	$500.00	$125.00
(k) Overall Wheel Base (Inner Bridge/External Bridge).	$10.00	$35.00	NOT ISSUED
(l) Implements of husbandry, farm equipment, agricultural trailers/products and forestry equipment (Local Moves Only).	$5.00	$17.00	NOT ISSUED
(3) SPECIAL PERMIT FEES			
Transmission Fee	$5.00	NOT APPLICABLE	NOT APPLICABLE
*Dimensions greater than 12 feet wide or 13 feet 6 inches high or 85 feet long will have an additional dimension fee with a combined fee of not to exceed $500.00. NOTE: For weights over 80,000 pounds [paragraphs (2)(a) through (h), above], add an administrative cost of $3.33 for issuance of permit, which does not include the costs charged by wire services for their services. Permit fees shall be based on 25 mile increments rounded up to the nearest dollar. Example: A 112,000 pound load traveling 67.5 miles would cost (75 miles X $0.32) plus $3.33 = $27.33 rounded up to $28.00 in addition to the $5.00 transmission fee when applicable.			

2.2   Assessment of Pavement Damage from OW Vehicles

The movement of OW vehicles with increased axle and tire loads imposes premature damage to highway pavements that leads to a fast deterioration of the highway system. As such, in order for SHAs to effectively manage their pavement system and consider alternative rehabilitation or design strategies with respect to OW vehicle movement, the impact of such vehicles on pavement and the extent of damage must be assessed. Evaluating and quantifying pavement damage due to the movement of OW vehicles requires consideration of several factors which are specific to each move. GVW, axle and tire loads and configurations, properties of existing pavement layers, pavement condition at the time of the move, traveling speed and pavement temperature (for asphalt surfaces) are critical factors for the damage analysis of OW vehicles.

The impact of OW vehicles on pavement and associated damage have been studied for a long time in many research studies. These studies used empirical, Mechanistic-Empirical (ME), or Finite Element (FE) methodologies along with the concept of load equivalency to evaluate pavement damage due to increased axle and vehicle loads. The load equivalency factor (LEF) defines the damage per pass to a pavement by the specific axle (or specific truck) relative to the damage per pass of a standard axle load (or standard track). Usually, the standard axle load is the 18,000 pounds single axle and the standard truck is the 18-wheel truck with a GVW of 80,000 pounds. A review of pavement damage methodologies for assessing the impact of OW and single-event overload vehicles on pavement performance is presented here.

- Impact of Heavy Vehicles on Low-Volume Roads (Sebaaly et al., 2003)
  The impact of agricultural equipment on the actual response of low-volume roads (gravel and blotter pavements) was evaluated using instrumented pavement sections in South Dakota. Pavement responses under various combinations of agricultural equipment as well as the 18,000 lb single-axle truck were collected using pressure cells and deflection gauges. Because rutting is the only distress that gravel and blotter pavements experience, rutting failure was selected as the criteria to develop LEFs. The rutting LEFs were calculated as the ratio of the number of repetitions of the 18,000 lb single-axle truck over the number of repetitions of a given agricultural equipment to cause 0.5-in. surface rutting. Analysis of the field data and the LEF data indicated that agricultural equipment can be significantly more damaging to low-volume roads than an 18,000 lb single-axle trucks. The impact also depends on factors such as season, load level, the thickness of base layer, and soil type. It was concluded that an agency can effectively reduce potential damage caused by agricultural equipment on gravel and blotter pavements by designing for a thicker base layer or by subjecting the agricultural equipment to the legal load limit (i.e., around 20,000 pounds).

- Determination of Equivalent Axle Load Factor of Trailer with Multiple Axle on Flexible Pavement Structures (Tjan and Fung, 2005)
  In this study, LEF for a 10-axle hauling unit with 80 tires carrying and GVW of 175 tons (350,000 pounds) traveling on flexible pavement structures was developed. ME method considering cracking (20 percent cracks on pavement surface) and permanent deformation in subgrade (13 mm rut depth) was used to develop LEF in this study. The Everstress FE program was selected for pavement response calculation to determine tensile and compressive strains. As the Everstress program can only handle 20 loaded tires, a quarter system of the trailer was analyzed and then superpositioned to obtain pavement response under all 80 tires. It was concluded that LEF depends on the thickness of pavement structure and subgrade modulus. Fatigue cracking is the determining failure criteria (i.e., higher LEF) for pavements with high subgrade modulus and thicker structure while permanent deformation LEF is higher for pavement structures with low subgrade modulus.

- Deterioration Analysis of Flexible Pavements under Overweight Vehicles (Sadeghi and Fathali, 2007)
  In this study, the influence of overloaded vehicles on the operational life of flexible pavements was studied and a deterioration model was developed. Fatigue cracking and rutting in subgrade were the main failure criteria used in the development of the deterioration model. A sensitivity analysis was conducted to determine the critical factors

that impact the deterioration of pavement under truck loading. The operational life reduction factor shown in Eq. (2) was used to determine the ticketing (i.e., permitting cost) by multiplying it to the travel length and pavement value (i.e., construction cost).
where:

$$F = \frac{1}{N} - \frac{1}{N_{all}} \qquad (2)$$

F = operational life reduction factor
N = allowable load repetition when each axle has excess loads
N_{all} = allowable load repetition when axles passing the road have the allowable load

- Pavement Damage Due to Different Tire and Loading Configurations on Secondary Roads (Al-Qadi and Wang, 2009)
  In this study, a three-dimensional (3-D) FE model was developed to predict pavement responses under various tire configurations on secondary road pavements. This model was capable of incorporating the measured 3-D tire-pavement contact stresses, linear viscoelasticity in asphalt layer, and continuously moving load. The impact of heavy trucks with wide-base tires as well as conventional dual-tire assemblies on secondary road pavement damage was analyzed using available damage models (fatigue cracking and rutting in asphalt and unbound layers). The damage ratio was defined as the following:
  where:

$$DR = \frac{N_{dual}}{N_{w455}} \qquad (3)$$

DR = damage ratio caused by the 455 wide-base tire with respect to the dual-tire
N_{dual} = allowable number of load applications to failure for dual-tire
N_{w455} = allowable number of load applications to failure for the 455 wide-base tire

- Evaluating the Effect of Natural Gas Developments on Highways: Texas Case Study (Banerjee et al., 2012)
  Natural gas development in the Barnett Shale region of Texas has been a major contributor to the economic prosperity of the region. However, from a highway infrastructure perspective, it has resulted in increased maintenance budgets for Texas DOT's Fort Worth and Dallas Districts. The associated damage caused by trucking operations was evaluated by the use of the mechanistic-empirical pavement design guide (MEPDG) with respect to four primary distress mechanisms: rutting, longitudinal cracking, alligator cracking, and roughness. As shown in Figure 2-5, the difference in the time to reach the terminal distress value (attributable to the design traffic and due to the combined effect of the design and natural gas traffic) reflects the service life reduction of the pavement sections caused by natural gas development.
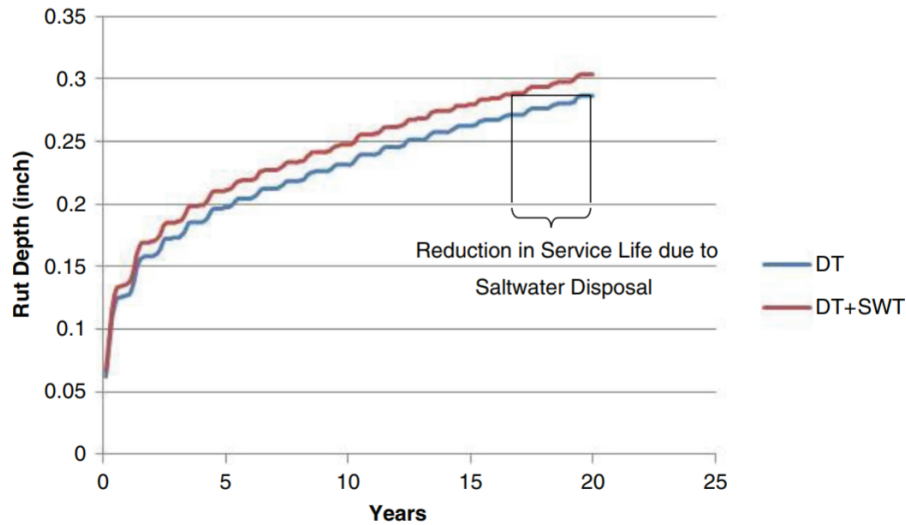
Figure 2-5: Reduction in service life due to extra OW truck (Banerjee et al., 2012)

- Framework for Determining Load Equivalencies with DARWin-ME (Banerjee et al., 2013)
  A methodology was developed to use ME design procedures to determine load equivalencies for various axle configurations and loads for OS and OW vehicles. In this study, the DARWin-ME was used to establish the equivalent damage factors (EDFs) for single, tandem, tridem, and quad axles. The framework defined a given axle load and configuration equivalent to a reference axle load based on equivalent pavement responses that resulted in the same distress level. Figure 2-6 shows EDFs computed for two types of five-axle vehicles under various loading configurations. This figure implies that for a given GVW, the distribution of loads and axle configuration greatly affects the EDFs.

(a) FHWA Class 9, steering plus two tandem axles   (b) FHWA Class 11, five single axles
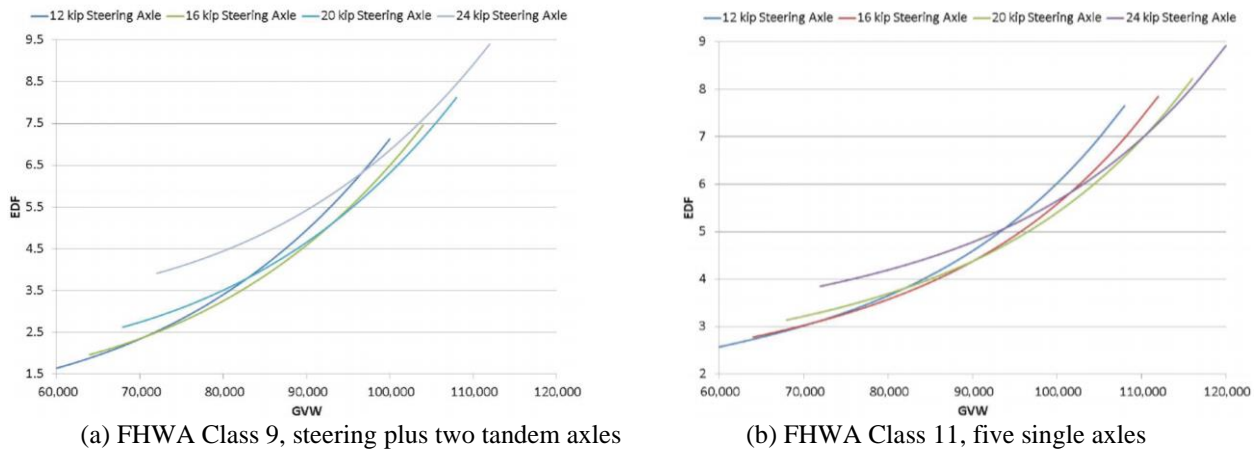
Figure 2-6: EDFs calculated for five-axle vehicles (Banerjee et al., 2013)

- Characterization of Overweight Permitted Truck Routes and Loads in Wisconsin (Titi et al., 2014)
  An OW permit database with over 95,000 entries along with the geographic information system and relational databases were used to conduct a statewide routing analysis to identify highways that are heavily used by OW permitted trucks. The routing and pavement

analyses were primarily used to assist the Wisconsin DOT in developing rehabilitation strategies for deteriorated pavements. Visual condition surveys were also performed to determine related pavement condition on the identified segments. A strong correlation between OW traffic level and observed pavement distress was found.

- Quantification of Accelerated Pavement Serviceability Reduction Due to Overweight Truck Traffic (Dey et al., 2015)
  In this study, deterioration of flexible pavement sections under OW vehicles was investigated using MEPDG. This was done to quantify the relative pavement damage attributable to OW vehicles compared to vehicles within legal axle and GVW limits in South Carolina. The study developed axle load distributions of several truck types using information from an OW permit database. Additionally, an analysis was conducted to evaluate the impact of each overweight truck type on representative pavement structures. It was found that among all distress types, fatigue cracking (top-down and bottom-up) was more sensitive to overweight trucks (up to the typical overweight permit limit) and trucks loaded above typical overweight permit limit (i.e., superload) compared to rutting and international roughness index (IRI).

- Modelling Pavement Response to Superheavy Load Movement (Khanal et al., 2016)
  In this study, FEM was used to carry out a pavement impact study for two different scenarios of superheavy load moves in spring and winter conditions in Canada. The stresses and strains determined using the FEM were then used to calculate and predict the key types of pavement damage; fatigue cracking of the asphalt concrete and rutting of the subgrade. It was found that although the spring move had about 55 percent less gross vehicle weight, the damage predicted is about three times higher when compared with the winter move.

- Mechanistic-Based Pavement Damage Associated Cost from Oversize and Overweight Vehicles in Nevada (Hajj et al., 2017)
  Assessing pavement damage attributable to OW vehicle moves in Nevada and providing a framework for a permit fee structure of single and multi OW trips in Nevada were the objectives of this study. The methodology was based on ME analysis of flexible pavements under OW vehicle loadings utilizing pavement performance models that have been locally calibrated to Nevada conditions. The presented methodology used information that was collected by the NDOT overdimensional office during the permit application process and addresses pavement damage and associated costs from single and multi-trip permitted vehicles. The overall flowchart for the cost allocation analysis method is presented in Figure 2-7.
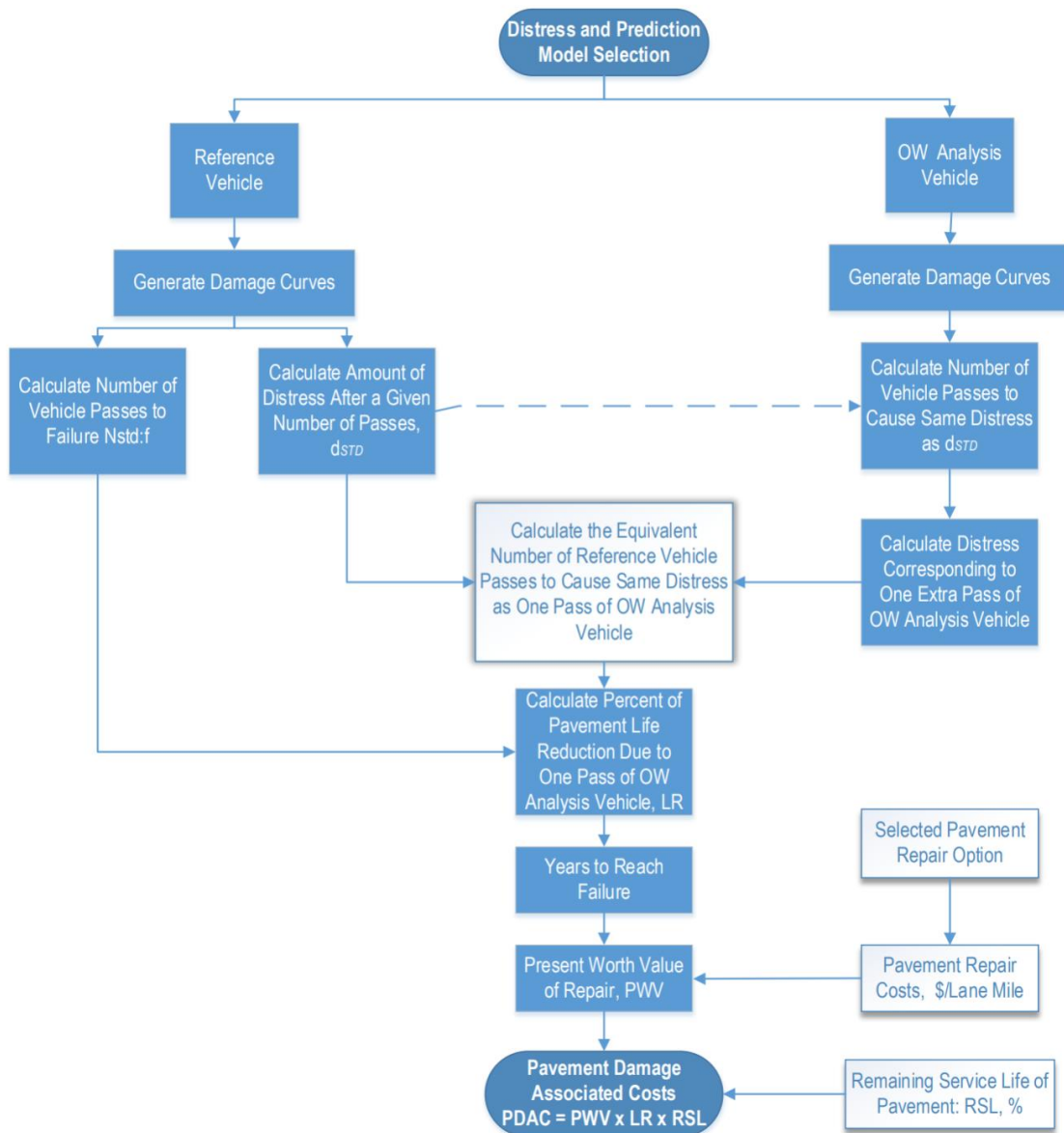
Figure 2-7: Flowchart of overall approach for the estimation of pavement damage and allocated cost (Hajj et al., 2017)

- Analysis Procedures for Evaluating Superheavy Load Movement on Flexible Pavements, Volume I: Final Report (Hajj et al., 2018)

  In this study which was part of an FHWA project on Analysis Procedures for Evaluating Superheavy Load Movement on Flexible Pavements, a comprehensive mechanistic-based methodology was developed which consisted of the following analysis procedures: (1) segmentation of SHL analysis vehicle, (2) subgrade bearing failure analysis, (3) sloped shoulder failure analysis, (4) buried utility risk analysis, (5) localized shear failure analysis, (6) deflection-based service limit analysis, and (7) cost allocation analysis. shows the flowchart of the overall approach developed as part of this study.

- The Assessment of Damage to Texas Highways due to Oversize and Overweight Loads Considering Climatic Factors (Wu et al., 2019)
  Different paradigms that influence pavement performance under OS/OW vehicles were combined into a single evaluation methodology by considering the characteristics of OS/OW vehicles (i.e. dimension and weight), their origin and destination, permitted routes, frequency of the routes, pavement condition data, and climatic effects. This study showed that higher axle loads from OW vehicles would cause a faster deterioration rate and reduction in the service life of road sections compare to regular traffic. This was particularly true when OW vehicles passed at the early age of roads. It was also found that the rate of road deterioration from OW vehicles decreased at the end of the road life.

As shown in Figure 2-8, the first step of the approach involves a risk analysis of instantaneous or rapid load-induced ultimate shear failure. As pavement subgrade is generally the weakest layer in the pavement structure, the bearing failure analysis investigates the likelihood of general bearing capacity failure under the SHL vehicle within the influenced zone of the subgrade layer. Next, the sloped-shoulder failure analysis examines the bearing capacity failure and the edge slope stability associated with the sloping ground under the SHL-vehicle movement. Once the ultimate failure analyses are investigated and ruled out, when applicable, a buried utility risk analysis is conducted. In this analysis, the stresses and deflections induced by the SHL vehicle on existing buried utilities are evaluated and compared to established design criteria. Subsequently, if no mitigation strategies are needed, service limit analyses for localized shear failure and deflection-based service limit are conducted. The localized shear failure analysis investigates the possibility of failure at the critical location on top of the subgrade layer under the SHL vehicle. The deflection-based service limit analysis assesses the magnitude of the load-induced pavement deflections during the SHL movement. For instance, this analysis may suggest the need for mitigation strategies to meet the imposed acceptable surface deflection limits. After successfully completing all previously described analyses (i.e., ultimate failure analyses, buried utility risk analysis, and service limit analyses), a cost allocation analysis is then conducted.
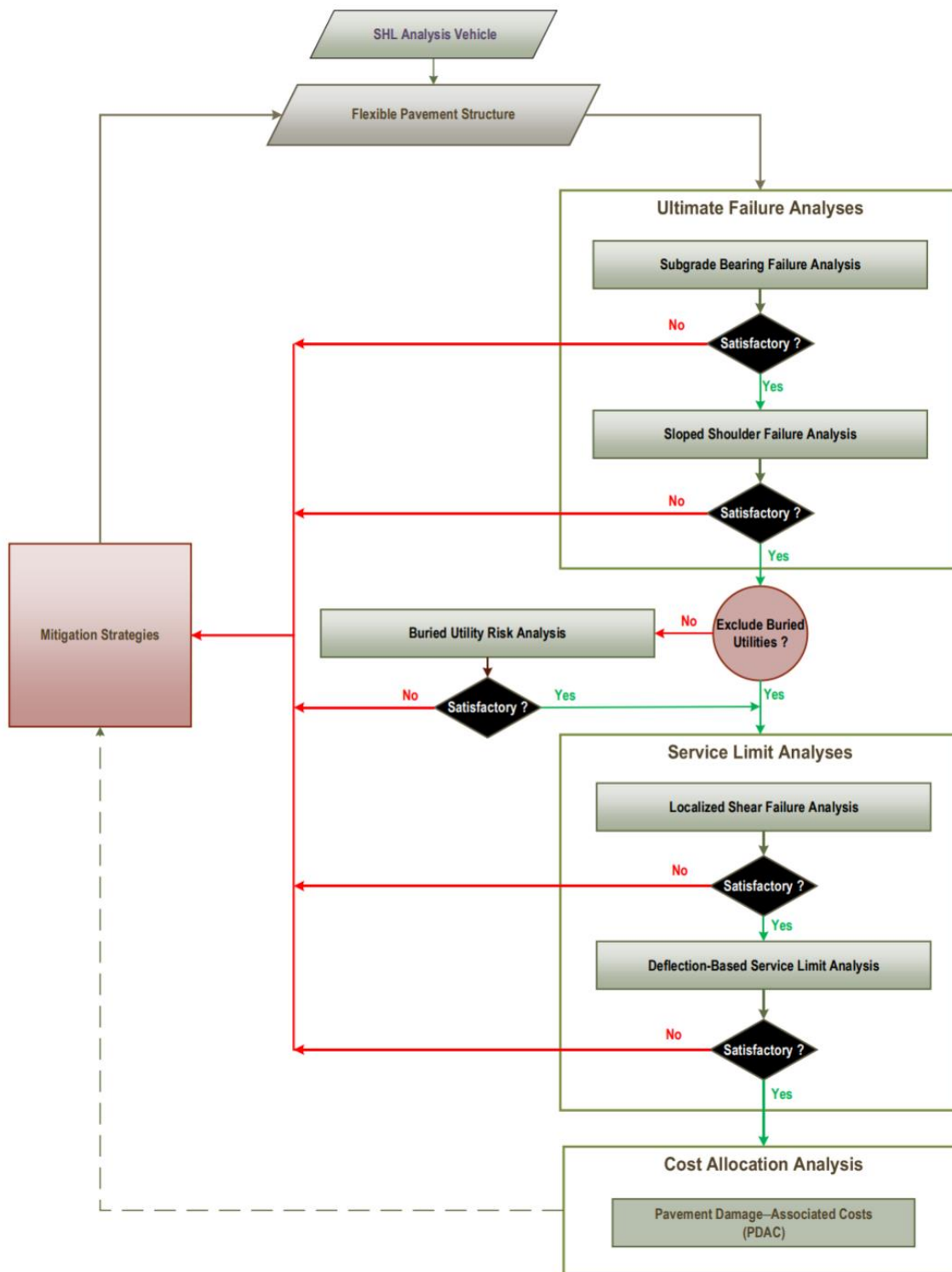
Figure 2-8: Overall SHL-vehicle analysis methodology (Hajj et al., 2018)

3   WEIGH-IN-MOTION DATA ANALYSIS

The FDOT Permit Office oversees OW/OS Permit issuance on all state-maintained highways and roadways. The Permit Application System (PAS) can be used to self-issue trip permits for loads up to 16 feet wide, 18 feet high, 150 long, and 200,000 pounds (140,000 pounds for self-propelled equipment). Specific consideration is given to the moves when any axle exceeds 30,000 pounds, or when the GVW is 300,000 pounds or more.

At the beginning, it was anticipated that the PAS database would provide detailed information regarding specific routes that are subjected to more frequent passes of the OS/OW vehicles. However, significant challenges were encountered with the PAS database. These challenges are summarized in the following.

- While the PAS database included the GPS coordinates (and/or the address) of the origin, destination, and other specific waypoints, the actual roadways travelled by the OS/OW vehicles were not available in the PAS route detail tables (e.g., "AP_RTE_DET" and other similar tables). I.e., there are many different routes that could be taken to get from the origin to the destination (or to another waypoint).
- Another table in the PAS database (namely "OVPT011_OVP_RTE") included the route description feature which provided the roadway names (or highway numbering) of the routes travelled by the OS/OW vehicles (e.g., "SR 426| SR 436| US 441| SR 19| SR 40"). However, these roadway names were not associated with FDOT's roadway section ID and mileposts. Furthermore, this particular table did not include any directional information, milepost limits, beginning and ending points, nor GPS coordinates.

Due to the above challenges, the Department and the research team had searched for additional sources of data. After a prolonged effort, it was concluded that the detailed and specific routes travelled by OS/OW vehicles are only available in PAS as captured images of Google maps that cannot be used by the research team in an efficient manner. Therefore, the Department and the research team agreed to focus on data from traditional portable WIM sites and newer WIM sites at Freight Operations Exchange (FOX) facilities for studying the trends in vehicle loads.

3.1   Weigh-In-Motion Data

Weigh-In-Motion (WIM) is the process of estimating the static (motionless) weight of a vehicle from measurements of the vertical component of dynamic tire forces applied to a sensor on a smooth, level road surface. Weigh-in-motion or weighing-in-motion devices capture and document the axle weights and gross vehicle weights as vehicles drive over a measurement site. WIM systems are capable of measuring vehicles traveling at a reduced or normal traffic speed and do not require the vehicle to come to a halt.

The WIM dataset contains individual records of buses/trucks (FHWA Classes 4 to 13) passing through each WIM site in Florida. The dataset includes date, time, travel direction, travel lane, gross vehicle weight, vehicle class, vehicle length, axle spacing and axle weights for each truck passing through the WIM station (FDOT, 2018).

3.2 Analysis of WIM and FOX Data

For the subsequent analysis of traffic data, FDOT provided the research team with WIM data between years 2015 and 2019, and FOX data between years 2017 and 2019. The raw dataset was transferred in the form of text files, with each file corresponding to the WIM data for a given year. In total, the WIM data included 246 million records over the 5-year period while the FOX data included 6.5 million records over the 3 year period.

Both the WIM and the FOX database included micro-level data for every vehicle that passed through the facility. The data included not only the FHWA Vehicle Class (shown in Appendix A) and Gross Vehicle Weight (GVW) of each vehicle, but also the total number of axles, axle spacings (WIM data only), and the weight of each axle (WIM data only). In addition, the database also included several supplementary information such as speed, length, and width of the vehicle. However, for the purpose of this Task, the primary focus was given to truck traffic counts and GVW.

For the purpose of this task, the WIM and FOX sites were grouped into the following categories: (1) Limited Access routes that generally represent high-speed Interstates and freeways with high-volume of traffic and (2) Non-Limited Access routes that include low-speed roadways with relatively lower volume of truck traffic.

Table 3-1 and Table 3-2 show the locations of WIM and FOX sites on limited and non-limited access roadways, respectively. In these tables, a unique ID was generated for each location. The WIM sites are designated with "W" followed by the last two digits of WIM site number. The FOX sies are designated with "F" followed by sequential integers as they appear in the tables.

A map of all WIM and FOX locations are shown in Figure 3-1.

Table 3-1: WIM and FOX locations for limited access routes

District	ID	Site	County	County Section	Mile post	Road-way	Lat.	Long.	Fun. Class	Class Description*
1	W50	9950	Collier	3175000	61.558	I-75	26.28657	-81.7427	11	P.A., Interstate - Urban
	W51	9951	Polk	16320000	17.789	I-4	28.15742	-81.8121	11	P.A., Interstate - Urban
	F1	I-75 NB Exit 158	Charlotte	1075000	9.754	I-75	26.8798	-81.9849	1	P.A., Interstate - Rural
2	W02	9902	Madison	35090000	24.61	I-10	30.38869	-83.3279	1	P.A., Interstate - Rural
	W04	9904	Alachua	26260000	4.927	I-75	29.54304	-82.3317	1	P.A., Interstate - Rural
	W05	9905	Duval	72280000	2.77	I-95	30.135	-81.5342	11	P.A., Interstate - Urban
	W14	9914	Duval	72001000	23.567	I-295	30.35556	-81.7607	11	P.A., Interstate - Urban
	W23	9923	Nassau	74160000	5.571	I-95	30.65499	-81.6624	1	P.A., Interstate - Rural
	W36	9936	Columbia	29170000	17.17	I-10	30.25136	-82.5149	17	Major Collector - Urban
	W56	9956	Hamilton	32100000	19.696	I-75	30.53374	-83.0701	1	P.A., Interstate - Rural
	F2	I-75 SB MM 451 White Springs	Hamilton	32100000	9	I-75	30.4372	-82.9157	1	P.A., Interstate - Rural
	F3	I-95 SB MM 377 Yulee	Nassau	74160000	8	I-95	30.6868	-81.674	1	P.A., Interstate - Rural
3	W49	9949	Escambia	48260000	8.7	I-10	30.5092	-87.2908	11	P.A., Interstate - Urban
	W58	9958	Walton	60002000	19.186	I-10	30.69121	-86.0952	1	P.A., Interstate - Rural
	F4	I-10 EB Exit 152 Grand Ridge	Jackson	53002000	25.2	I-10	30.6581	-85.041	1	P.A., Interstate - Rural
	F5	I-10 EB Pensacola MM2	Escambia	48260000	1.77	I-10	30.5628	-87.3778	1	P.A., Interstate - Rural
	F6	I-10 WB Exit 158	Jackson	53002000	31.22	I-10	30.6373	-84.9422	1	P.A., Interstate - Rural
4	W13	9913	St. Lucie	94470000	2.933	SR-91 (TP)	27.2464	-80.3466	12	P.A., Freeway And Expressway – Urban
	W33	9933	Broward	86472000	4.258	SR-869 (TP)	26.1801	-80.3062	12	P.A., Freeway And Expressway - Urban
	W52	9952	Palm Beach	93220000	42.741	I-95	26.91501	-80.1439	12	P.A., Freeway And Expressway - Urban
	F7	I-95 NB Indiantown Rd	Palm Beach	93220000	44.1	I-95	26.9347	-80.1496	11	P.A., Interstate - Urban

Table 3-1: continued

District	ID	Site	County	County Section	Mile post	Road-way	Lat.	Long.	Fun. Class	Class Description*
	F8	I-95 SB Becker Rd	St. Lucie	94001000	0.095	I-95	27.2121	-80.401	11	P.A., Interstate - Urban
	F9	I-95 SB MM 113	Martin	89095000	22.1	I-95	27.19	-80.4005	1	P.A., Interstate - Rural
5	W06	9906	Volusia	79110000	4.678	I-4	28.88769	-81.279	11	P.A., Interstate - Urban
	W19	9919	Brevard	70220000	39.08	I-95	28.32948	-80.7746	11	P.A., Interstate - Urban
	W20	9920	Sumter	18130000	17.589	I-75	28.80062	-82.088	1	P.A., Interstate - Rural
	W31	9931	Sumter	18470000	3.379	SR-91 (TP)	28.79894	-81.9982	2	P.A., Expressway - Rural
	W60	9960	Orange	75002000	29.641	SR-482	28.45244	-80.9906	2	P.A., Expressway - Rural
	W61	9961	Osceola	92471000	33.446	SR-91 (TP)	28.25515	-81.3308	12	P.A., Freeway And Expressway - Urban
	F10	I-95 SB Palm Coast	Flagler	73001000	8	I-95	29.52477	-81.2034	11	P.A., Interstate - Urban
6	W34	9934	Miami-Dade	87471000	36.09	SR-821 (TP)	25.91201	-80.3811	1	P.A., Interstate - Rural
7	W53	9953	Hillsborough	10075000	19.073	I-75	27.88979	-82.3485	11	P.A., Interstate - Urban
	W55	9955	Hillsborough	10320000	13.076	I-275	28.13385	-82.4138	11	P.A., Interstate - Urban
	W62	9962	Hillsborough	10190000	23.689	I-275	28.02732	-82.2038	11	P.A., Interstate - Urban

Note*: P.A. = Principal Arterial

Table 3-2: WIM and FOX locations for non-limited access routes

District	ID	Site	County	County Section	Milepost	Roadway	Lat.	Long.	Fun. Class	Class Description*
1	W18	9918	Hendry	7030000	10.618	US-27 / SR-80	26.75383	-81.055	4	P.A., Other - Rural
	W27	9927	Polk	16100000	0.816	SR-546	28.05319	-82.0049	14	P.A., Other - Urban
	W48	9948	Polk	16170000	17.539	US-27 / SR-25	27.87903	-81.5971	14	P.A., Other - Urban
	F11	US-27 SB Hendry	Hendry	7030000	10.195	US-27	26.7554	-81.0461	4	P.A., Other - Rural
2	W09	9909	Levy	34010000	3.184	US-19 / SR-500	29.55086	-82.9004	4	P.A., Other - Rural
	W63	9963	Bradford	28010000	0.06	US-301	29.84037	-82.1627	4	P.A., Other - Rural
	F12	US-90 EB Madison	Madison	35010000	20.965	US-90	30.469	-83.3978	6	Minor Arterial - Rural
3	W07	9907	Bay	46040000	22.531	US-231 / SR-75	30.39718	-85.435	4	P.A., Other - Rural
	W16	9916	Escambia	48040000	9.399	US-29 / SR-95	30.54365	-87.2815	14	P.A., Other - Urban
	W40	9940	Gadsden	50080000	13.079	SR-267	30.55475	-84.5927	6	Minor Arterial - Rural
	W43	9943	Jackson	53020000	12.386	US-90 / SR-10	30.71938	-85.0393	14	P.A., Other - Urban
	W57	9957	Jackson	53060000	5.205	SR-77	30.90482	-85.5223	4	P.A., Other - Rural
	W59	9959	Walton	60060000	21.435	US-331	30.99143	-86.3092	4	P.A., Other - Rural
	F13	SR-77 SB Panama City	Bay	46060000	11	SR-77	30.3084	-85.6517	14	P.A., Other - Urban
	F14	US-231 SB Welcome Center	Jackson	53050000	17.7	US-231	30.9861	-85.4075	4	P.A., Other - Rural
	F15	US-27 SB Gadsden	Gadsden	50040000	3.442	US-27	30.6604	-84.4121	4	P.A., Other - Rural
	F16	Gadsden CR-12B (Deactivated)	Gadsden	NA	NA	CR-12B	30.6602	-84.4053	NA	NA
4	W64**	9964	Palm Beach	93290000	3.064	SR-715	26.70774	-80.684	16	Minor Arterial - Urban
	W65**	9965	Palm Beach	93160000	22.815	US-27	26.61724	-80.7117	4	P.A., Other - Rural
5	W25	9925	Volusia	79060000	6.903	SR-600	29.10369	-81.2098	4	P.A., Other - Rural
	W29	9929	Volusia	79010000	11.126	SR-546	28.93191	-80.8773	14	P.A., Other - Urban

Table 3-2: continued

District	ID	Site	County	County Section	Milepost	Roadway	Lat.	Long.	Fun. Class	Class Description*
	F17	CR-475 EB Wildwood	Sumter	NA	NA	CR-475	28.9307	-82.1156	NA	NA
	F18	CR-484 SB Wildwood	Marion	NA	NA	CR-484	29.0236	-82.1564	NA	NA
	F19	SR-40 EB Marion	Marion	36080000	31.7	SR-40	29.1743	-81.6713	4	P.A., Other - Rural
	F20	US-1 NB Palm Coast	Flagler	73010000	18.2	US-1	29.5596	-81.268	4	P.A., Other - Rural
	F21	US-1 SB Palm Coast	Flagler	73010000	18.2	US-1	29.57409	-81.276	4	P.A., Other - Rural
6	W47	9947	Miami-Dade	87090000	8.1	US-27 / SR-25	25.87372	-80.3491	14	P.A., Other - Urban
7	F22	US-92 EB Seffner	Hillsborough	10030000	11.253	US-92	28.0088	-82.2677	14	P.A., Other - Urban

Note*: P.A. = Principal Arterial
Note**: These WIM sites only included data for 2019 and were not included in the analyses for traffic trends
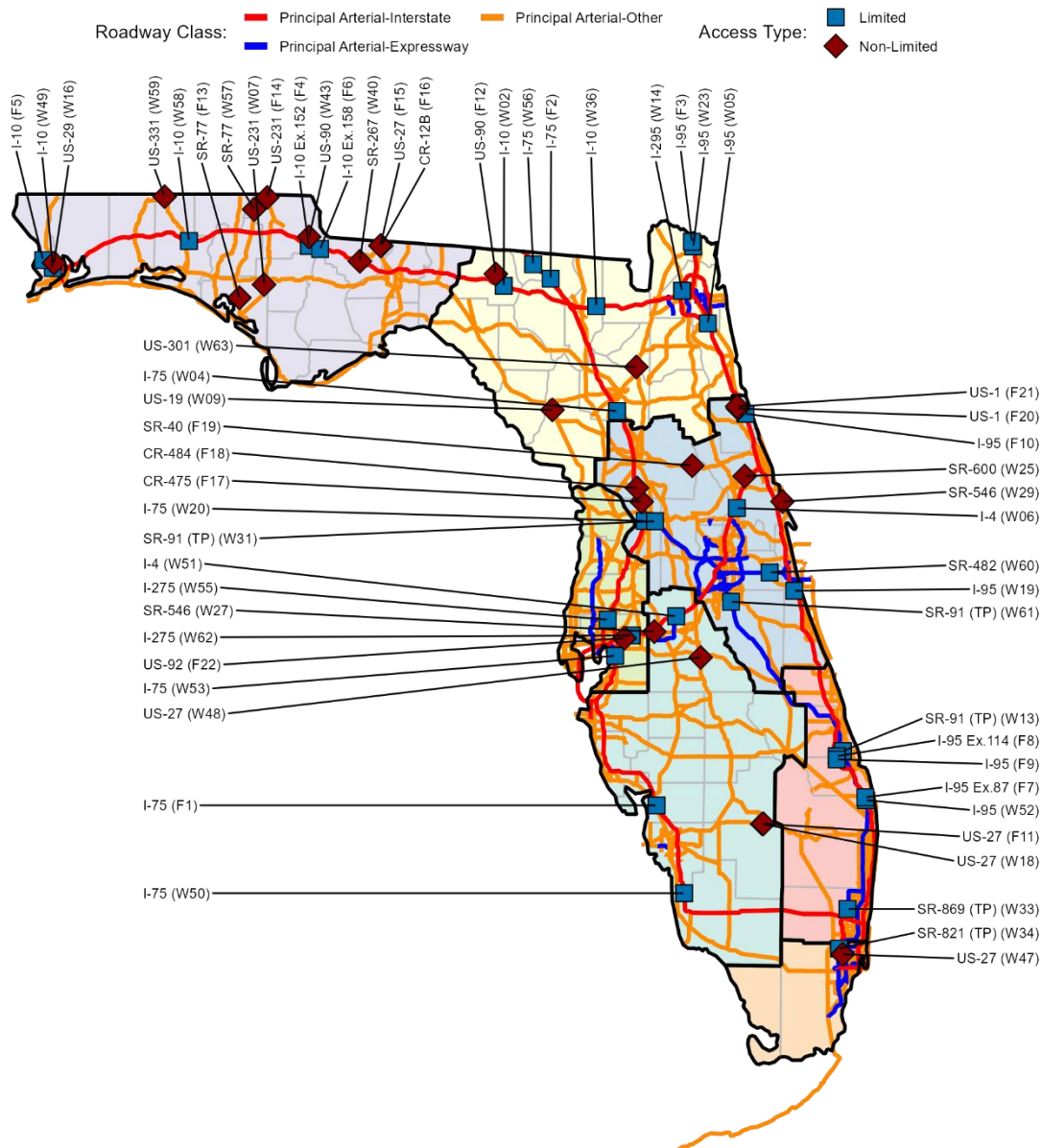
Figure 3-1: Map of WIM and FOX locations

3.3   Limited Access Roadways

3.3.1   Summary of Overall Trends for Limited Access Roadways

In this section of the report, an overall summary of the WIM and FOX data and the relevant observations are provided for the limited access roadways.

Figure 3-2 shows the total amount of truck traffic observed from the limited access WIM and FOX sites while Figure 3-3 shows the corresponding, average GVW broken down by vehicle class and year. In general, the following observations are made from these figures.

1. Vehicle Class 9 (i.e., 5-axle, tractor-trailers) comprises the predominant trucks on Florida's limited access highways, followed by Vehicle Classes 5 and 8. The average GVW of these vehicles remained relatively consistent over the years (e.g., the average GVW of Class 9 vehicles varied from 51.8 kip to 53.1 kip within the 5-year period).

2. Although the combined number of trucks for Vehicle Classes 7, 10, 11, 12, and 13 only makes up approximately 5.0 percent of the entire truck volume, these vehicles are the heaviest trucks found on Florida's limited access highways. With a few exceptions, the average GVW of these vehicles was mostly in excess of 55 kip for the 5-year period. Moreover, the average weight of Class 13 vehicles was over 75 kip between 2015 and 2017.

As discussed in the Task 1 report, the maximum GVW legally allowed on FDOT's roadways is 80 kip. In other words, any vehicle whose GVW is in excess of this limit is categorized as an OW vehicle and an appropriate permit is required for the vehicle to travel on FDOT's roadways.

The average vehicle load of 55 kip to 75 kip for certain vehicle classes mentioned above implies that a good portion of OW vehicles may be included in the vehicle mix. Figures 3-4 show the total amount of OW traffic per vehicle class and year from the limited access WIM and FOX sites. Figures 3-5 show the relative proportions of the OW vehicle weights for each vehicle class and year. The observations made from these figures are summarized in the following.

1. The number of OW vehicles have increased significantly from 2015 to 2019, regardless of the vehicle class. It is also noted that in general, the percentage of vehicles with GVW over 100 kip has increased over the years, i.e., not only the number of OW trucks but also their GVWs have increased on Florida's limited access roadways.

2. Vehicle Class 9 has the most number of overweight vehicles followed by Class 10. The OW vehicle counts have continuously increased for these vehicle classes. The GVW for most of the OW vehicles in these classes was between 80 kip and 100 kip. More specifically, only 5 percent of Class 9 OW vehicles and 15 percent of Class 10 OW vehicles (approximately) were in excess of 100-kip GVW in 2019.

3. The greatest proportions of OW vehicles with GVW in excess of 100 kip were found for Vehicle Classes 13 and 8. For Class 13, approximately 70 percent (or 47,000) of the OW vehicles were loaded to GVW in excess of 100 kip in 2019. For Class 8, approximately 55 percent (or 29,000) of the OW vehicles exceeded 100 kip in 2019.

4. Although their OW vehicle counts are relatively insignificant compared to other classes, Class 4 (i.e., buses), Class 5 (i.e., 2-axle, single unit), and Class 6 (3-axle, single unit) vehicles also showed a growth both in terms of the number of OW vehicles as well as the proportions of the vehicles loaded in excess of 100 kip.
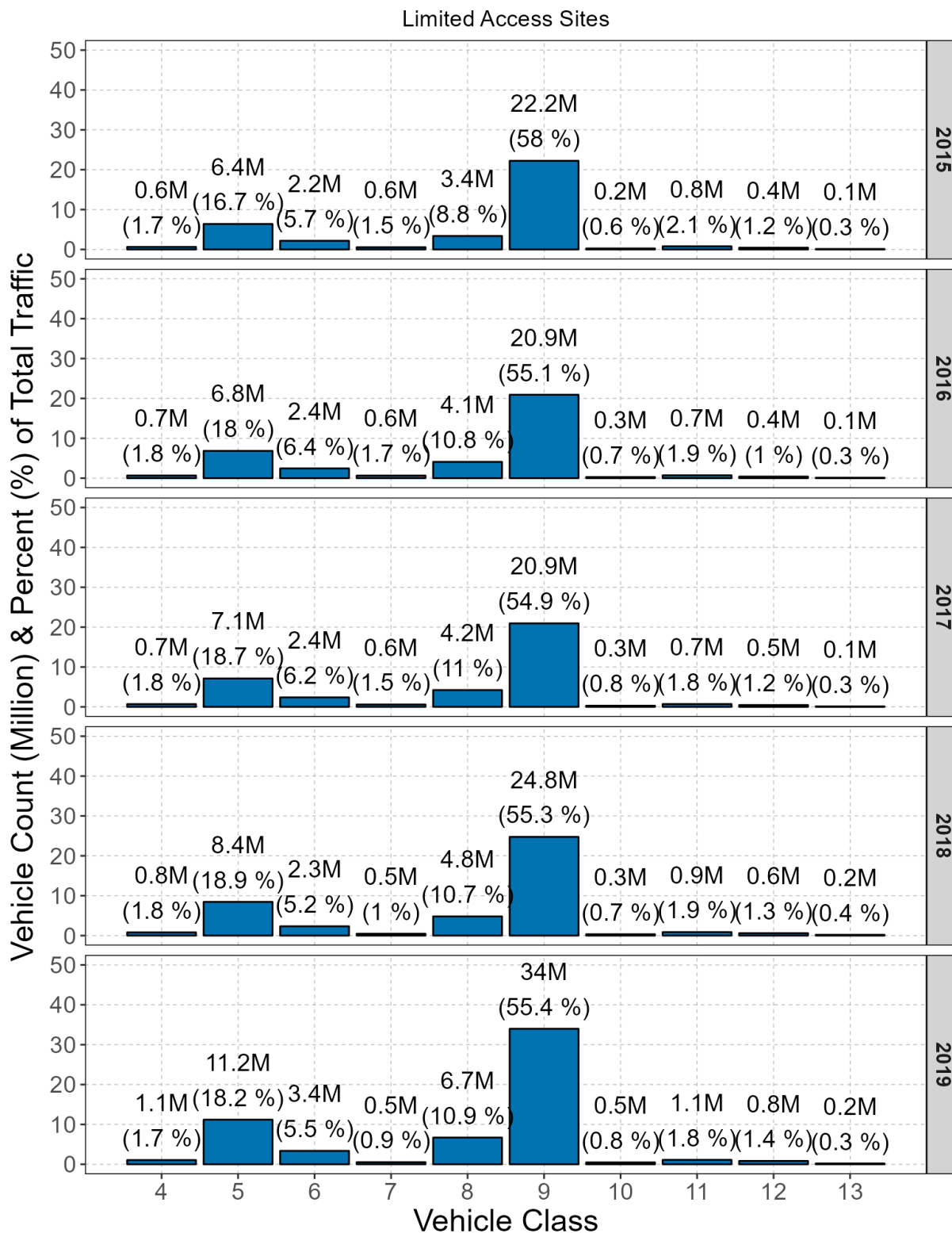
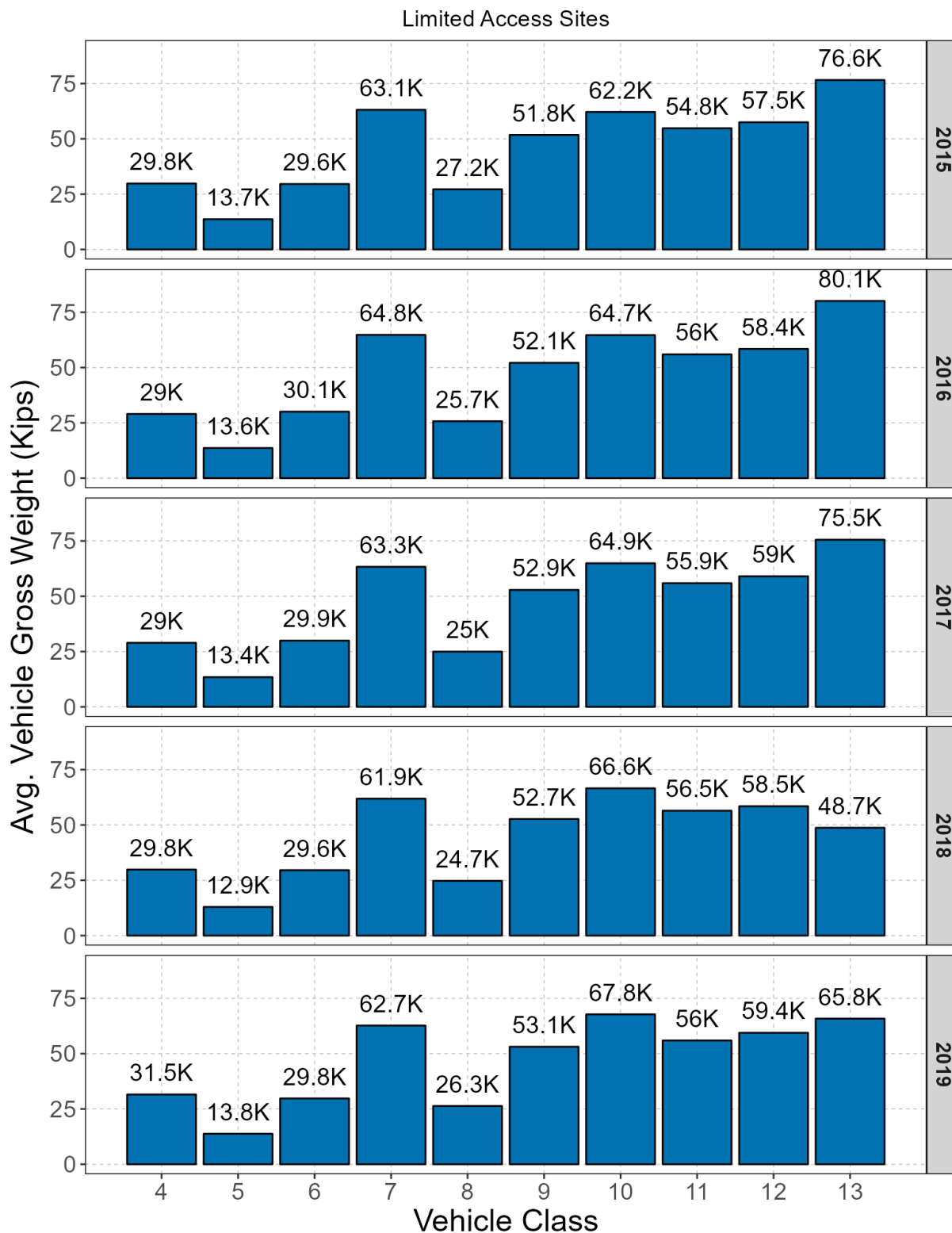**Figure 3-2: Total truck count per vehicle class for limited access roadways**

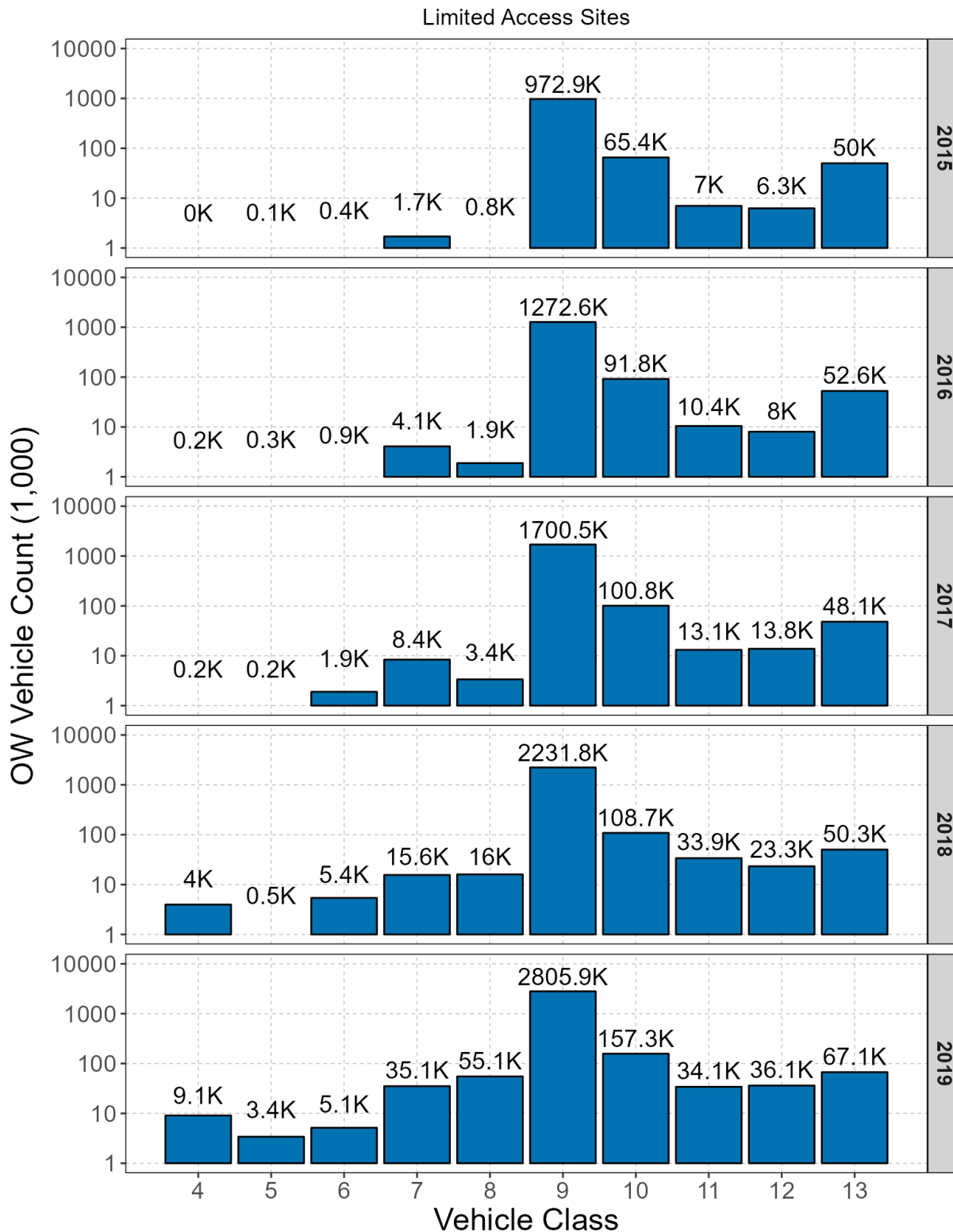Figure 3-3: Average gross vehicle weight per vehicle class for limited access roadways

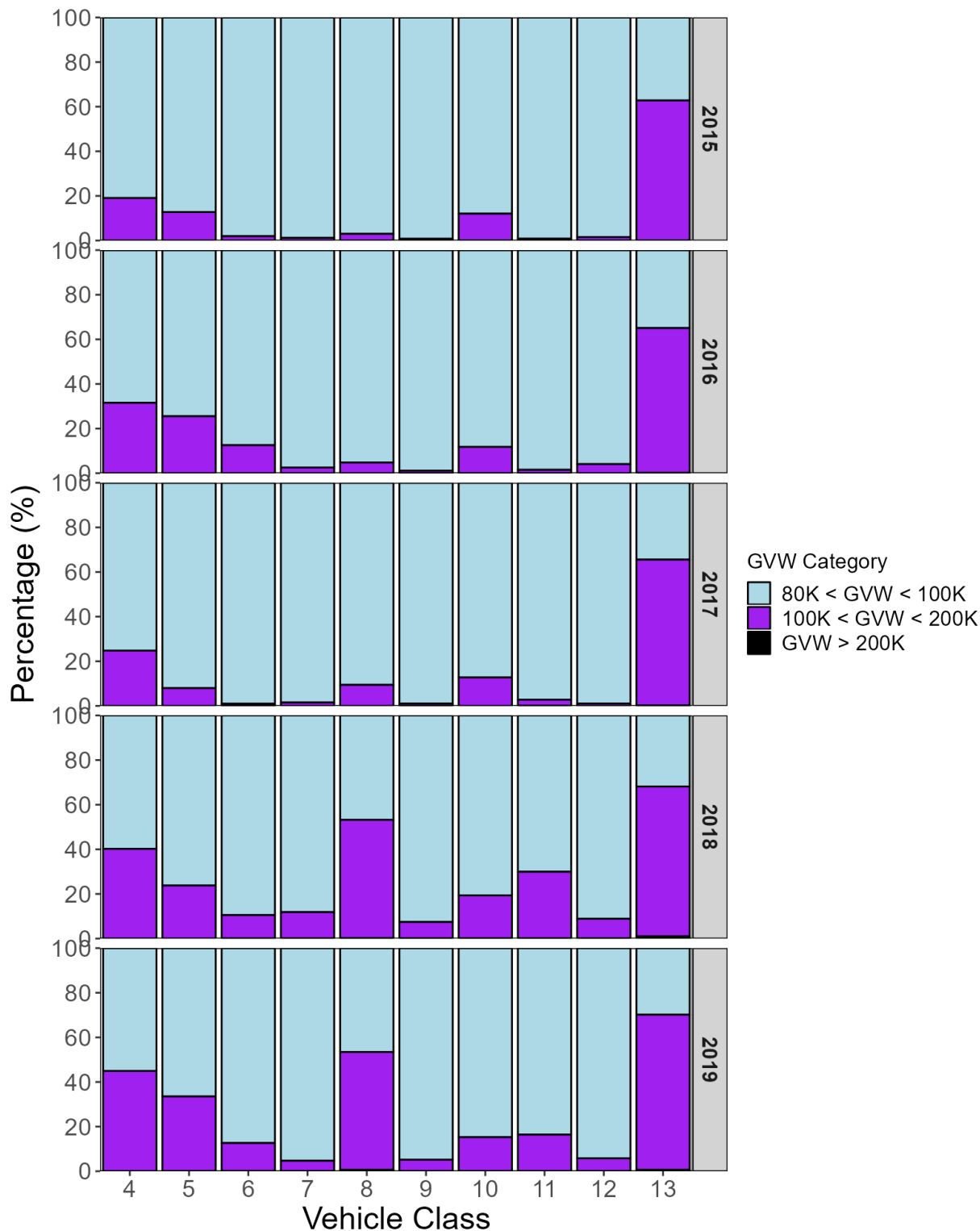**Figure 3-4: Total OW truck count per vehicle class for limited access roadways**

Figure 3-5: Distribution of OW vehicle weights for limited access roadways

3.3.2   Analysis of WIM and FOX Data by Route

In addition to the overall trends and summary provided above, the WIM and FOX data was analyzed for traffic counts and trends at every site. More specifically, the annual average counts for total trucks and OW trucks were determined, along with their trends (i.e., increasing or decreasing).

As mentioned previously, the secondary objective of this task is to identify the highway corridors that are likely to be impacted by increased truck loads (and OW trucks) anticipated in the future. As such, the results are provided on a route-by route basis in the following sections.

The tabulated results for all WIM and FOX sites on limited access roadways are provided in Appendix B.

3.3.2.1   Interstate Route 10

Figure 3-6 shows the annotated locations of the WIM and FOX sites along I-10. The following provides a summary of observations.

1. The data from all WIM sites (W49, W58, W02, and W36 from west to east) indicate that I-10 generally carried a significant amount of truck traffic, estimated to be between 1.2M trucks/year (W58 in Walton County) and 2.1M trucks/year (W02 in Madison County). In addition, these sites have seen a growth of truck traffic between 5 percent (W02) and 163 percent (W58) during the 5-year period.

2. Similarly, I-10 carried between 64K OW trucks/year (W02) and 126K OW trucks/year (W58), with their 5-year growth found to be between 13 percent (W02) and 251 percent (W58).

3. The FOX site located near the Alabama border, namely F5, shows a significantly lower amount of truck traffic (and OW traffic) compared to W49 located 6.5 miles to the east of F5. It should be noted that in between these two sites, I-10 intersects another major truck route, i.e., US-90. As such, it is postulated that the majority of the trucks are taking US-90 (rather than I-10) to cross the Florida/Alabama border.

4. The two FOX sites located in Jackson County are at the exits. F4 connects to SR-69 and F6 connects to SR-286. However, both these sites carry relatively insignificant amount of truck traffic compared to the mainline I-10 traffic.

Figure 3-6: Summary of WIM and FOX data along I-10

3.3.2.2 Interstate Route 75

Figure 3-7 shows the annotated locations of the WIM and FOX sites along I-75. The following provides a summary of observations.

1. I-75 has carried most significant amount of traffic within District 2. As shown by the data from W56 in Hamilton County and W04 in Alachua County, this route has carried over 3.0M truck traffic and 52K OW traffic per year. Moreover, both these sites have shown a relatively high growth rate for truck traffic, between 69 percent and 144 percent.
   a. The Fox site F2 is located approximately 25 miles south of W56 but shows a significantly lower amount of truck traffic (92K per year) and OW traffic (42K per year). Although a solid evidence is not available, it is possible that a significant amount of truck traffic is taking SR-6 or US-129 located between these two sites.

2. W20 in Sumter County and W53 in Hillsborough County carried somewhat reduced amount of truck traffic (between 1.3M and 1.8M per year) compared to those in District 2. It is likely that over 50 percent of traffic is routed to SR-91, Florida's Turnpike which intersects I-75 at north of W20.

3. The truck traffic on I-75 is reduced at Fox site F1 in Charlotte County. It is possible that the trucks are taking alternative routes to avoid the urban areas (i.e., near Fort Myers and Cape Coral) that I-75 goes through in District 1. Nonetheless, this site still exhibited a good amount of OW traffic of 46K per year, and has seen more OW trucks in 2019 than in 2017.

4. Wim site W50 carried over 2.0M truck traffic per year, indicating that I-75 may be one of the major truck routes connecting the east and the west coasts of South Florida.
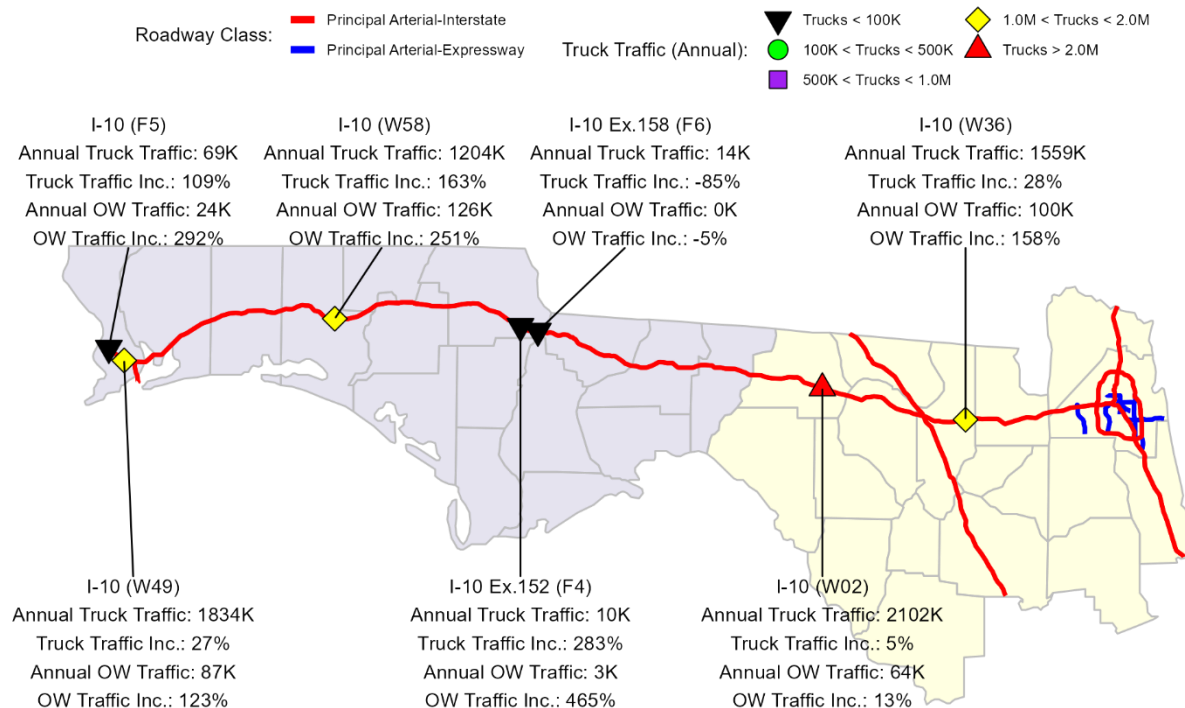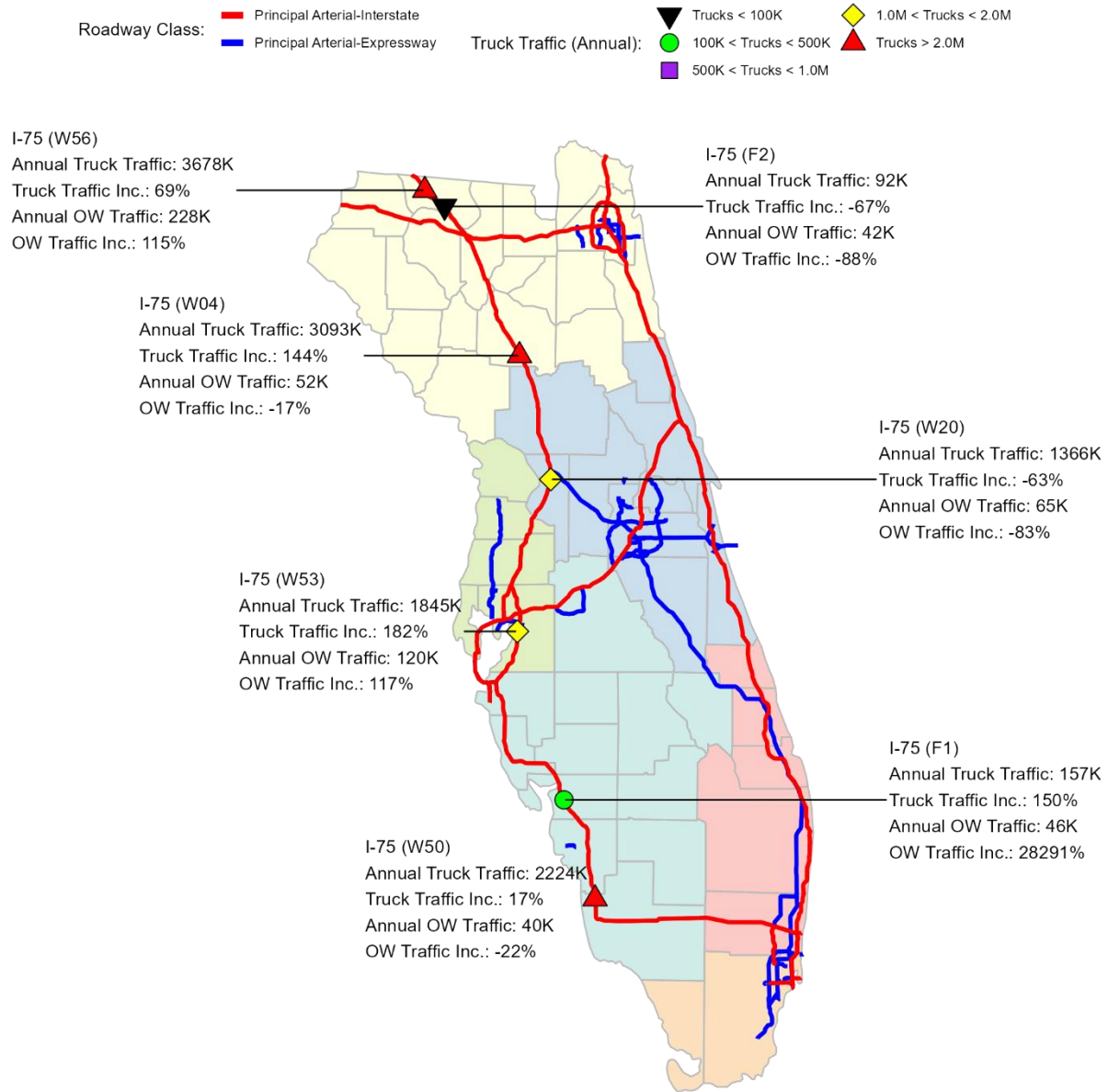

Figure 3-7: Summary of WIM and FOX data along I-75

3.3.2.3   Interstate Route 95

Figure 3-8 shows the annotated locations of the WIM and FOX sites along I-95. The following provides a summary of observations.

1. The two Wim sites to the north (W23) and south (W05) of Jacksonville indicate that I-95 has carried a significant amount of truck traffic (between 2.4M and 3.6M per year) and OW traffic (between 88K and 370K per year).
   a. Note that the Fox site F3, located just north of W23, shows significantly lower amount of traffic. Since there are no exits on I-95 between F3 and W23, the cause of such discrepancy cannot be assessed at this time.

2. Compared to WIM sites, the amount of truck traffic was reduced significantly on Fox site F10 in Flagler County, between Jacksonville and Daytona Beach (60K truck traffic per year).

3. The truck traffic on I-95 significantly increased to the south of Cape Canaveral as seen from sites W19 in Brevard County and W52 in Palm Beach County.
   a. The exception might be at F9 in Martin County, where I-95 and the Turnpike route go in "parallel".
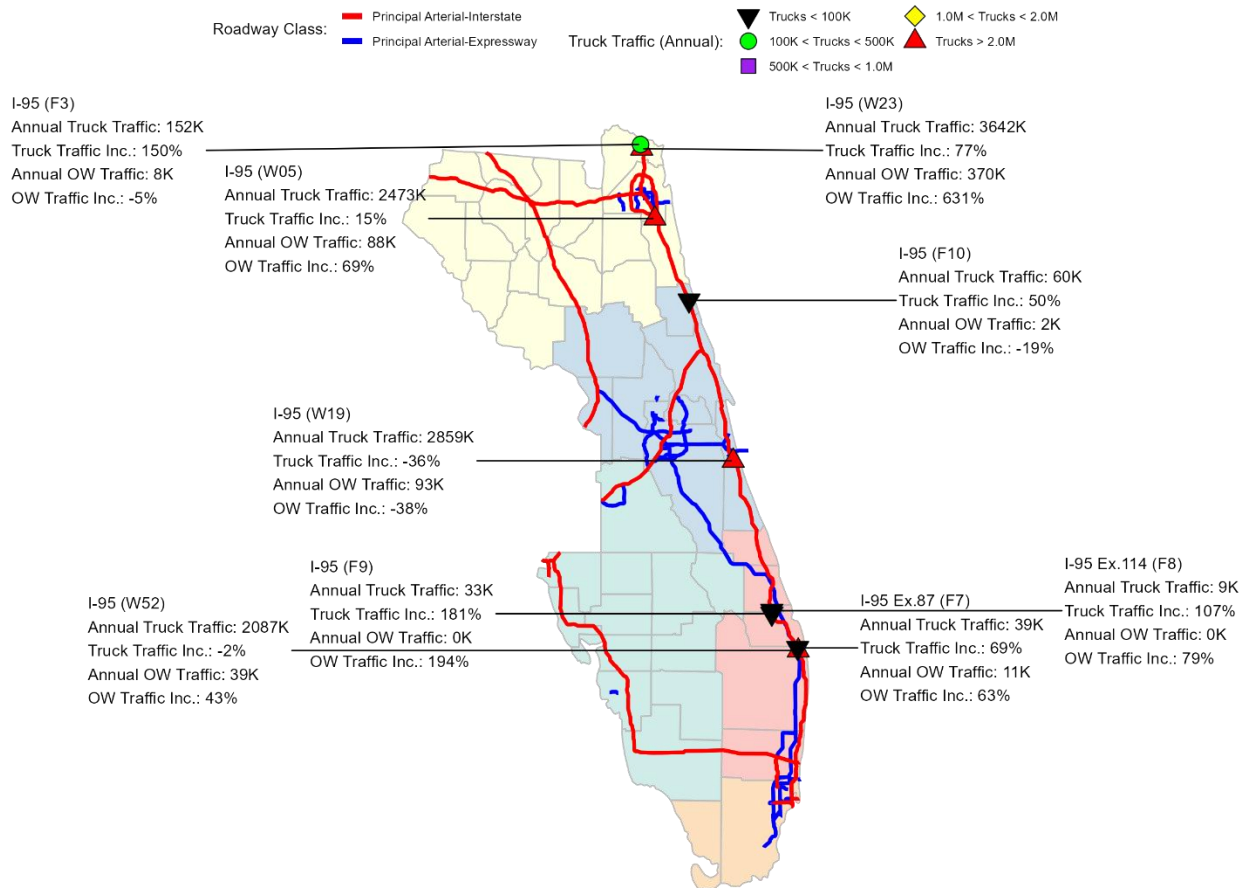
Figure 3-8: Summary of WIM and FOX data along I-95

3.3.2.4 SR-91, Florida Turnpike

Figure 3-9 shows the annotated locations of the WIM sites along SR-91, Florida's Turnpike. The following provides a summary of observations.

1. At the north end of SR-91, W31 in Sumter County carried the most truck traffic compared to the other sites. This significant amount of truck traffic at this site (2.3M per year) explains the significant reduction on I-75 traffic from W04 to W20 (see Figure 3-7).

2. Site W61 in Osceola County carried the least amount of truck traffic (362K per year) among the three WIM sites on SR-91. It is possible that the SR-91 traffic is spread out to I-4 and other local routes while traversing through Orlando.

3. W13 in St. Lucie County indicates 1.5M truck traffic with 145K OW truck traffic. The relatively higher amount of traffic observed from this site may explain the reduced amount of traffic on F9 located on I-95 which runs in parallel to SR-91 in the region (see Figure 3-8).
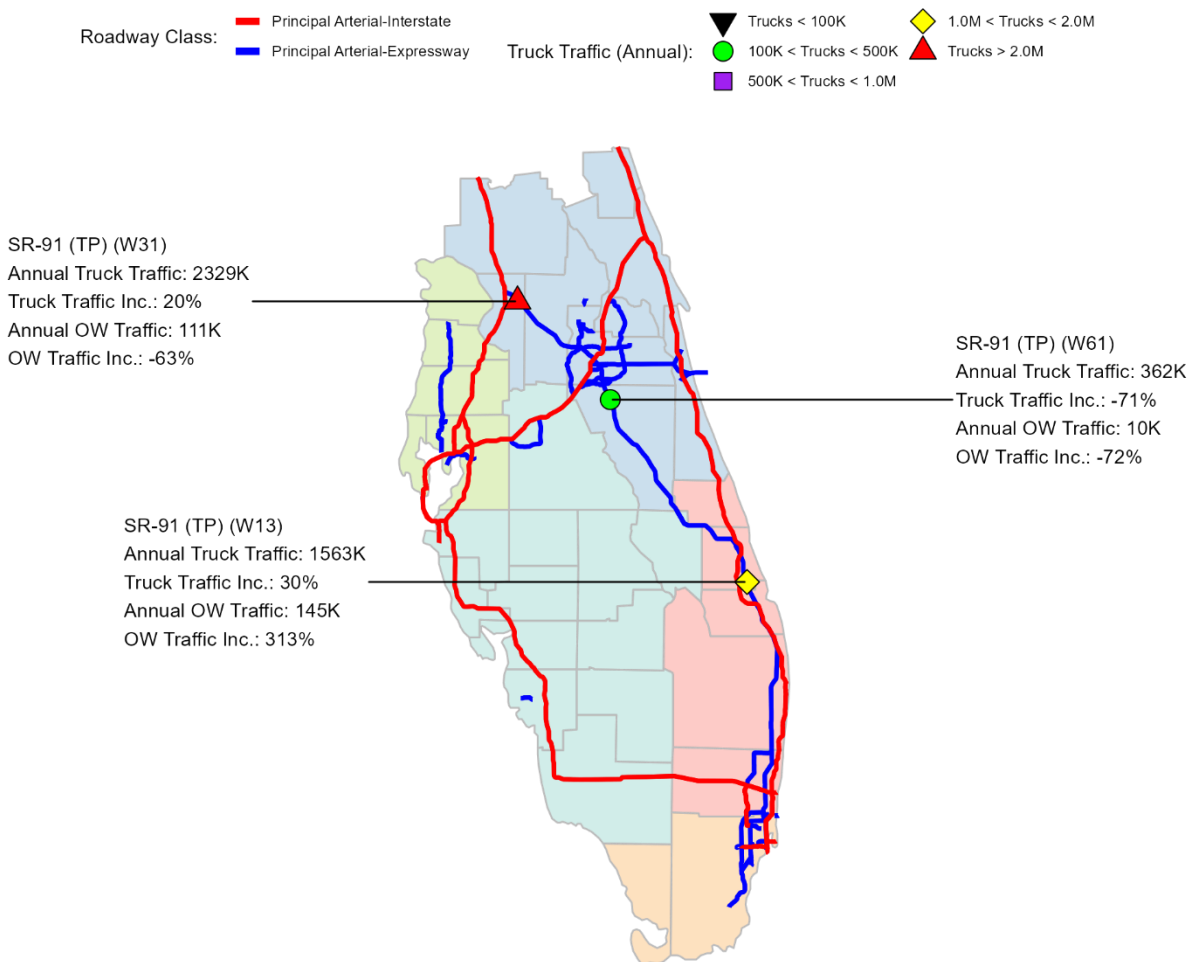
Figure 3-9: Summary of WIM and FOX data along SR-91, FL Turnpike

3.3.2.5   Interstate Route 4

Figure 3-10 shows the annotated locations of the two WIM sites along I-95. The following provides a summary of observations.

1. As a major connector between Tampa and Orlando, I-4 carried a significant amount of truck traffic and OW traffic. W62 in Hillsborough County carried 2.8M trucks per year, while W51 in Polk County carried over 3.0M per year. Although the OW traffic was relatively lower on W62, both W51 and W62 showed a significantly increasing trend in OW truck counts.

2. The I-4 traffic was somewhat reduced to the east of Orlando. W61 in Osceola County measured about half of truck traffic (1.6M per year) compared to W51.
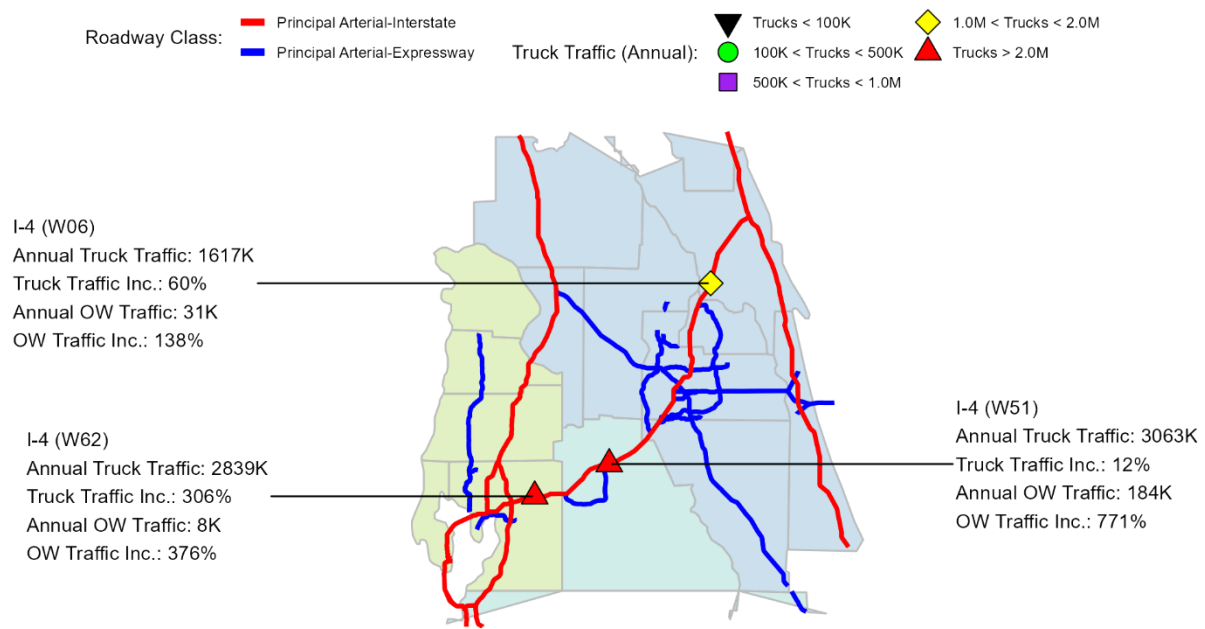
Figure 3-10: Summary of WIM and FOX data along I-4

3.3.2.6   Other Limited Access Routes

Figure 3-11 shows the annotated locations of the WIM and FOX sites along I-95. The following provides a summary of observations.

1. Located on a major connector between I-95 and I-10 in Duval County, W14 on northwestern loop of I-295 carried almost 3.5M truck traffic per year of which 91K was OW.

2. W60 located on SR-482 between Orlando and Florida's east coast (Titusville and Cocoa area) carried about 732K truck traffic and 49K OW traffic per year. This roadway also showed a significant increase in both total truck traffic as well as OW traffic (174 percent and 198 percent, respectively).

3. W55 on I-275 near Tampa area also showed a significant amount of truck traffic, i.e., almost 1.0M trucks and 51K OW trucks per year.

4. SR-869 (W33 in Broward County) and SR-821 (W34 in Miami-Dade County), both of which are Florida's Turnpike roadways, carried over 1.7M trucks per year. Although the average truck traffic was higher on W34, W33 had seen more OW traffic (80K per year) with significantly higher growth rate for both total truck traffic and OW traffic.
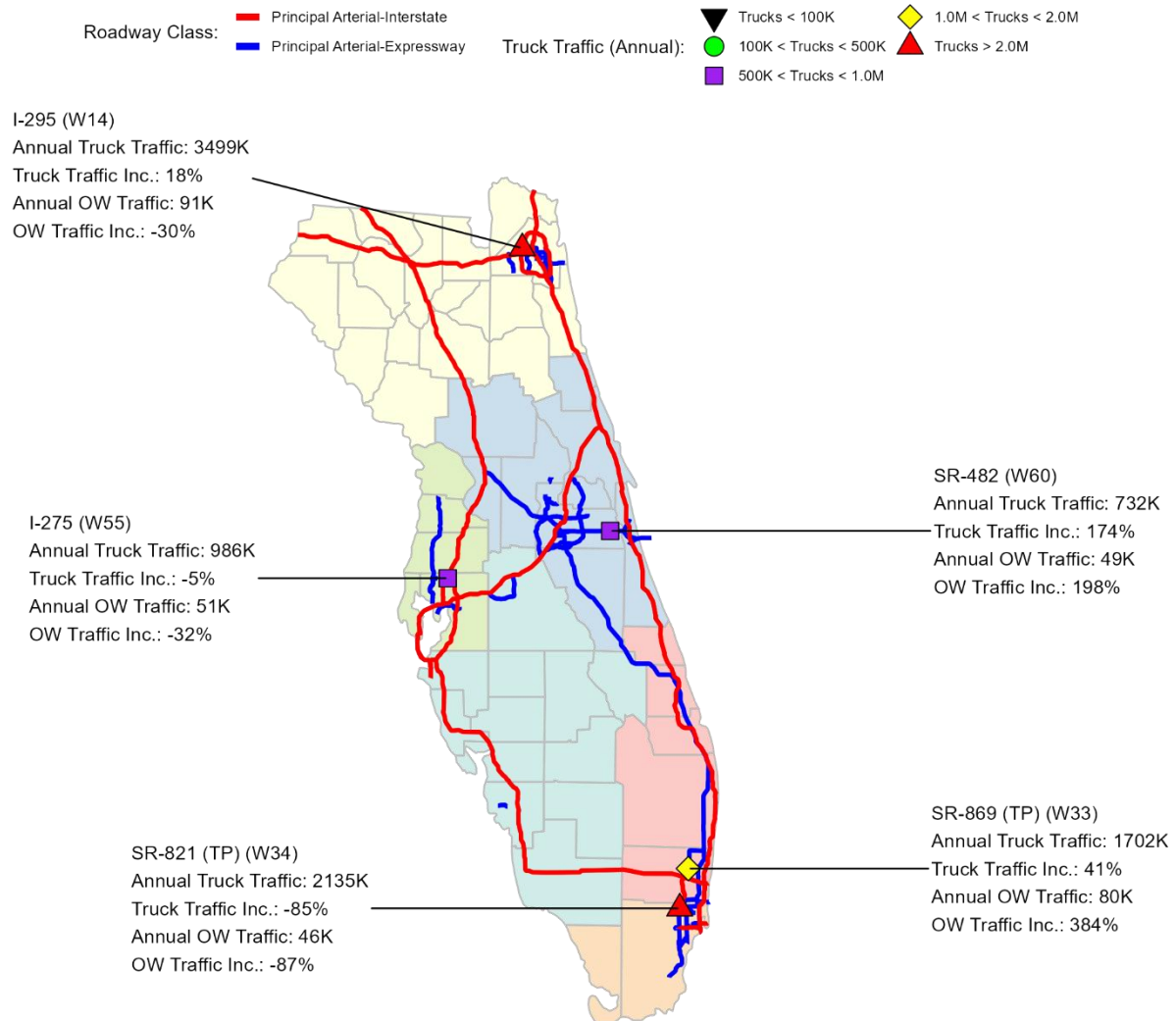
Figure 3-11: Summary of WIM and FOX data (others)

3.3.3   Summary of Traffic Trends on Limited Access Routes

As an overall summary of the traffic trends for limited access routes, Table 3-3 provides a list of roadway routes that were subjected to heavier and more frequent truck traffic between 2015 and 2019. More specifically, these are the segments that carried at least 1.0M total truck traffic per year or have experienced over 100 percent increase in OW truck counts. While the OW traffic

count and the estimates of the percent increase in traffic vary substantially between roadway segments, it is anticipated that these roadways segments will experience higher rate of deterioration if the traffic trends continue to increase both in terms of count and weight. Broadly speaking, these roadway segments are identified as the following.

1. Most of I-10 between Jacksonville and the Florida/Alabama border (Figure 3-6)
2. Most of I-4 between Tampa and Daytona Beach (Figure 3-10).
3. I-75 between Florida/Georgia border and Tampa (Figure 3-7).
4. I-95 between Florida/Georgia border and St. Johns/Flagler County line (Figure 3-8).
5. Florida's Turnpike, SR-869 in Broward County (Figure 3-11).
6. Florida's Turnpike, SR-91 in St. Lucie and Martin Counties (Figure 3-9).

Table 3-3: Limited access routes subjected to heavier traffic

Road way	ID	District	County	County Section	Milepost	Avg. Truck Traffic per Year (× 1000)	OW Truck Traffic per Year (× 1000)	% Inc. in Truck Count	% Inc. in OW Truck Count
I-10	W02	2	Madison	35090000	24.61	2102	64	5%	13%
	W36	2	Columbia	29170000	17.17	1559	100	28%	158%
	W49	3	Escambia	48260000	8.7	1834	87	27%	123%
	W58	3	Walton	60002000	19.186	1204	126	163%	251%
I-4	W51	1	Polk	16320000	17.789	3063	184	12%	771%
	W06	5	Volusia	79110000	4.678	1617	31	60%	138%
	W62	7	Hillsborough	10190000	23.689	2839	8	306%	376%
I-75	W56	2	Hamilton	32100000	19.696	3678	228	69%	115%
	W53	7	Hillsborough	10075000	19.073	1845	120	182%	117%
I-95	W05	2	Duval	72280000	2.77	2473	88	15%	69%
	W23	2	Nassau	74160000	5.571	3642	370	77%	631%
SR-869 (TP)	W33	4	Broward	86472000	4.258	1702	80	41%	384%
SR-91 (TP)	W13	4	St. Lucie	94470000	2.933	1563	145	30%	313%

3.4 Non-Limited Access Roadways

3.4.1 Summary of Overall Trends for Non-Limited Access Roadways

The overall summary of the WIM and FOX data from the non-limited access roadways are provided in this section.

The total amount of truck traffic measured from non-limited access WIM and FOX sites and their corresponding average GVW are shown in Figure 3-12 and Figure 3-13, respectively. Clearly and as expected, the number of total truck traffic observed from these sites are far less then those of

the limited-access roadways. The observations made from these figures are similar to those previously made for the limited access roadways.

1. Vehicle Class 9 (i.e., 5-axle, tractor-trailers) comprises the predominant trucks, followed by Vehicle Classes 5 and 8. The average GVW of these vehicles remained relatively consistent over the years (e.g., the average GVW of Class 9 vehicles varied from 50.0 kip to 53.4 kip within the 5 year period, which is in the same range as those observed for limited access roadways).

2. Based on the average GVW, the heaviest trucks are also found within Vehicle Classes 7, 10, 11, 12, and 13, although they these classes only occupy approximately 8.0 percent of the entire truck volume. Excluding the possible outlier (GVW of Class 13 in 2017), the average GVW of these vehicles was between 40 kip and 75 kip.

Figure 3-14 shows the total amount of OW traffic while Figure 3-15 shows the relative proportions of the OW vehicle weights. The following provides a summary of observations.

1. The number of OW vehicles have increased significantly from 2015 to 2019, regardless of the vehicle class.

2. Vehicle Class 9 has the most number of overweight vehicles followed by Class 10. The OW vehicle counts have continuously (and significantly) increased for these vehicle classes.

3. The greatest proportions of OW vehicles with GVW in excess of 100 kip were found for Vehicle Classes 11 and 13. Also note the significant portion of vehicles with GVW over 200 kip for Class 13 in 2017. While the actual cause of such unusual trend is not known, it is noted that these OW vehicles were mostly found from the following Fox sites: Eastbound US-90 in Madison County (F12), Eastbound CR-475 in Sumter County (F17), and Eastbound CR-484 in Marion County (F18).
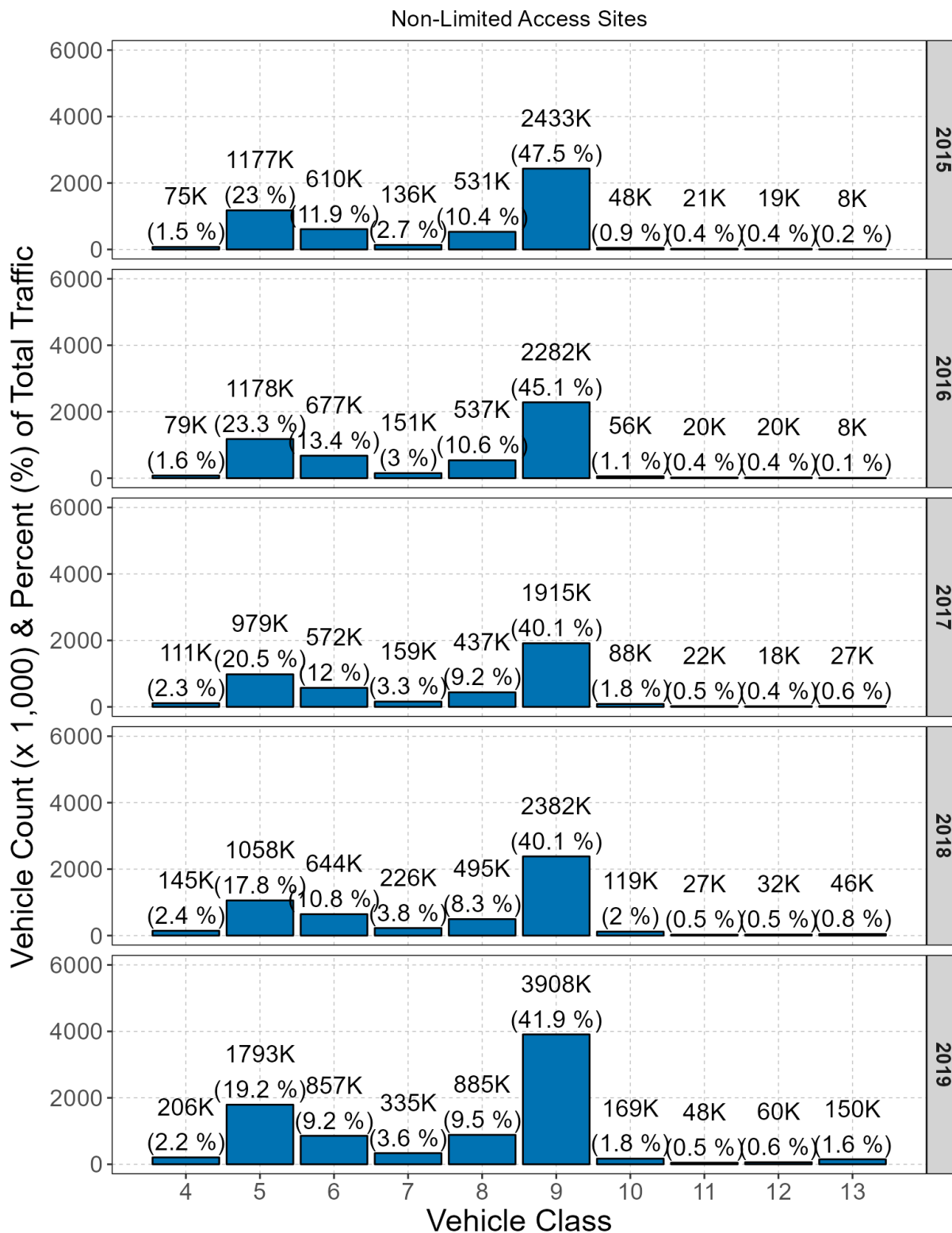
Figure 3-12: Total truck count per vehicle class for non-limited access roadways
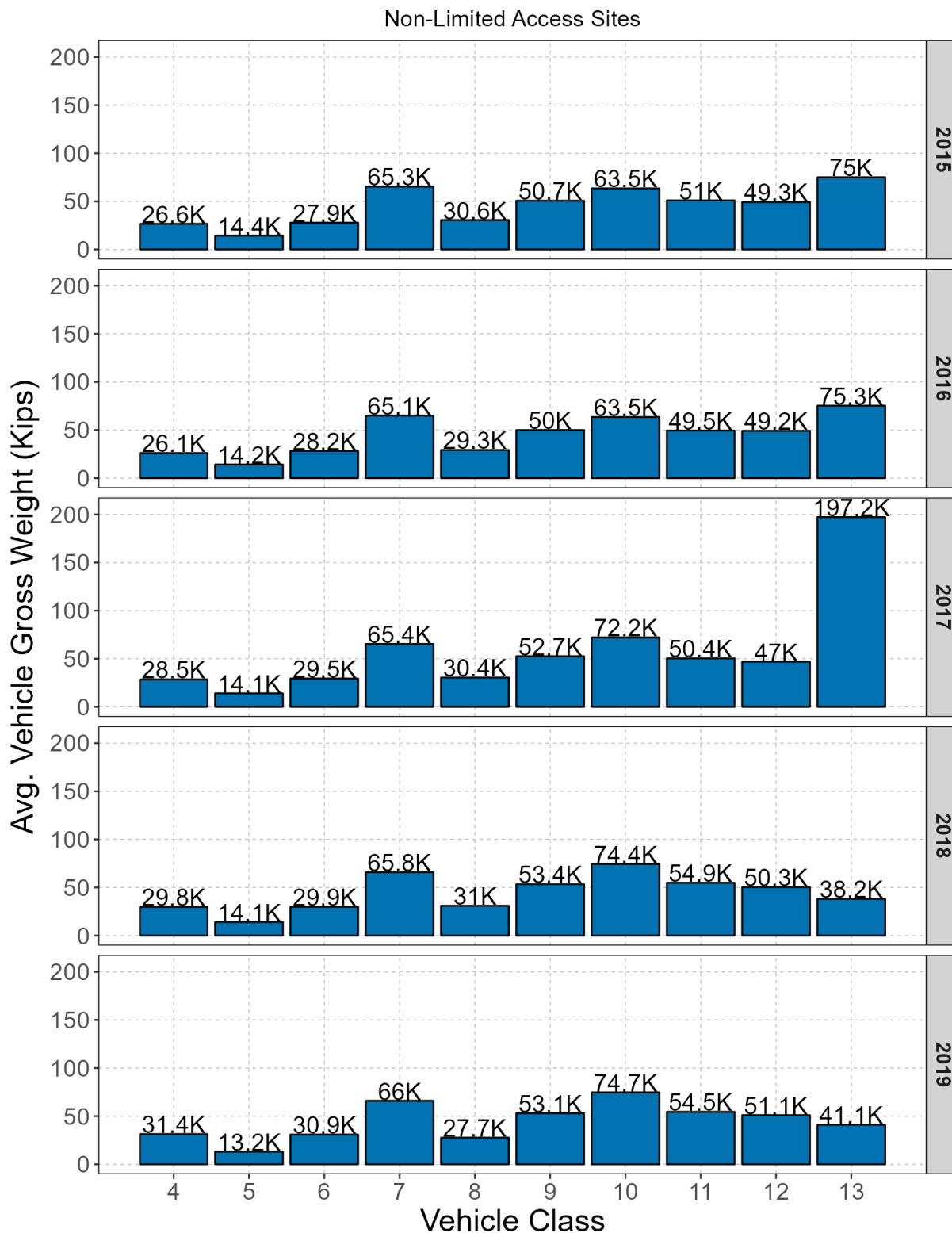
Figure 3-13: Average gross vehicle weight per vehicle class for non-limited access roadways
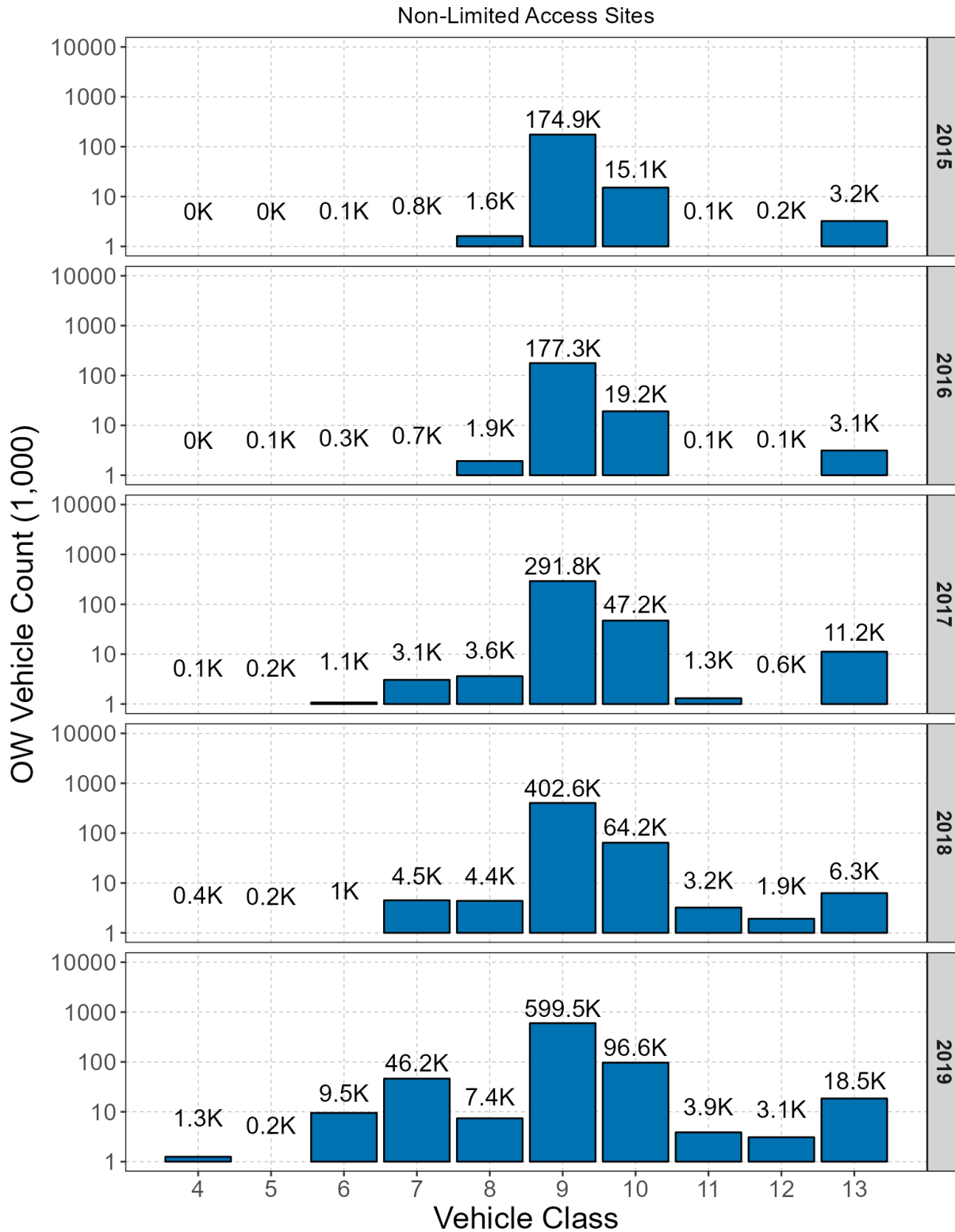
Figure 3-14: Total OW truck count per vehicle class for non-limited access roadways
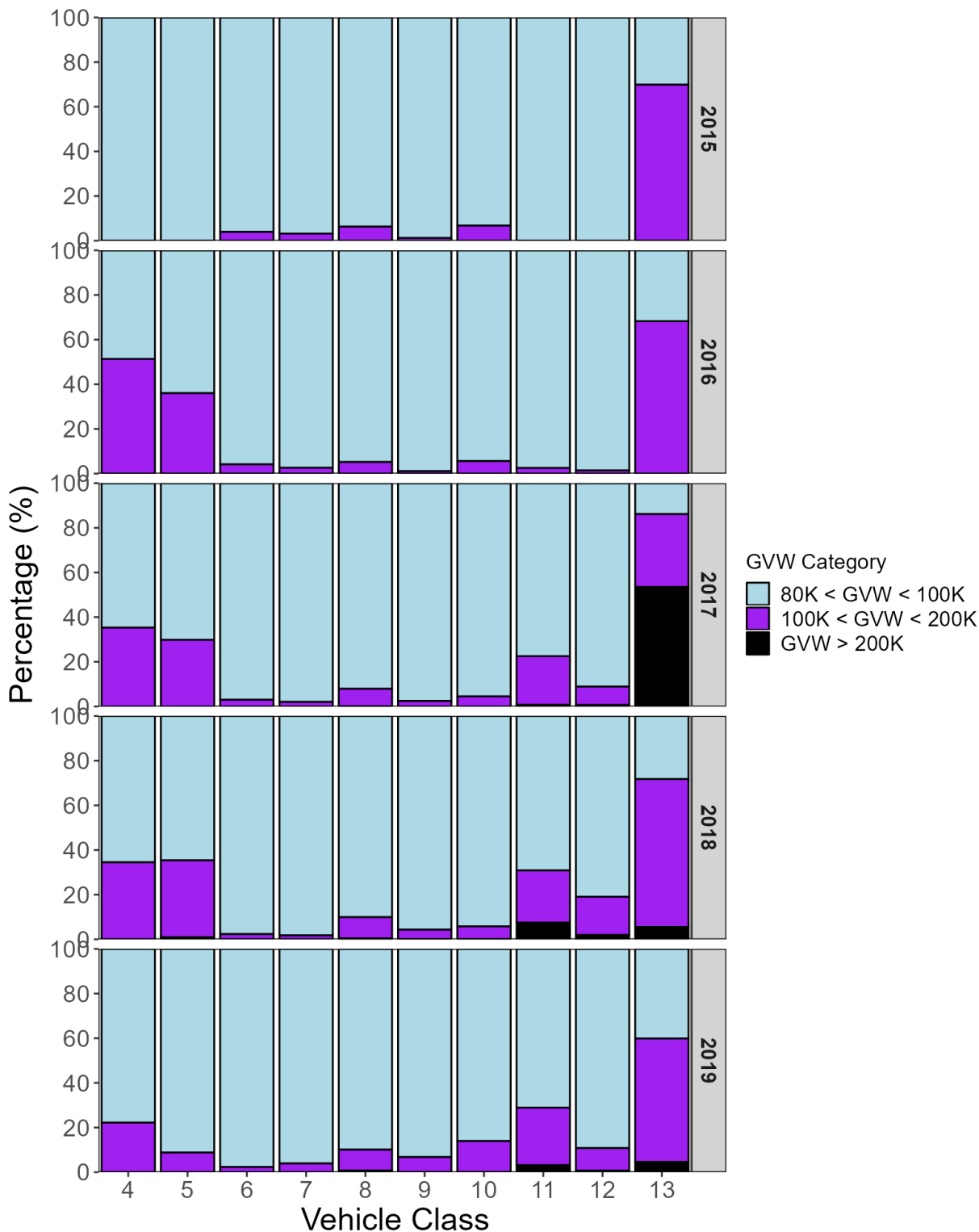
Figure 3-15: Distribution of OW vehicle weights for non-limited access roadways

3.4.2   *Analysis of WIM and FOX Data by Region*

Since the locations of the WIM and FOX sites for non-limited access roadways are more "sporadic" than those on limited access highways, these sites were grouped on a regional basis (rather than a route-by-route basis).

The tabulated results for all WIM and FOX sites on non-limited access roadways are provided in Appendix B.

3.4.2.1   <u>Northern Florida</u>

Figure 3-16 shows the annotated locations of the non-limited access WIM and FOX sites in Northern Florida. The following provides a summary of observations.

1. With the exception of F12 (US-90 in Madison County) and F16 (CR-12B in Gadsden County), all WIM and FOX sites showed significant increase in OW truck counts ranging between 27 percent from W57 (SR-77 in Jackson County) and 730 percent from W16 (US-29 in Escambia County).

2. Higher truck traffic was observed in the following roadways.
   a. US-301 (W63 in Bradford County) between Jacksonville and Gainesville, which carried 1.0M trucks per year.
   b. US-231 (W07 in Bay County) between Panama City and I-10 carried 331K trucks per year.
   c. US-29 (W16 in Escambia County) between Florida/Alabama border and I-10, which carried 301K trucks per year.
   d. US-19 (W09 in Levy County) between Perry and Otter Creek carried 233K trucks per year.
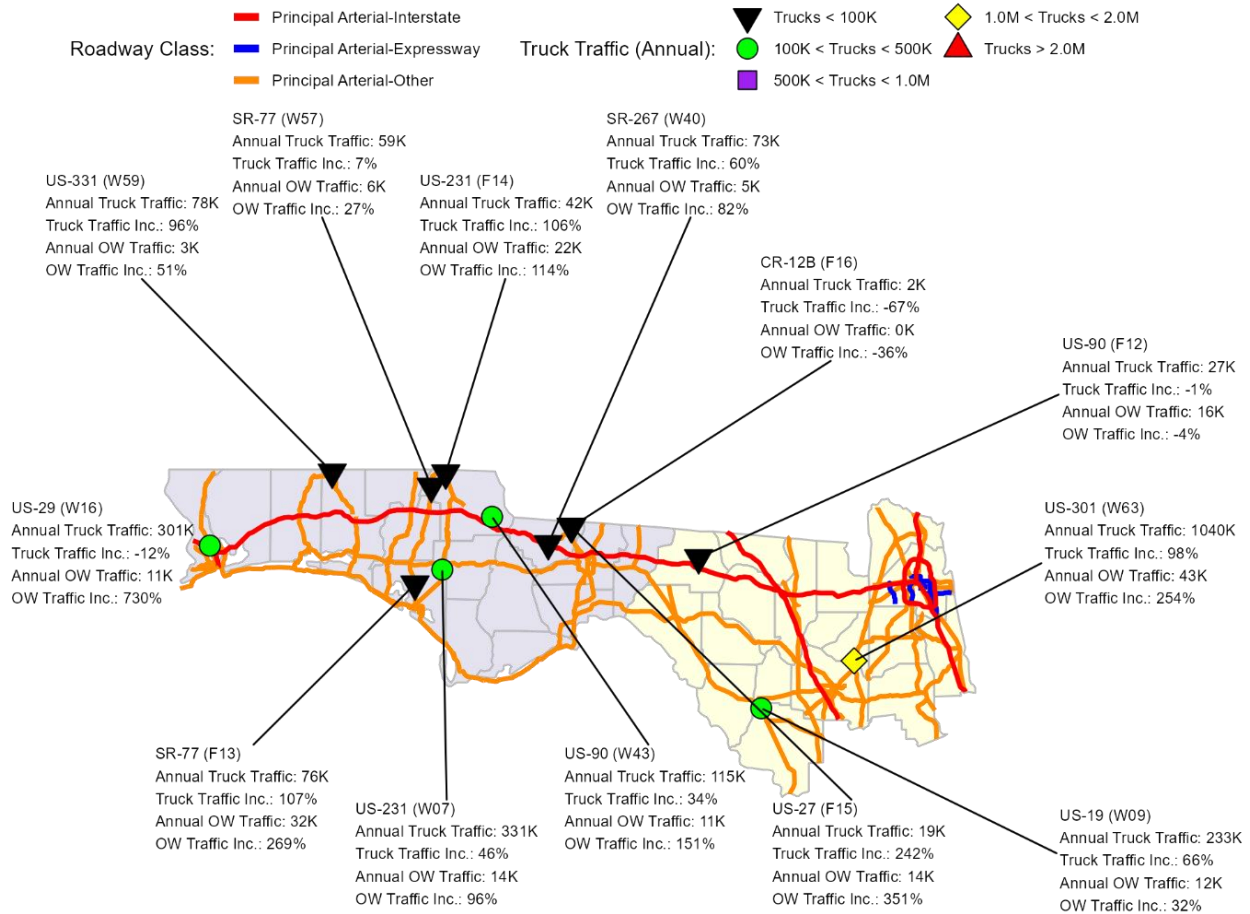
Figure 3-16: Summary of WIM and FOX data on non-limited roadways in Northern Florida

3.4.2.2   Central Florida

Figure 3-17 shows the annotated locations of the non-limited access WIM and FOX sites in Central Florida. The following provides a summary of observations.

1. Although the amount of trucks varied quite substantially (between 6K and 860K), all WIM and FOX sites in Central Florida has experienced increasing truck traffic over the years.
   a. The highest truck traffic growth in excess of 300 percent was seen from F20 (NB US-1) and F21 (SB US-1) in Flagler County, which may explain the reduced amount of truck traffic on I-95 in the same region.

2. Higher truck traffic was observed in the following roadways.
   e. US-27 in Lake Wales (W48 in Polk County) carried 860K trucks per year.
   f. US-92/SR-546 in Lake Land (W27 in Polk County) 303K trucks per year.
   g. US-92/SR-600 (W25 in Volusia County) between Daytona Beach and DeLand carried 211K trucks per year.
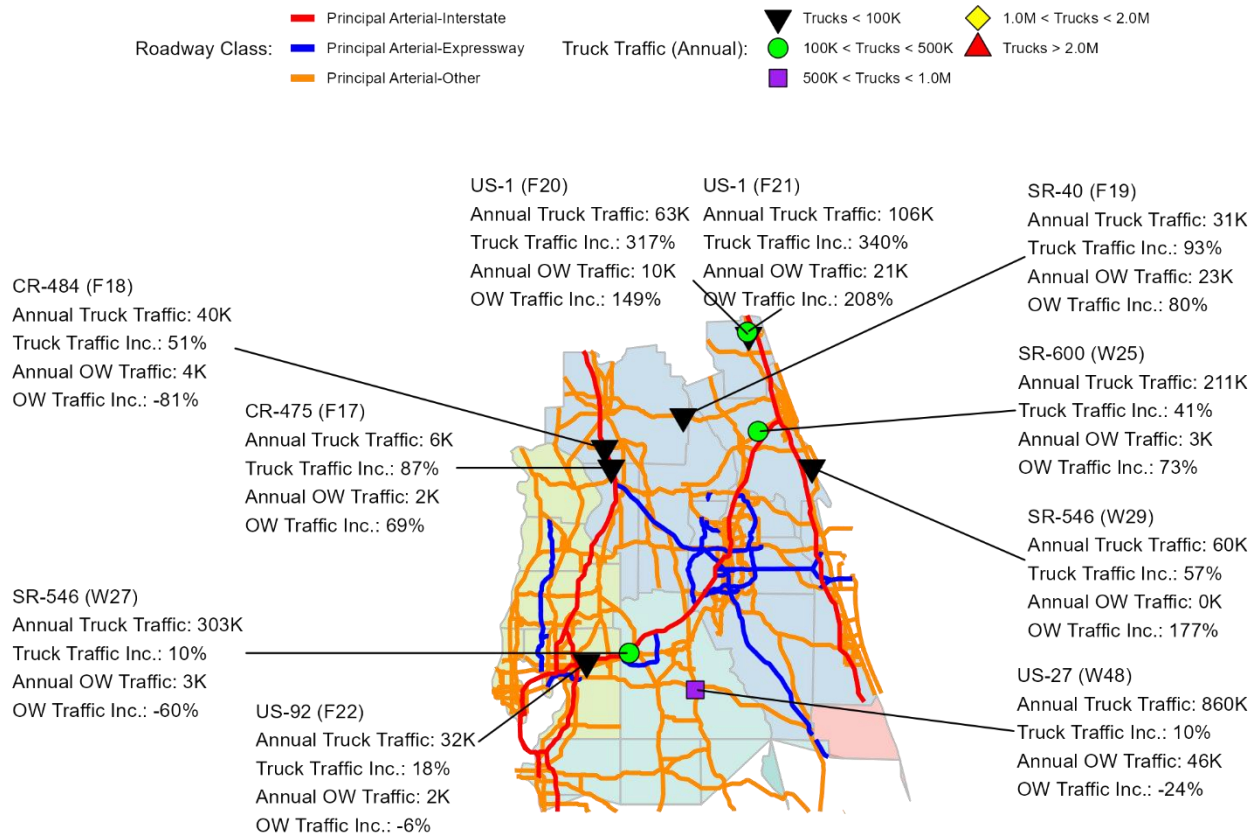
Figure 3-17: Summary of WIM and FOX data on non-limited roadways in Central Florida

3.4.2.3   Southern Florida

Figure 3-18 shows the annotated locations of the non-limited access WIM and FOX sites in Southern Florida. The following provides a summary of observations.

1. All three sites in Southern Florida were located on US-27 in Hendry and Miami-Dade Counties, and carried relatively higher amount of truck traffic (over 680K per year). All US-27 sites showed increasing trends for both the total truck count and the OW truck count.

2. US-27 in Miami-Dade County carried over 1.5M truck traffic and 42K OW trucks per year with increasing trends.
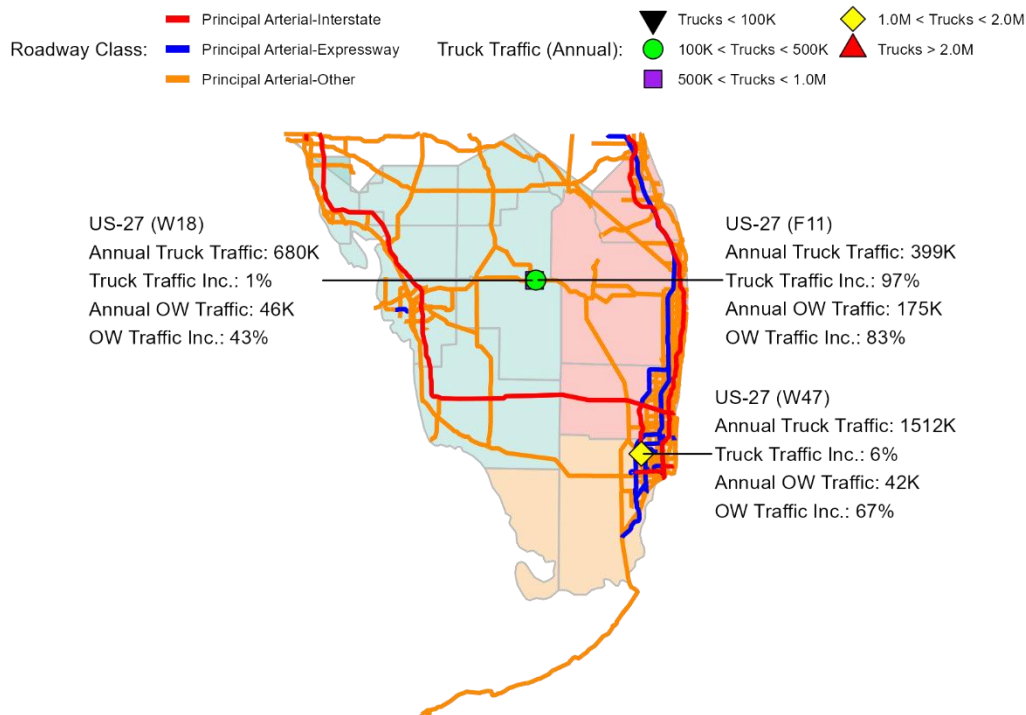
Figure 3-18: Summary of WIM and FOX data on non-limited roadways in Southern Florida

3.4.3 Summary of Traffic Trends on Non-Limited Access Routes

Table 3-4 provides a short list of WIM and FOX sites on non-limited access roadways that carried at least 100K total truck traffic per year.

Note that although the total truck traffic count may not be as significant as those of the limited access roadways, these sites are showing a significantly growing trend in both the total traffic count and the OW traffic count. More specifically, the number of OW traffic on these roadways has grown between 32 percent to 730 percent within the studied time frame (mostly between 2015 and 2019).

Of significance to the current study is that these roadways may not have been designed and constructed for such an increasing amount of OW trucks, and may undergo a higher rate of deterioration.

The roadway segments with the highest growth rate for OW trucks are identified as the following.

1. US-29 in Escambia County (W16) between Florida/Alabama border and I-10 with 730 percent growth (Figure 3-16)
2. US-301 between Jacksonville and Gainesville (W63) with 254 percent growth (Figure 3-16).
3. US-90 in Jackson County (W43) with 151 percent growth (Figure 3-16).
4. US-231 between Panama City and I-10 (W07) with 96 percent growth (Figure 3-16).
5. US-1 in Flagler County (F21) with 208 percent growth (Figure 3-17).

6. YS-27 in Miami-Dade County (W47) with 67 percent growth (Figure 3-18).

Table 3-4: Limited access routes subjected to heavier traffic

Roadway	ID	District	County	County Section	Milepost	Avg. Truck Traffic per Year (× 1000)	OW Truck Traffic per Year (× 1000)	% Inc. in Truck Count	% Inc. in OW Truck Count
US-27 / SR-80	W18	1	Hendry	7030000	10.618	680	46	1%	43%
US-19 / SR-500	W09	2	Levy	34010000	3.184	233	12	66%	32%
US-301	W63	2	Bradford	28010000	0.06	1040	43	98%	254%
US-231 / SR-75	W07	3	Bay	46040000	22.531	331	14	46%	96%
US-29 / SR-95	W16	3	Escambia	48040000	9.399	301	11	-12%	730%
US-90 / SR-10	W43	3	Jackson	53020000	12.386	115	11	34%	151%
SR-600	W25	5	Volusia	79060000	6.903	211	3	41%	73%
US-1	F21	5	Flagler	73010000	18.2	106	21	340%	208%
US-27 / SR-25	W47	6	Miami-Dade	87090000	8.1	1512	42	6%	67%

4   LONG TERM WEIGH-IN-MOTION DATA ANALYSIS

In the previous chapter, five years of WIM data were analyzed to identify the variations in traffic pattern. In this chapter, a longer period of WIM data was analyzed and the impact of the overweight traffic loads on the pavement design, particularly in the thickness of the surface layer, was evaluated. FDOT provided the research team with the weigh-in-motion (WIM) data from 2009 to 2022. Due to formatting issues, WIM data from 2009 and 2010 were excluded from further analysis. The headers for WIM data were obtained from the supplementary WIM dictionary data provided by FDOT. According to the WIM data dictionary, there should be 55 column headers. For all the available years of WIM data except 2009 and 2010, there were 55 columns that matched the order of the information provided in the WIM data dictionary. WIM data from 2009 and 2010 had 53 columns. Thus, these two years of data were excluded from the analysis. In total, around 595 million data points were processed and analyzed over the period between 2011-2022.

In this chapter, each year of WIM data for a particular class was divided into two categories before analysis, i.e., legal weight (LW) and overweight (OW). Based on the axle spacing and number of axles, the maximum allowable weight or legal weight in Florida can be determined from Table 4-1.

Table 4-1: Maximum weight allowed in Florida

Distance between any group of 2 or more consecutive axles (ft)	Maximum weight allowed on 2 Axles (lbs)	Maximum weight allowed on 3 Axles (lbs)	Maximum weight allowed on 4 Axles (lbs)	Maximum weight allowed on 5 Axles (lbs)	Maximum weight allowed on 6 Axles (lbs)	Maximum weight allowed on 7 Axles (lbs)
4	44,000					
5	44,000					
6	44,000					
7	44,000					
8	44,000	44,000				
9	44,000	44,000				
10	44,000	44,000				
11	44,000	44,500				
12	44,000	45,000	50,000			
13	44,000	46,000	50,500			
14	44,000	46,500	51,500			
15	44,000	47,500	52,000			
16	44,000	48,000	52,500	58,000		
17	44,000	49,000	53,500	58,500		
18	44,000	49,500	54,000	59,500		
19	44,000	50,500	54,500	60,000		
20	44,000	51,000	55,500	60,500	66,000	
21	44,000	52,000	56,000	61,000	66,500	
22	44,000	52,500	56,500	62,000	67,000	
23	44,000	53,500	57,500	62,500	68,000	
24	44,000	54,500	58,000	63,000	68,500	74,000
25	44,000	55,000	58,500	63,500	69,000	74,500
26	44,000	55,500	59,500	64,500	69,500	75,000
27	44,000	56,500	60,000	65,000	70,000	76,000
28	44,000	57,000	60,500	65,500	71,000	76,500
29	44,000	58,000	61,500	66,000	71,500	77,000
30	44,000	58,500	62,000	67,000	72,000	77,500
31	44,000	59,500	62,500	67,500	72,500	78,000
32	44,000	60,000	63,500	68,000	73,000	78,500
33	44,000	61,000	64,000	68,500	74,000	79,500
34	44,000	61,500	64,500	69,500	74,500	80,000
35	44,000	62,500	65,500	70,000	75,000	
36	44,000	63,000	68,000	70,500	75,500	
37	44,000	64,000	68,000	71,000	76,000	
38	44,000	64,500	68,000	72,000	77,000	
39	44,000	65,500	68,000	72,500	77,500	
40	44,000	66,000	68,500	73,000	78,000	
41	44,000		69,500	73,500	78,500	
42	44,000		70,000	74,500	79,000	
43	44,000		70,500	75,000	80,000	
44	44,000		71,500	75,500		
45	44,000		72,000	76,000		
46	44,000		72,500	77,000		
47	44,000		73,500	77,500		
48	44,000		74,000	78,000		
49	44,000		74,500	78,500		
50	44,000		75,500	79,500		
51	44,000		76,000	80,000		

After a vehicle was categorized based on its weight limit, information about the axle type, such as single, tandem, or tridem, for that vehicle was determined. Scheme "F" (i.e., the vehicle class defined by the Federal Highway Administration), vehicle type, and axle spacing were used to determine the axle type. The relation between scheme "F" class and vehicle type, which FDOT uses, is shown in Table 4-2. It is essential to mention that one of the columns that were missing in the 2009 and 2010 WIM data was the vehicle type.

Table 4-2: Relation between Scheme F class and vehicle type

Scheme "F" (Class)	Vehicle Type	Number of axles
1	1	2
2	3	3
2	2	2
2	4	4
3	7	4
3	6	3
3	8	5
3	5	2
4	10	2
4	11	3
5	20	2
5	21	3
5	22	4
5	23	5
6	24	3
7	28	4
8	30	3
8	34	4
8	38	4
9	40	5
9	44	5
10	50	6
10	54	7
11	60	5
12	70	6
13	80	7
13	84	8
13	88	8
13	90	9

4.1 Equivalent Axle Load Factor (EALF)

The Equivalent Axle Load Factor (EALF) is a relative measure to determine the damage in the pavement due to the passing of an axle compared to the damage caused to the pavement due to the passing of a standard axle. The standard axle is the 18-kip (80-kN) single axle load. For the

empirical pavement design methodologies (including FDOT's flexible pavement design method), a pavement is typically designed based on the total number of standard axles passing during the design period, which is known as Equivalent Single Axle Load (ESAL). ESAL is calculated using Eq. (4)

$$ESAL = \sum_{i=1}^{m} F_i n_i \qquad (4)$$

where, m = number of axle load groups,
F_i = EALF for the *i*-th axle load group,
n_i = number of passes for the *i*-th load group during the design period

EALF is a function of several factors, such as pavement type (flexible or rigid), thickness or structural capacity, and terminal conditions. EALF can be determined using both the theoretical and widely used empirical regression-based equations developed based on the results from the AASHO Road Test. The theoretical determination of EALF is based on the critical stresses, strains, and failure criteria of the pavement.

In this study, EALF will be determined based on the regression equations. EALF for flexible pavements can be determined using Eq. (5) to (8)

$$log\left(\frac{W_{tx}}{W_{18}}\right)_f = 4.79\,log(18+1) - 4.79\,log(L_x + L_2) + 4.33\,log(L_2) + \frac{G_t}{\beta_x} - \frac{G_t}{\beta_{18}} \qquad (5)$$

$$G_t = log\left(\frac{4.2 - p_t}{4.2 - 1.5}\right) \qquad (6)$$

$$\beta_x = 0.4 + \frac{0.081(L_x + L_2)^{3.23}}{(SN+1)^{5.19}L_2^{3.23}} \qquad (7)$$

$$EALF_{flexible} = \frac{W_{18}}{W_{tx}} \qquad (8)$$

where, W_{tx} = number of *x* load applications at the end of time *t*
W_{18} = number of 18-kip (80-kN) load applications at the end of time *t*
L_x = load in one single, tandem or tridem axle (in kip)
L_2 = axle code: 1- single axle, 2-tandem axles, 3-tridem axles
SN = structural number of the pavement
P_t = terminal condition of pavement, considered to be 2.5
$\beta_{18} = \beta_x$ when L_x is equal to 18 and L_2 equals to 1

Similar to flexible pavement, the following Eq. (9) to (11) can be used to determine EALF for rigid pavements.

$$log\left(\frac{W_{tx}}{W_{18}}\right)_r = 4.62\,log(18+1) - 4.62\,log(L_x + L_2) + 3.28\,log(L_2) + \frac{G_t}{\beta_x} - \frac{G_t}{\beta_{18}} \qquad (9)$$

$$G_t = log\left(\frac{4.5 - p_t}{4.5 - 1.5}\right) \qquad (10)$$

$$\beta_x = 1.00 + \frac{3.63(L_x + L_2)^{5.20}}{(D+1)^{8.46} L_2^{3.52}} \qquad (11)$$

where, *D* is the slab thickness in inches.

4.2 Thickness Determination

Once the EALF was determined from the analysis of WIM data for the vehicles in a particular year, they were grouped according to the WIM stations and subsequently by the functional class of pavements. The following functional classes of pavements were considered in this study:

- Limited Rural
- Limited Urban
- Non-Limited Rural
- Non-Limited Urban

Freeways are considered as pavements with limited access, while arterials and collectors are considered as pavements with non-limited access for this study.

The average EALF for each functional class of pavement was then used to determine the thickness of the Asphalt Concrete (AC) or Portland Cement Concrete (PCC) layer. AASHTO 1993 pavement design method was used to determine the thickness of the flexible and rigid pavement.

4.2.1 Flexible Pavement

According to AASHTO 1993, the Structural Number (SN) of the flexible pavement can be determined using Eq. (12)

$$log\,W_{18} = Z_R S_o + 9.36\,log(SN+1) - 0.2 + \frac{log\left[\frac{\Delta PSI}{(4.2 - 1.5)}\right]}{0.4 + \frac{1094}{(SN+1)^{5.19}}} + 2.32\,log\,M_R - 8.07 \qquad (12)$$

here, M_R = effective roadbed soil resilient modulus, a series of values ranging between 4 to 32 ksi were considered for the analysis for representing Florida conditions

Z_R = normal deviate for a given reliability *R*,
S_0 = standard deviation
ΔPSI = change in serviceability index

FDOT uses the following Eq. (13) to determine the number of 18-kip (80-kN) load application, ESAL, during the design period in the design lane (W_{18}) (FDOT Pavement Design Section, 2023).

$$ESAL = W_{18} = \sum_{y=1}^{y=x} (AADT \times 365 \times T_{24} \times D_F \times L_F \times E_{18}) \qquad (13)$$

where, $AADT$ = Annual average daily traffic,
T_{24} = percentage of heavy truck,
D_F = directional factor, taken as 1.0
L_F = lane factor, a series of values ranging between 0.66 to 0.94 were considered for the analysis.
E_{18} = EALF, determined from WIM data analysis.

The directional distribution factor D_F considers the proportion of traffic travelling in higher volume direction in peak hour. According to FDOT, if one-way traffic is counted then a value of 1.0 is used for D_F. For two-way traffic, 0.5 is used as D_F (FDOT, 2024).

Lane factor (L_F) converts the directional trucks to the design lane trucks. Generally, lane factors are adjusted to the unique features of the roadway known to the designer, such as designated truck lanes. Based on the Annual Average Daily Traffic (AADT) and number of lanes, FDOT adopts the value of L_F from Table 4-3. Table 4-3 shows that based on the AADT, L_F varies from 0.66 to 0.94 for two lanes, and 0.49 to 0.82 for three lanes.

Table 4-3: Lane factors for different types of facilities (FDOT, 2024)

Total AADT	Number of Lanes in One Direction	
	Two Lanes, L_F	Three Lanes, L_F
4,000	0.94	0.82
8,000	0.88	0.76
12,000	0.85	0.72
16,000	0.82	0.7
20,000	0.81	0.68
30,000	0.77	0.65
40,000	0.75	0.63
50,000	0.73	0.61
60,000	0.72	0.59
70,000	0.7	0.58
80,000	0.69	0.57
100,000	0.67	0.55
120,000	0.66	0.53
140,000		0.52
160,000		0.51
200,000		0.49

As no information was available on how the WIM station collected the data, i.e., whether one-way or two-way traffic was counted in two-lane or three-lane roadways, a D_F of 1.0 was assumed. Moreover, information regarding the total AADT was also unavailable. Thus, lane factors were taken to vary between 0.66 and 0.94 as per FDOT, assuming a two-lane roadway in one direction (FDOT, 2024).

FDOT uses the following EALFs based on the functional classes of the pavements, which is shown in Table 4-4.

Table 4-4: EALF for different functional classes of pavements

Functional Class	Flexible		Rigid	
	Rural	Urban	Rural	Urban
Freeways (Limited Access)	1.05	0.9	1.6	1.27
Arterials and Collectors (Non-Limited Access)	0.96	0.89	1.35	1.22

The resultant of the first three quantities on the right side of Eq. (13) are obtained directly from the WIM data analysis. The total number of truck traffic in a particular year can be obtained from the WIM data. This total number of truck traffic is same as the AADT $\times$ 365 $\times T_{24}$, which is the first three quantities of Eq. (13). This is the average of the yearly truck traffic in each functional pavement class. It is worth mentioning that the WIM data only includes FHWA vehicle class from 4 to 13, which is the truck traffic. After that using the EALF from FDOT (Table 4-4) and WIM analysis, two W_{18} can be determined- W_{18}^{FDOT} and W_{18}^{WIM}. Using the two W_{18} in Eq. (12), two SNs can be determined. One is the design SN used by FDOT, and the other is the SN from WIM data analysis.

After the SNs corresponding to FDOT's design EALF values and those from WIM analysis were obtained for each functional class, they were used to find the thickness differences to identify if the FDOT is over or under-designing the functional classes of the pavements based on the available traffic data, as shown in Eq. (14)

$$\Delta t = \frac{SN_{FDOT} - SN_{WIM}}{a} \tag{14}$$

where, t = thickness, and a = structural coefficient of the AC layer, taken as 0.44. The structural coefficient value for AC layer was taken from AASHTO, which is also the same value adopted by FDOT (FDOT, 2024).

4.2.2 Rigid Pavement

Although FDOT uses the Mechanistic-Empirical method for rigid pavement design, this study used the AASHTO 1993 empirical design equation for rigid pavement to determine the slab thickness to demonstrate the effect of EALF. The equation for rigid pavement design is shown in Eq. (15)

$$log\,W_{18} = Z_R S_o + 7.35\,log(D+1) - 0.06 + \frac{log\left[\frac{\Delta PSI}{(4.2-1.5)}\right]}{0.4 + \frac{1.624 \times 10^7}{(D+1)^{8.46}}}$$

$$+ (4.22 - 0.32p_t)\,log\left\{\frac{S_c C_d (D^{0.75} - 1.132)}{215.63J\left[D^{0.75} - \frac{18.42}{\left(E_c/k\right)^{0.25}}\right]}\right\} \tag{15}$$

where, D = slab thickness,
k = modulus of subgrade reaction, a range of values between 40~380 pci were considered to represent Florida conditions
S_c = modulus of rupture taken as 635 psi
J = load transfer coefficient, adopted 3.2
E_c = modulus of concrete, 4.0×10⁶ psi

The values presented above were obtained from the FDOT's rigid pavement design manual to represent the local condition (FDOT, 2022). Similar to the flexible pavement, W_{18} was determined twice. One is from the FDOT-adopted EALF shown in Table 4-4, and the other is from the WIM data analysis. Using the two W_{18} values, two slab thicknesses can be determined from Eq. (15). The difference in the slab thicknesses determined from the FDOT design and actual WIM analysis can be used to identify the over or under design in the rigid pavement, if any. Slab thickness difference (Δt) for rigid pavements is determined using Eq. (16)

$$\Delta t = D^{FDOT} - D^{WIM} \tag{16}$$

Further details on the formulation of Eq. (12) and (15) can be found elsewhere (Huang, 2004).

4.3 EALF by WIM Stations

This section of the report presents EALF determined from the WIM data. The results are grouped by WIM stations situated in various functional classes of pavements. In addition, EALF was also determined by dividing the WIM data into LW and OW vehicles by considering both flexible and rigid pavements.
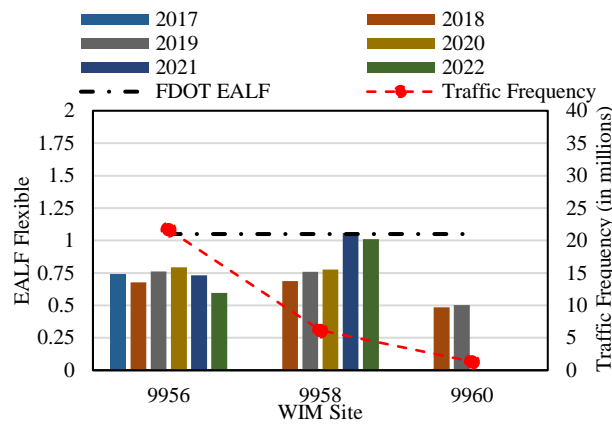
4.3.1 Limited Rural

Figure 4-1 through Figure 4-4 show the yearly average EALF for nine WIM stations, assuming all the stations are located on flexible and rigid pavements, respectively. These graphs have two vertical axes. EALF is shown on the primary vertical axis on the left. The secondary right vertical axes show the total traffic passing through a particular WIM station. The total number of trucks that have passed through the WIM stations in limited rural pavements in the last 12 years is around 183 million. The yearly average LW and OW traffic per WIM sites is around 1.6 and 0.1 million, respectively.

FDOT uses 1.05 as design EALF for limited rural flexible pavements. Figure 4-1 shows that EALF for LW vehicles never exceeded the design value for all the WIM sites and all the years considered, except for WIM station 9958, in Walton County, in 2021, where the EALF was found to be around 1.058. The average EALF for LW vehicles in flexible pavements was around 0.65. From Figure 31, the average EALF for flexible pavements for OW vehicles were 3.26.
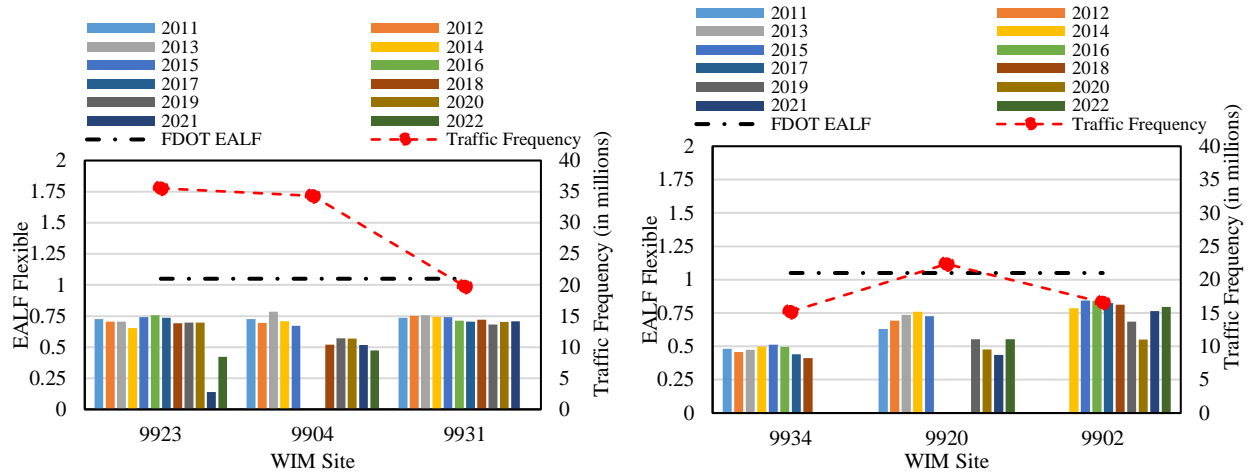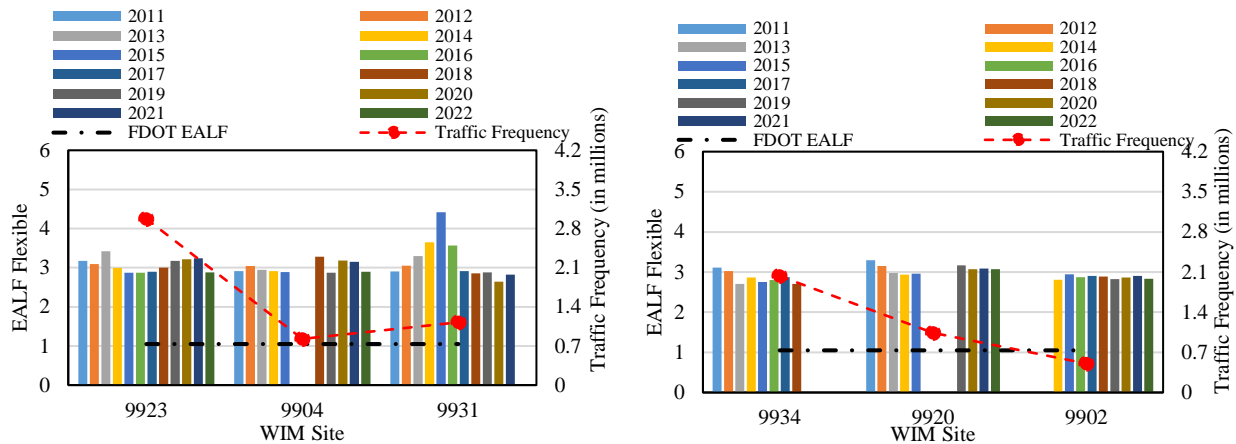

(a) WIM Station 9923, 9904, and 9931

(b) WIM Station 9934, 9920, and 9902

(c) WIM Station 9956, 9958, and 9960

Figure 4-1: EALF of limited rural flexible pavements with legal weights

(a) WIM Station 9923, 9904, and 9931

(b) WIM Station 9934, 9920, and 9902
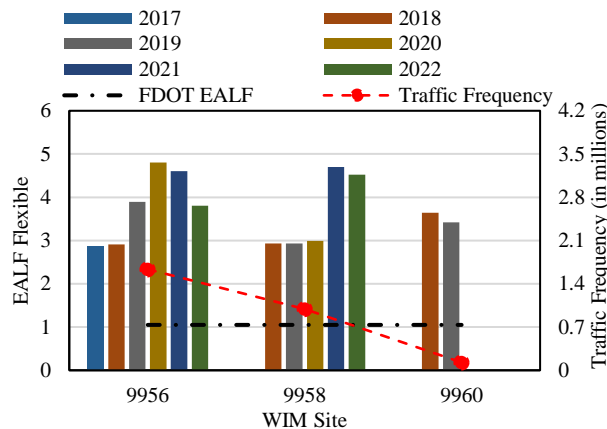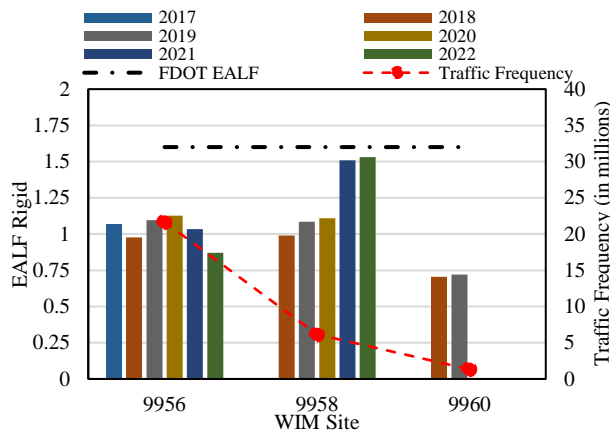
(c) WIM Station 9956, 9958, and 9960

Figure 4-2: EALF of limited rural flexible pavements with over weights

Similar to flexible pavements, Figure 4-3 shows that EALF for limited rural rigid pavements never exceeded the FDOT design value of 1.6. The average EALF for LW vehicles in limited rural rigid pavements was around 0.94. from Figure 4-4, the average EALF for OW vehicles in limited rural rigid pavements was 5.45.
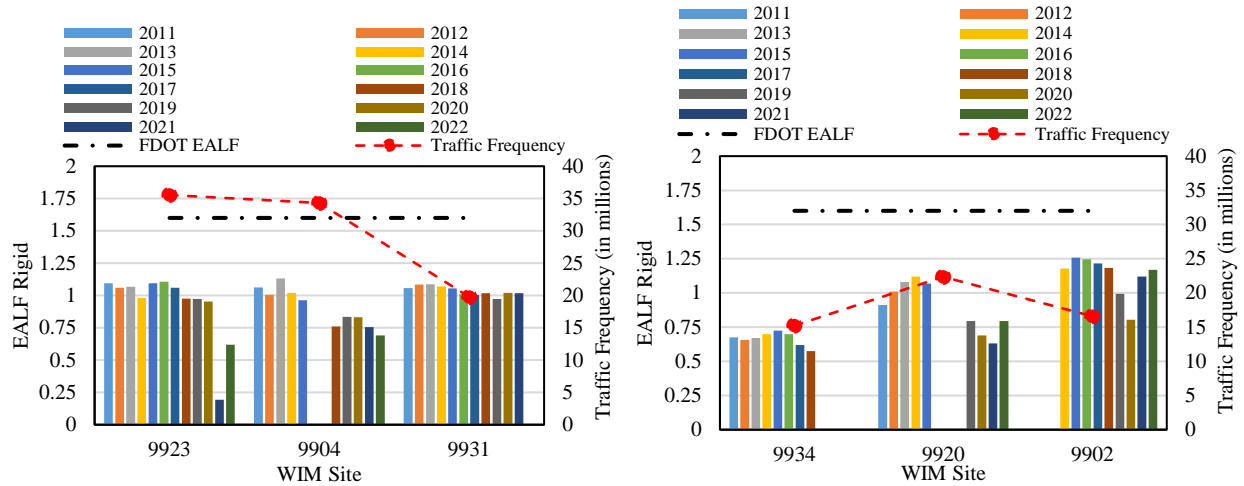
(a) WIM Station 9923, 9904, and 9931

(b) WIM Station 9934, 9920, and 9902

(c) WIM Station 9956, 9958, and 9960

Figure 4-3: EALF of limited rural rigid pavements with legal weights

(a) WIM Station 9923, 9904, and 9931

(b) WIM Station 9934, 9920, and 9902
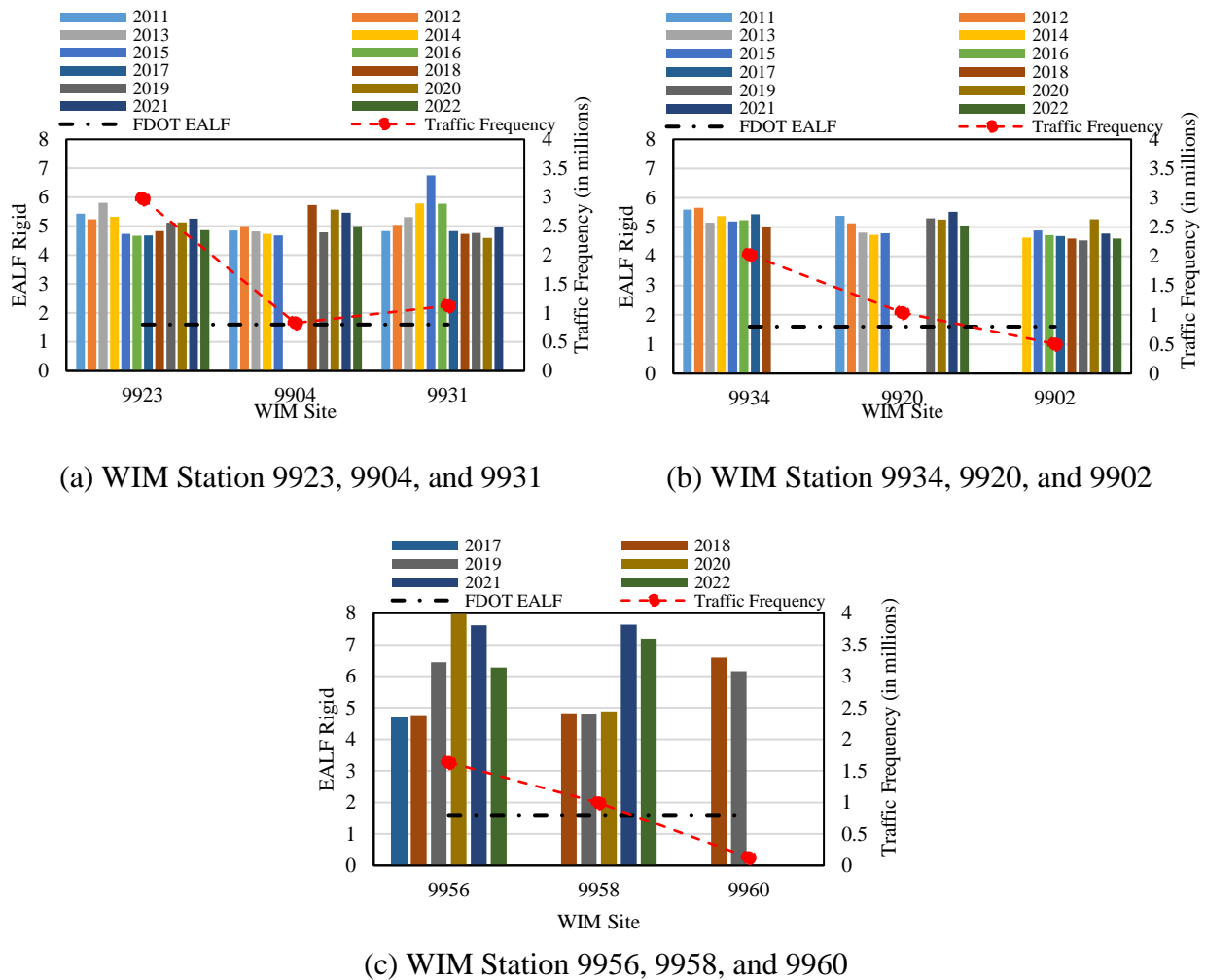

(c) WIM Station 9956, 9958, and 9960

Figure 4-4: EALF of limited rural rigid pavements with over weights

From the above two graphs for flexible and rigid pavements, it can be observed that EALF remains almost the same for all the years considered in a particular limited rural WIM station, except the newer WIM stations, such as 9956 and 9958 in Hamilton and Walton County, respectively. In these newer WIM stations, the EALF was higher in recent years, from 2020 and beyond, particularly for OW vehicles.

4.3.2 Limited Urban

Figure 4-5 through Figure 4-8 show the yearly average EALF for 15 WIM stations located on limited urban pavements. The total number of truck traffic passing through these WIM stations in the last 12 years is around 313 million. The yearly average LW and OW traffic per WIM sites is around 1.64 and 0.1 million, respectively.

FDOT uses 0.9 as design EALF for limited urban flexible pavements. Figure 4-5 shows that EALF for LW vehicles never exceeded the threshold for all the WIM sites and all the years considered, except for WIM station 9933 in Broward County in 2021, where the EALF was found to be 1.33.

The average EALF for LW vehicles on limited flexible urban pavements was around 0.53. Figure 4-6 shows that the average EALF for limited urban flexible pavements for OW vehicles was 4.42.
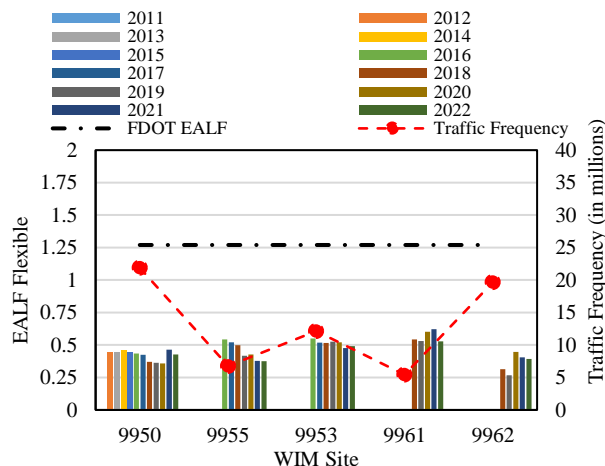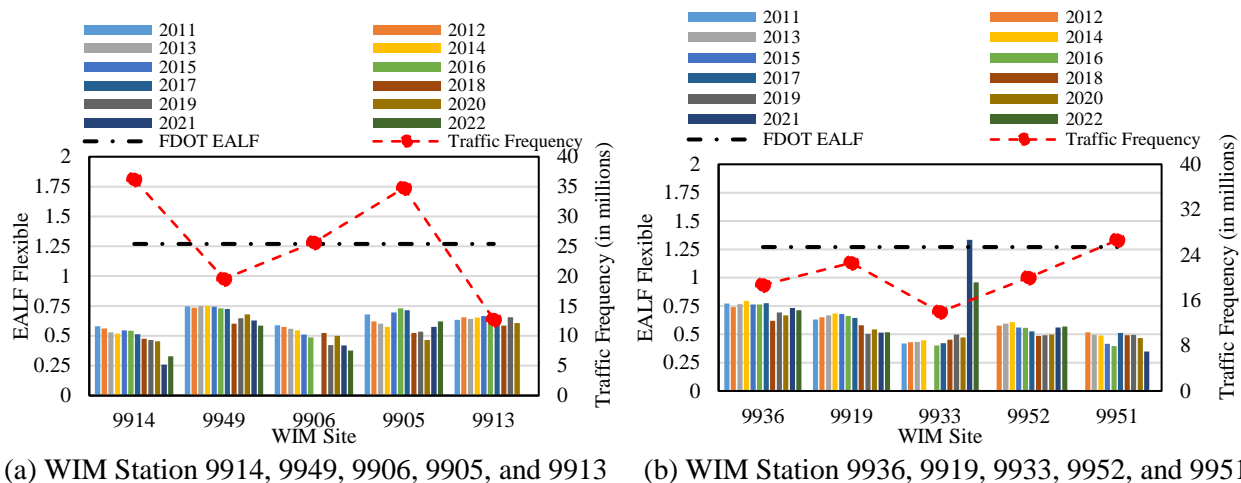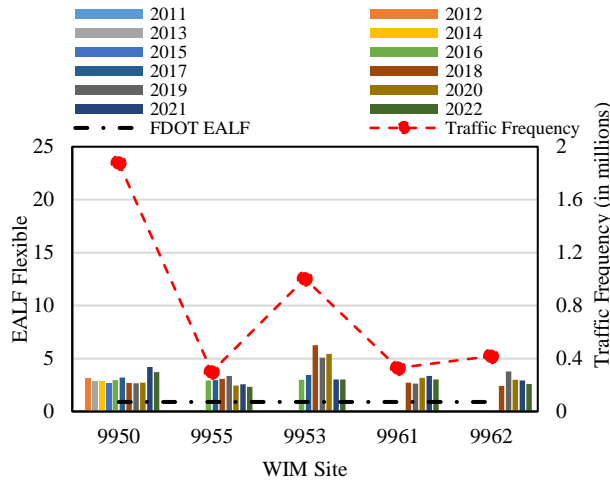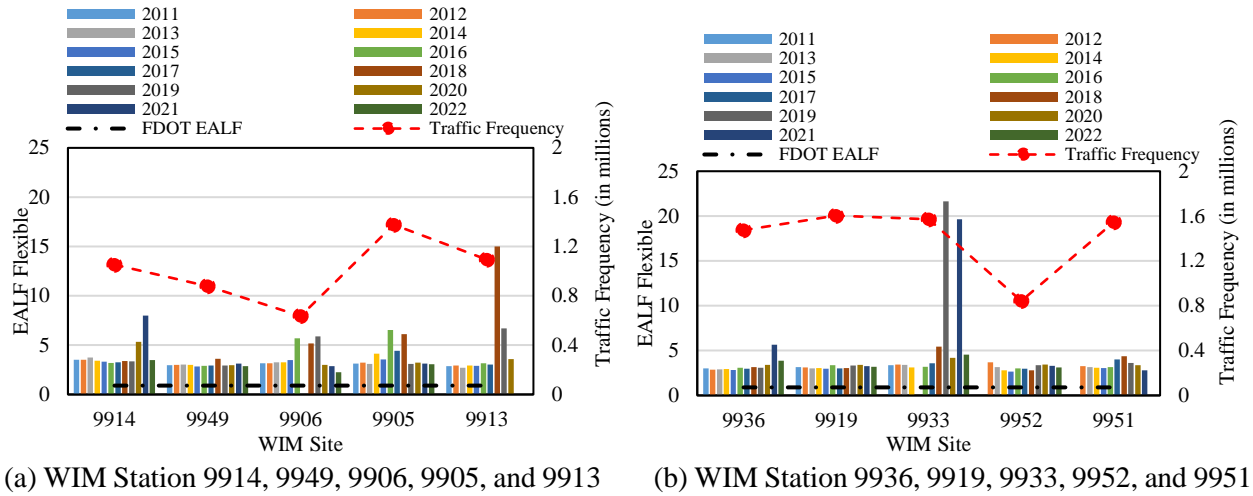

(a) WIM Station 9914, 9949, 9906, 9905, and 9913

(b) WIM Station 9936, 9919, 9933, 9952, and 9951

(c) WIM Station 9950, 9955, 9953, 9961, and 9962

Figure 4-5: EALF of limited urban flexible pavements with legal weights

(a) WIM Station 9914, 9949, 9906, 9905, and 9913

(b) WIM Station 9936, 9919, 9933, 9952, and 9951

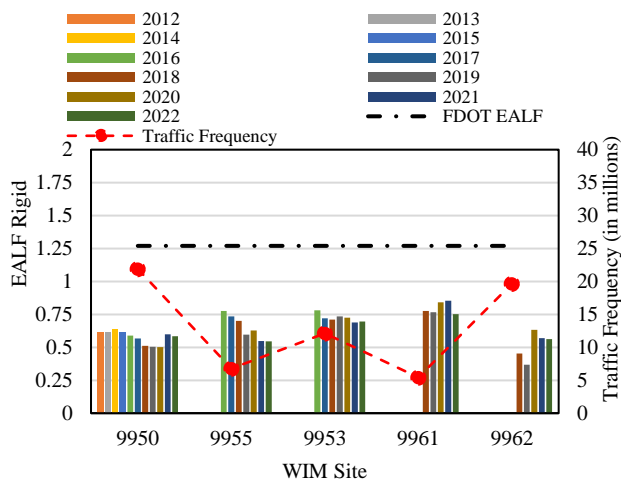(c) WIM Station 9950, 9955, 9953, 9961, and 9962

Figure 4-6: EALF of limited urban flexible pavements with over weights

Figure 4-7 shows that EALF for legal weight vehicles in limited urban rigid pavements never exceeded the FDOT design value of 1.27. The average EALF for LW vehicles on limited urban rigid pavements was around 0.77. According to Figure 37, the average EALF for OW vehicles in limited urban rigid pavements was 7.6.
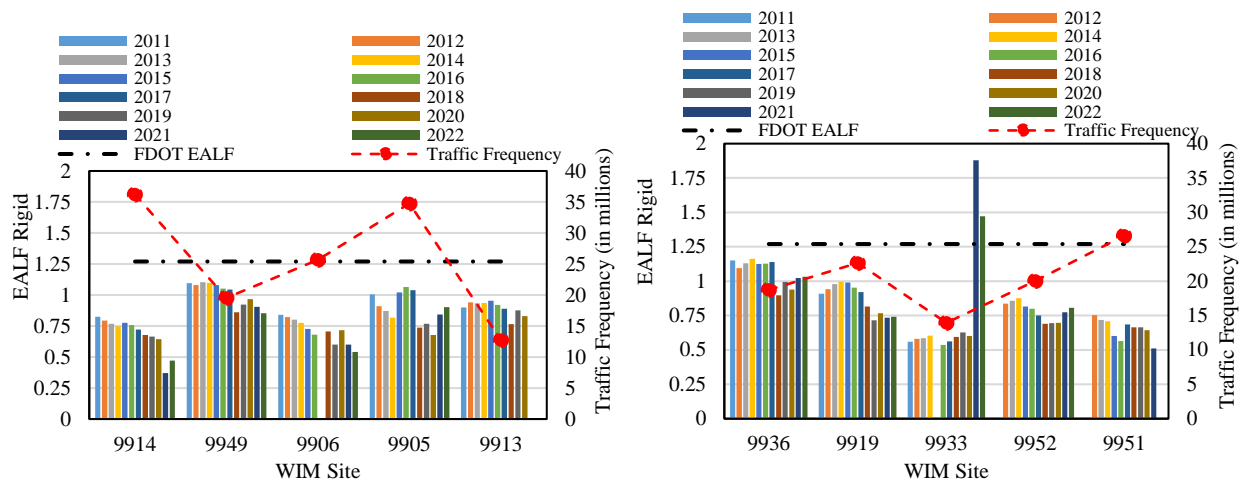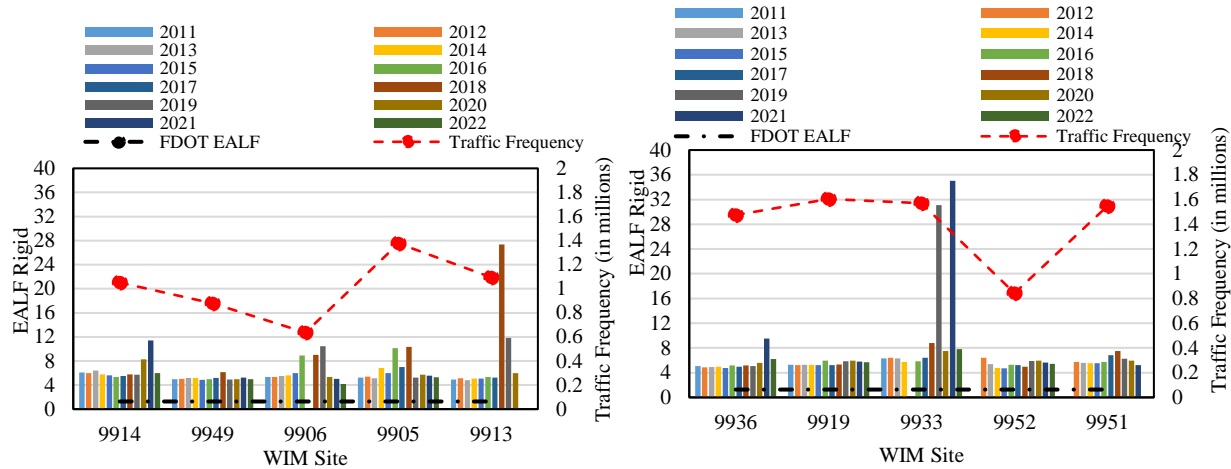
(a) WIM Station 9914, 9949, 9906, 9905, and 9913

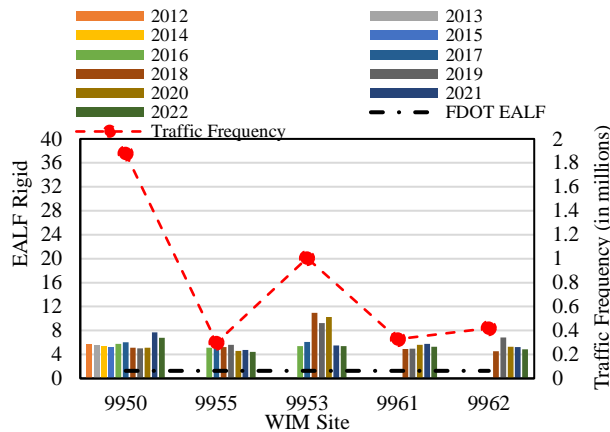(b) WIM Station 9936, 9919, 9933, 9952, and 9951

(c) WIM Station 9950, 9955, 9953, 9961, and 9962

Figure 4-7: EALF of limited urban rigid pavements with legal weights

(a) WIM Station 9914, 9949, 9906, 9905, and 9913

(b) WIM Station 9936, 9919, 9933, 9952, and 9951

(c) WIM Station 9950, 9955, 9953, 9961, and 9962

Figure 4-8: EALF of limited urban rigid pavements with over weights
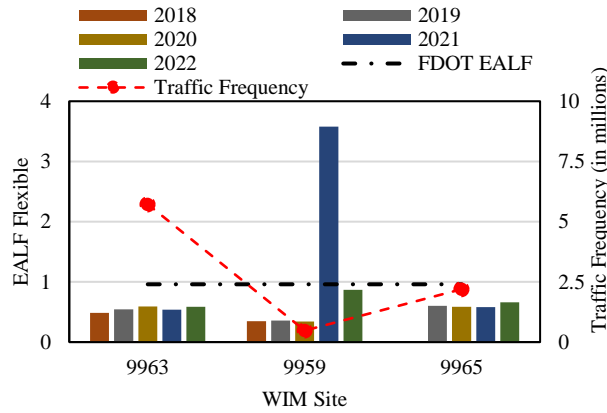
4.3.3 Non-Limited Rural

Figure 4-9 through Figure 4-12 show the yearly average EALF for nine WIM stations located on non-limited rural pavements. The total number of truck traffic passing through these WIM stations in the last 12 years is 29.3 million. The yearly average LW and OW traffic per WIM sites is 0.24 and 0.02 million, respectively.

FDOT uses 0.96 as design EALF for non-limited rural flexible pavements. Figure 4-9 shows that apart from WIM station 9959, all the WIM sites and all the years considered had EALF below the design value. The average EALF for LW vehicles in non-limited rural flexible pavements was around 0.54. The average EALF for non-limited rural flexible pavements for OW vehicles was 5.27.
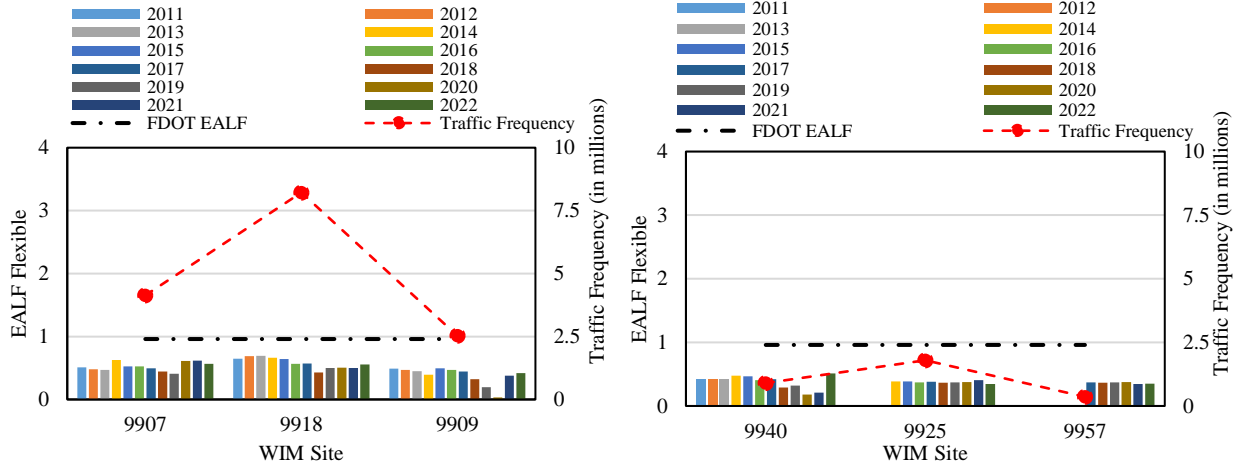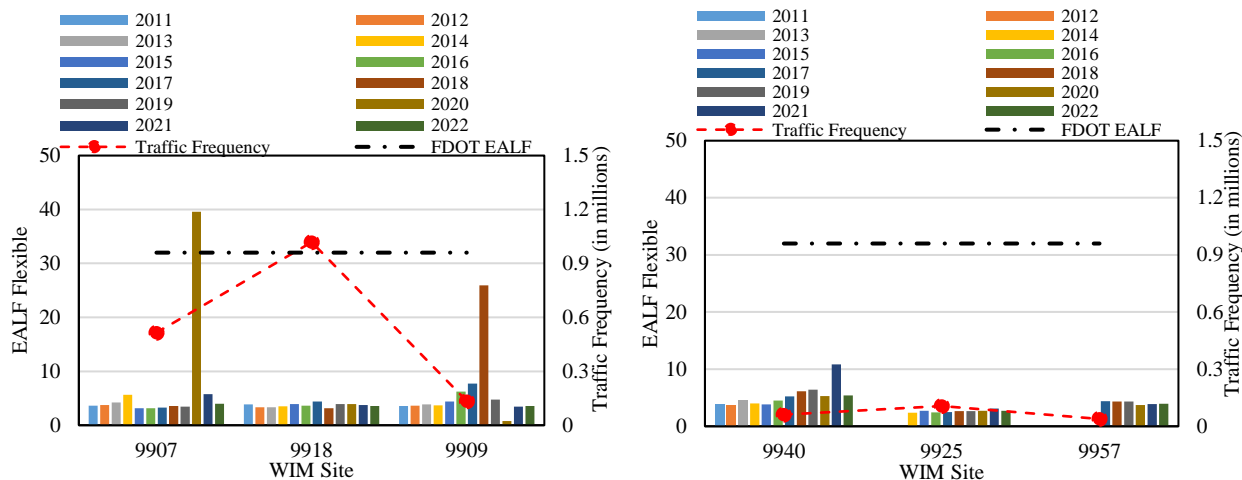
(a) WIM Station 9907, 9918, and 9909
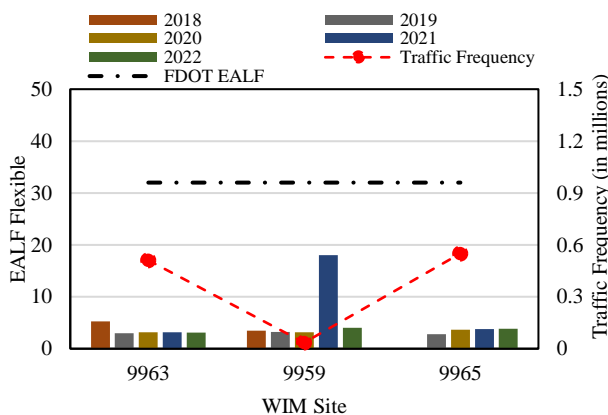
(b) WIM Station 9940, 9925, and 9957

(c) WIM Station 9963, 9959, and 9965

Figure 4-9: EALF of non-limited rural flexible pavements with legal weights

(a) WIM Station 9907, 9918, and 9909

(b) WIM Station 9940, 9925, and 9957

(c) WIM Station 9963, 9959, and 9965

Figure 4-10: EALF of non-limited rural flexible pavements with over weights

Similar to flexible pavements, Figure 4-11 and Figure 4-12 shows the EALF variations for the legal and over-weight vehicles in non-limited rural rigid pavements. FDOT adopted design EALF for non-limited rural rigid pavements is 1.35. The average EALF for LW and OW vehicles in non-limited rural rigid pavements were around 0.77 and 9.54, respectively.

(a) WIM Station 9907, 9918, and 9909

(b) WIM Station 9940, 9925, and 9957

(c) WIM Station 9963, 9959, and 9965

Figure 4-11: EALF of non-limited rural rigid pavements with legal weights

(a) WIM Station 9907, 9918, and 9909

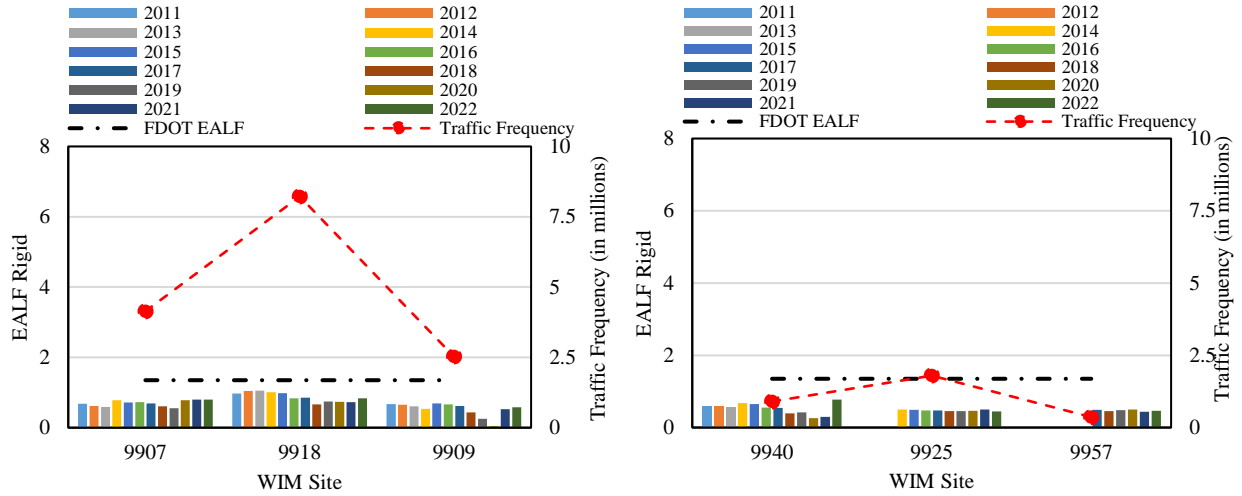(b) WIM Station 9940, 9925, and 9957
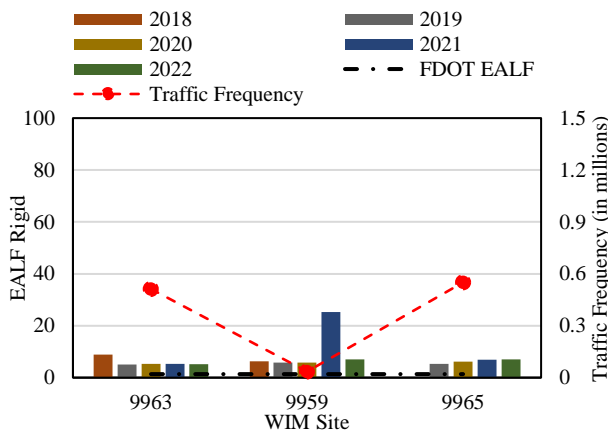
(c) WIM Station 9963, 9959, and 9965

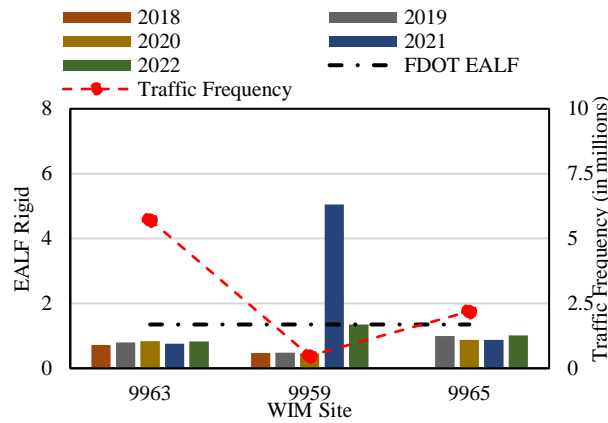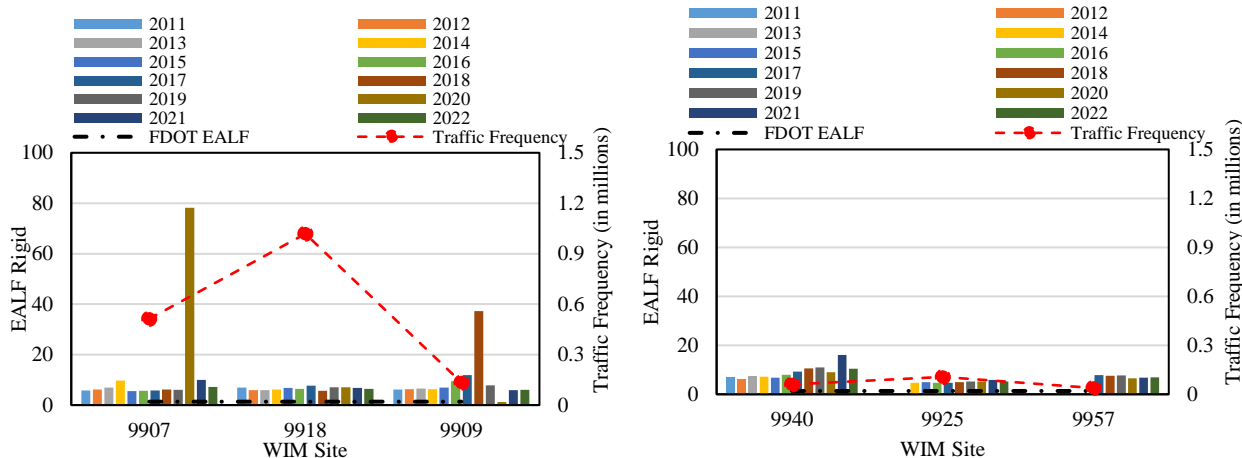**Figure 4-12: EALF of non-limited rural rigid pavements with over weights**

Figure 4-9(c) and Figure 4-11(c) show that highest EALF for LW vehicles occur at WIM station 9959 in Walton County in 2021. Figure 4-13 shows the breakdown of EALF and traffic frequency for LW vehicles at WIM station 9959 by FHWA vehicle class for the year 2021. It also shows that an EALF of around 50 or more was observed for vehicle classes 4, 7, 10, and 13, with vehicle class 13 being the highest. These vehicle classes made up around 3% of the total traffic passed through WIM site 9959 in 2021.
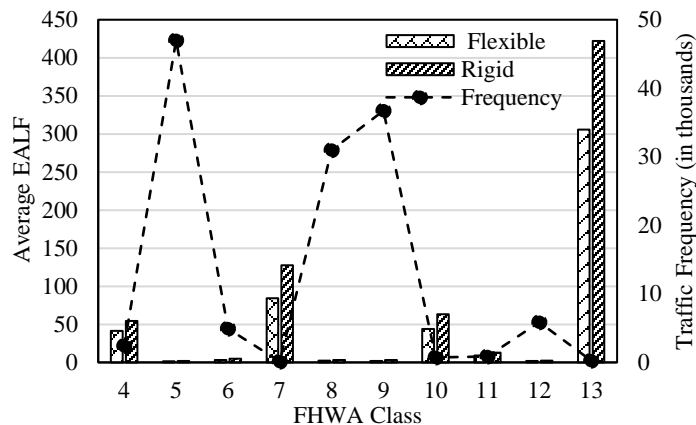
Figure 4-13: EALF for legal weight vehicles at WIM station 9959 in 2021

Figure 4-10(a) and Figure 4-12(a) show that the highest EALF for OW vehicles occurred at WIM station 9907 in Bay County in 2020. For all the truck classes, the average EALF was close to 50 or more for both the flexible and rigid pavement. The highest number of OW vehicles was observed for Class 9 vehicles, around 67,000, with flexible and rigid EALF of around 40 and 80. With a total truck count of around 336, Class 13 vehicles were the heaviest, with EALFs for flexible and rigid pavements around 100 and 220.
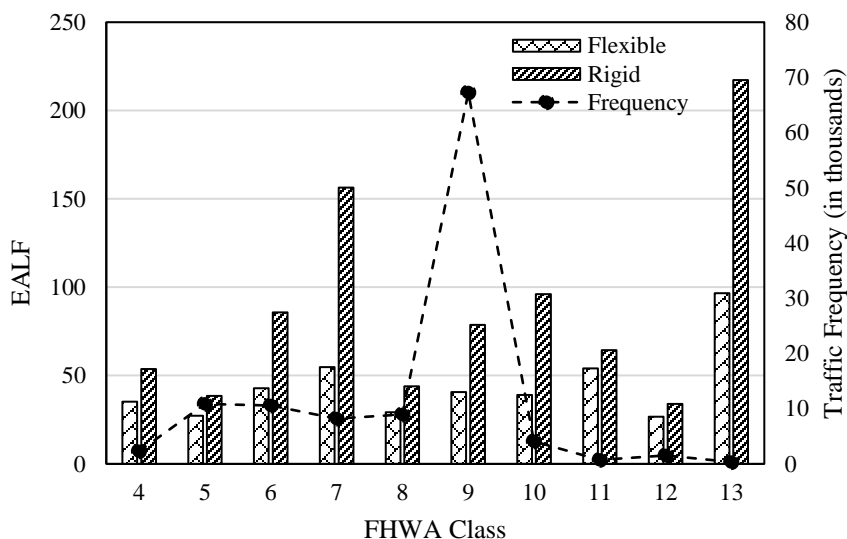
Figure 4-14: EALF for over-weight vehicles at WIM station 9907 in 2021

4.3.4   Non-Limited Urban

Figure 4-15 through and Figure 4-18 show the yearly average EALF of seven WIM stations on non-limited urban pavements. The total truck traffic passing through these WIM stations is around 39 million. The yearly average LW and OW traffic per WIM sites is 0.42 and 0.05 million, respectively.

The average EALF for LW vehicles in non-limited urban flexible pavements was around 0.604. The average EALF for non-limited urban flexible pavements for OW vehicles was 15.2. FDOT uses 0.89 as the design EALF for non-limited flexible pavements. Except for WIM station 9947 in Miami-Dade County in 2021 and 2022, all the stations had lower EALF than the design value for the LW vehicles, as shown in Figure 4-15. Figure 4-16 shows that for OW vehicles, the highest EALF of around 160 was observed for WIM station 9916 in Escambia County in 2021.

(a) WIM station 9948 and 9927

(b) WIM station 9947 and 9943

(c) WIM station 9916, 9929 and 9964
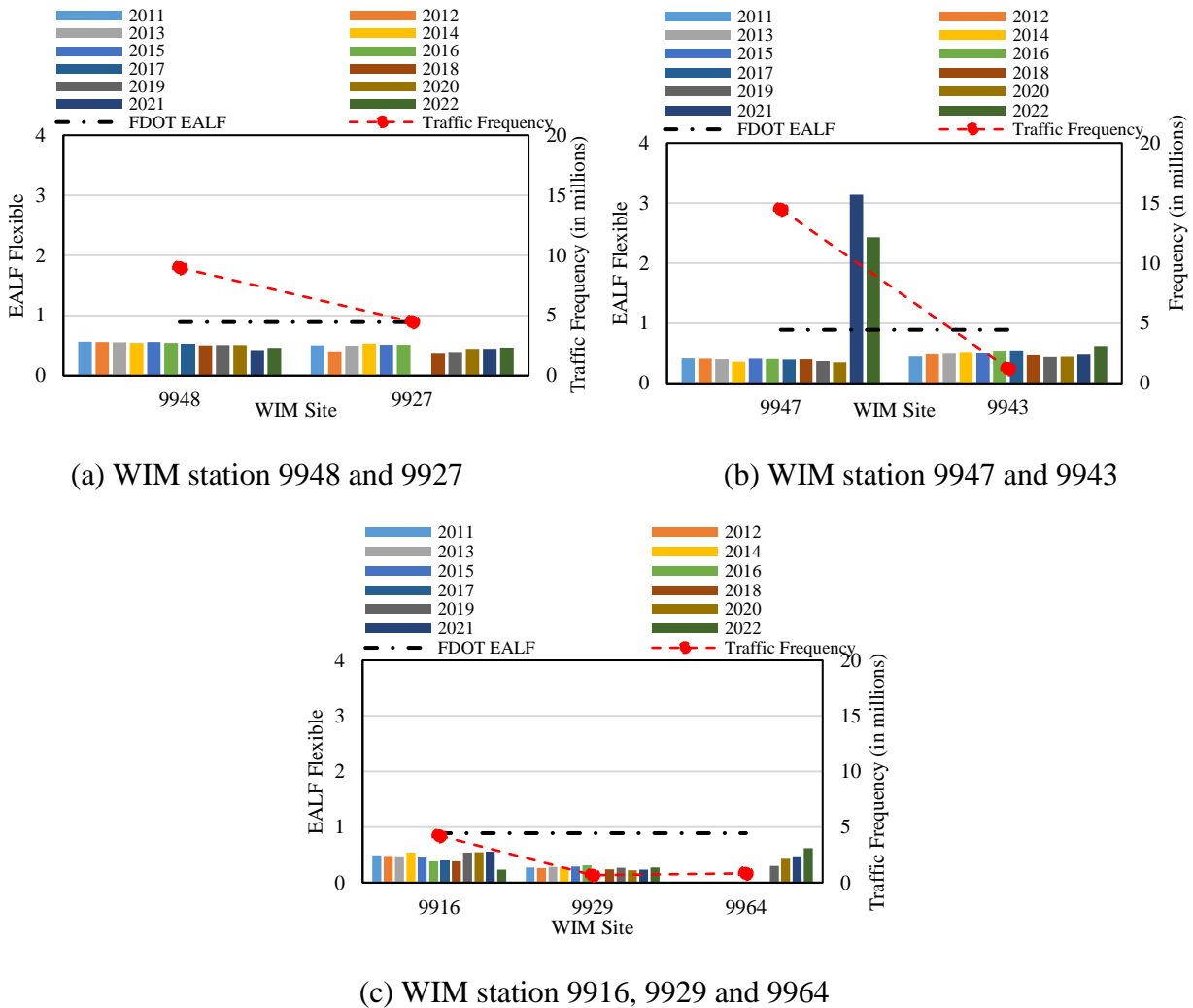
Figure 4-15: EALF of non-limited urban flexible pavements with legal weights

(a) WIM station 9948 and 9927

(b) WIM station 9947 and 9943

(c) WIM station 9916, 9929 and 9964
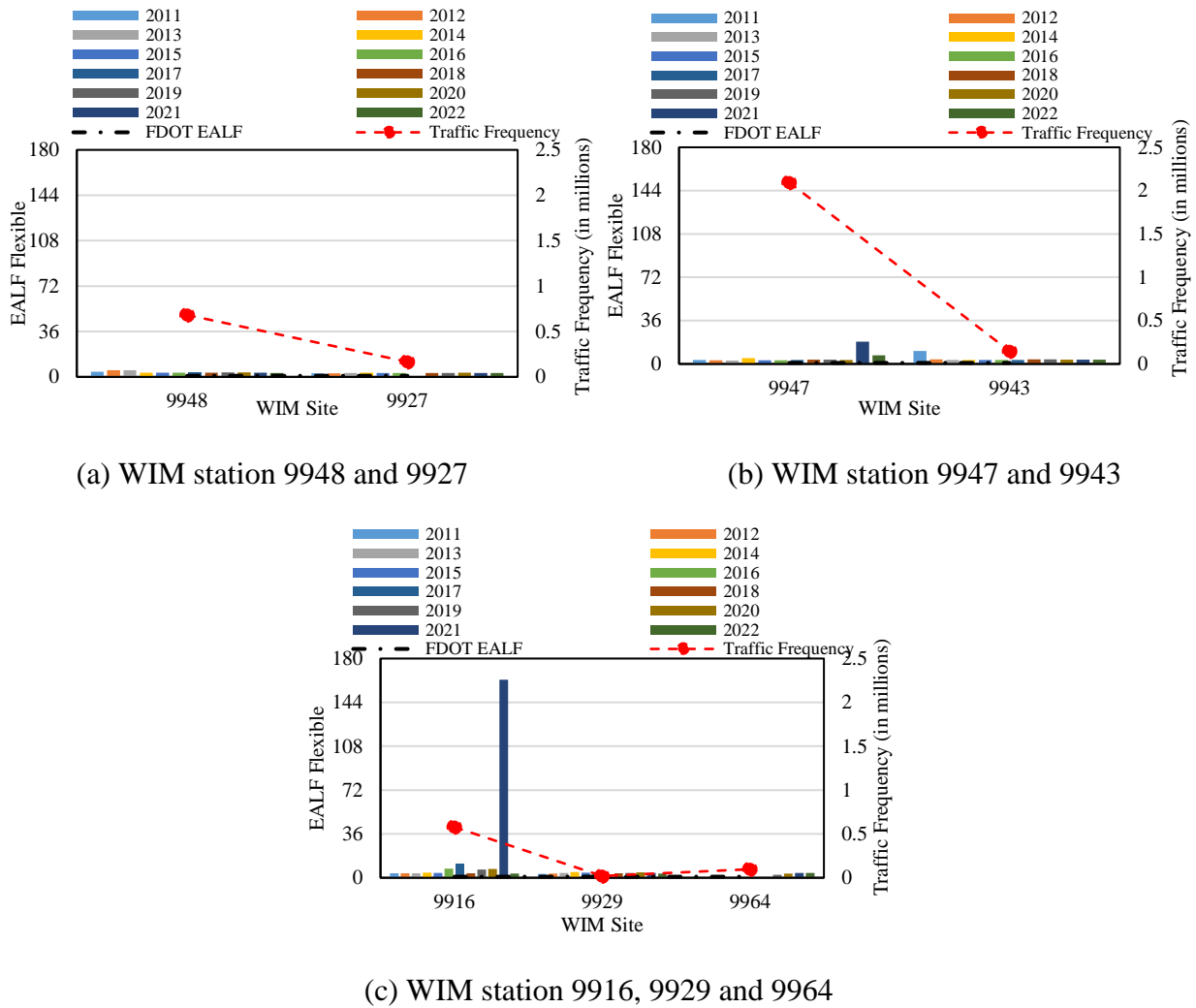
Figure 4-16: EALF of non-limited urban flexible pavements with over weights

Figure 4-17 and Figure 4-18 show the EALF variations for the LW and OW vehicles in non-limited urban rigid pavements. The average EALF for LW and OW vehicles were around 0.93 and 27.5, respectively.
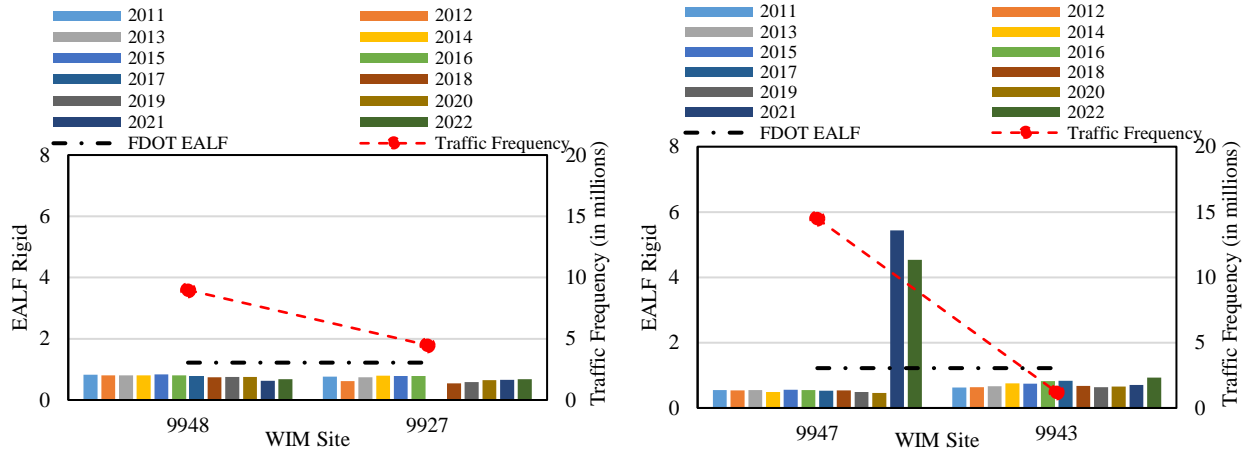
(a) WIM station 9948 and 9927

(b) WIM station 9947 and 9943
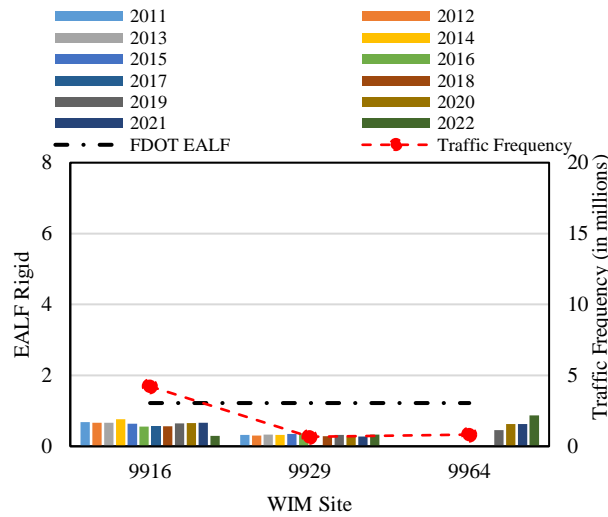
(c) WIM station 9916, 9929 and 9964

Figure 4-17: EALF of non-limited urban rigid pavements with legal weights
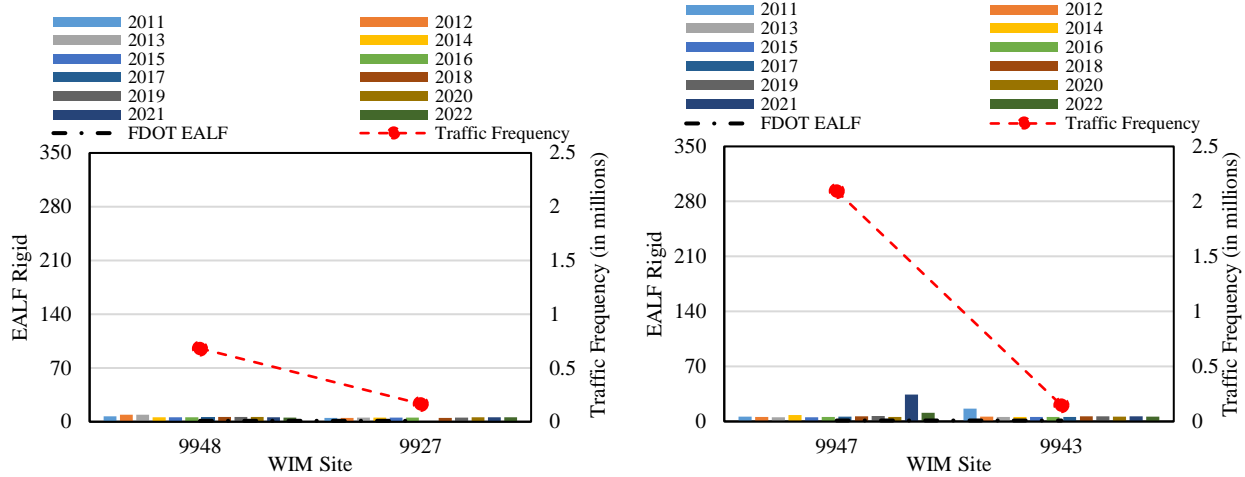
(a) WIM station 9948 and 9927

(b) WIM station 9947 and 9943
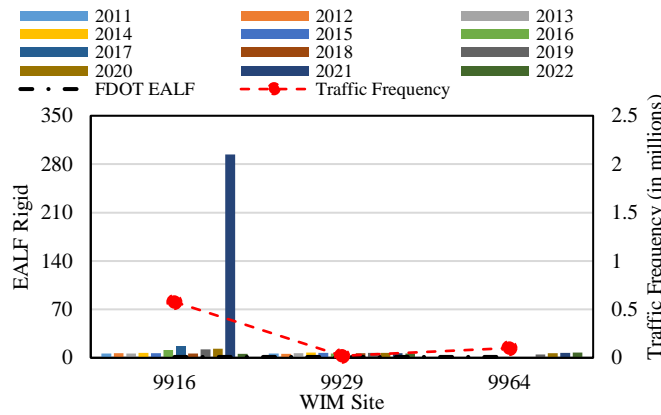
(c) WIM station 9916, 9929 and 9964

Figure 4-18: EALF of non-limited urban rigid pavements with over weights

It was already mentioned that the WIM station 9947 in Miami-Dade County exceeds the FDOT-adopted design EALF for the years 2021 and 2022, as shown in Figure 4-15(b) and Figure 4-17(b). Figure 4-19 shows the EALF distribution by vehicle class along with the respective traffic frequency for the LW vehicles in 2021 and 2022. For LW vehicles in 2021, the highest impact from EALF was observed for Class 7 vehicles, while in 2022, it was Class 13. For both years, the EALF and frequency of Class 9 vehicles were relatively higher. From 2021 to 2022, the frequency of Class 9 vehicles increased by around 80%, while the EALF for both the flexible and rigid pavement decreased by around 20%.

(a) 2021   (b) 2022
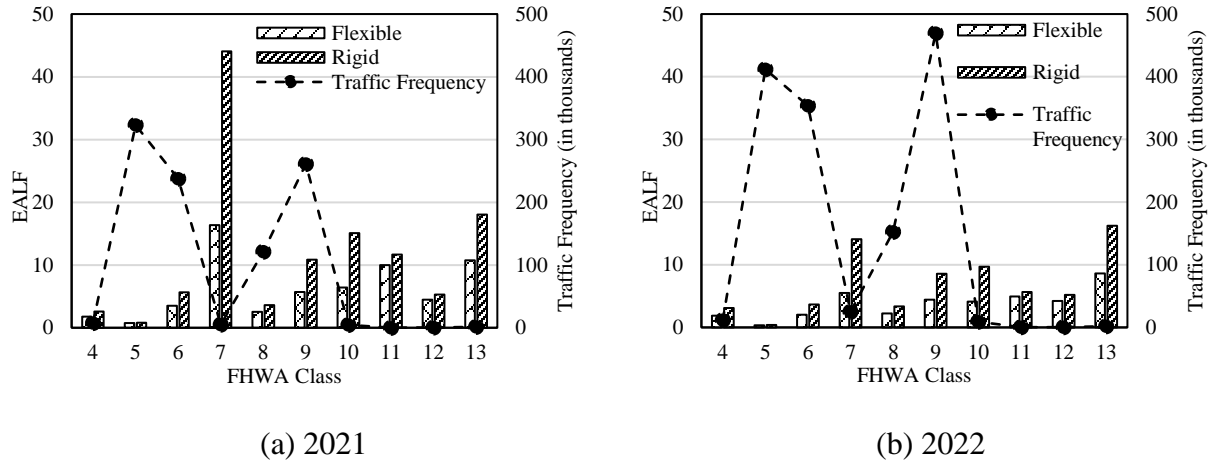
Figure 4-19: EALF for legal weight vehicles at WIM station 9947

Figure 4-20 shows the EALF distribution by vehicle class for the OW vehicles that passed the WIM station 9916 in Escambia County in 2021. Unlike other OW distributions, this graph also shows that the highest EALF can be from different classes of vehicles based on the pavement type. For example, Class 7 has the highest EALF of around 700 for rigid pavement, while Class 11 has the highest EALF of around 350 for flexible pavement.
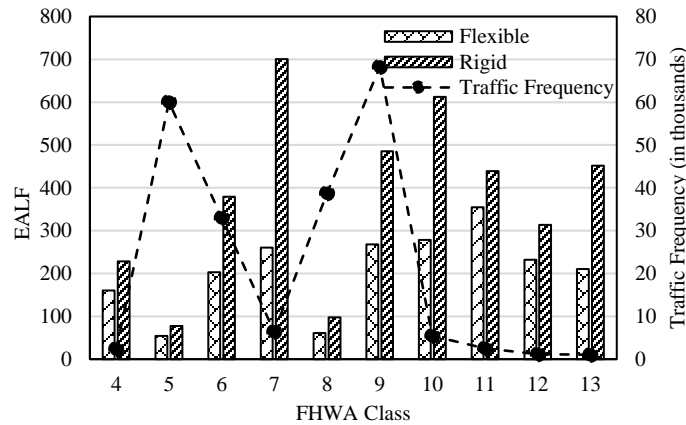
Figure 4-20: EALF for over-weight vehicles at WIM station 9916 in 2021

The EALF variations depends on both the axle configuration and the weight of the axle. This can be demonstrated by a simple example of a Class 5 vehicle. It is assumed that the total weight of the Class 5 vehicle is 75 kip. Class 5 vehicles can be made up of 2, 3, 4, or 5 axles. For this demonstration, Class 5 vehicles with 2, 3, or 4 axles are considered. Different configurations of Class 5 vehicles considered in this study are shown in Figure 4-21.

a) Two single axles   (b) Three single axles

(c) One single and one tandem axle   (d) One single and one tridem axle
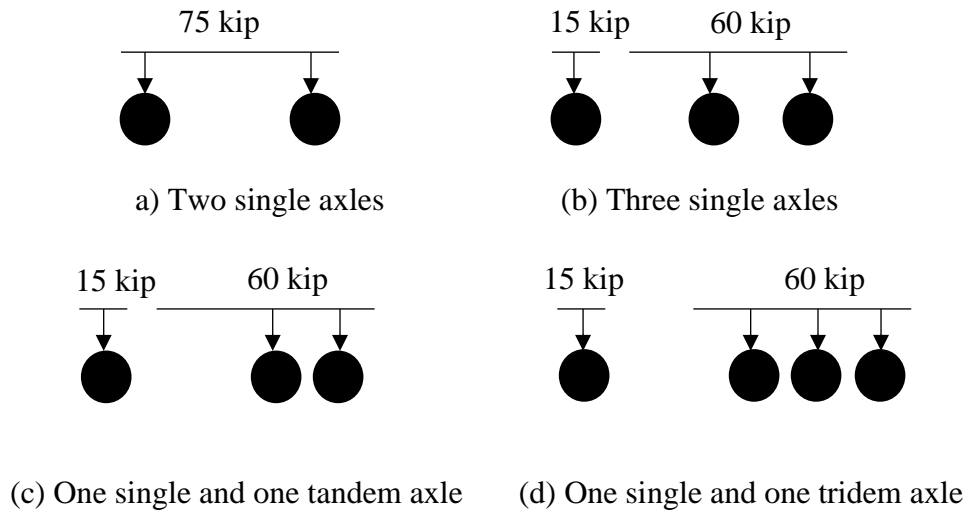
Figure 4-21: Different configurations considered for a Class 5 vehicle

Figure 4-21(a) shows a Class 5 vehicle with two single axles. Thus, each axle carries a load of 37.5 kip. Figure 4-21(b) shows the Class 5 vehicle with one single steering axle and two single trailer axles. It is assumed that the steering axle carries a weight of 15 kip, while the two single axles in the trailer carry 30 kip loads each. For Figure 4-21(c) and (d), it is assumed that the trailer axle is comprised of one tandem and one tridem axle, respectively. Thus, the total trailer load of 60 kip is carried by the respective axles. There will be no division of load for the tandem and tridem axles, like the single axles in Figure 4-21(a) and (b). As an example, the procedure of EALF determination is presented for two single axles, as shown in Figure 4-21(a).

4.3.4.1 Two Single Axles

Previously mentioned values of p_t, and SN of 2.5 and 5, respectively, were also used in this example as well. The axle code (L_2) for the single, tandem and tridem axle are 1, 2 and 3, respectively. G_t, β_x, and β_{18} are determined as shown in Eqs. (17) to (19)

$$G_t = \log\left(\frac{4.2 - 2.5}{4.2 - 1.5}\right) = -0.2 \tag{17}$$

$$\beta_x = 0.4 + \frac{0.081(37.5 + 1)^{3.23}}{(5 + 1)^{5.19}1^{3.23}} = 1.38 \tag{18}$$

$$\beta_{18} = 0.4 + \frac{0.081(18 + 1)^{3.23}}{(5 + 1)^{5.19}1^{3.23}} = 0.5 \tag{19}$$

Using the values of G_t, β_x, and β_{18}, the EALF can be determined using the Eqs. (20) and (21)

$$log\left(\frac{W_{tx}}{W_{t18}}\right)_f = 4.79\,log(18+1) - 4.79\,log(L_x + L_2) + 4.33\,log(L_2) + \frac{G_t}{\beta_x} - \frac{G_t}{\beta_{18}}$$

$$= 4.79\,log(18+1) - 4.79\,log(37.5+1) + 4.33\,log(1) + \frac{(-0.2)}{1.38} - \frac{(-0.2)}{0.5} = -1.21 \tag{20}$$

$$EALF = \frac{1}{10^{-1.21}} = 16.33 \tag{21}$$

The EALF determined above is for one single axle. As there are two single axles, the total EALF for the axle configuration shown in Figure 4-21(a) is 16.33+16.33 = 32.66.

4.3.4.2 One Single and One Tandem Axle

For a Class 5 vehicle with one single axle and one tandem axle shown in Figure 4-21(c), first, the EALF for single axle is determined. Then, the EALF for the tandem axle is determined. Total EALF is the summation of EALFs from single steering axle and tandem trailer axle. For the sake of completeness, the steps involved in the determination of EALF of a Class 5 vehicle with one single axle and one tandem axle (Figure 4-21(c)) will be presented below.

The weight of the single steering axle is 15 kip.

$$G_t = log\left(\frac{4.2 - 2.5}{4.2 - 1.5}\right) = -0.2 \tag{22}$$

$$\beta_x = 0.4 + \frac{0.081(15+1)^{3.23}}{(5+1)^{5.19}1^{3.23}} = 0.457 \tag{23}$$

$$\beta_{18} = 0.4 + \frac{0.081(18+1)^{3.23}}{(5+1)^{5.19}1^{3.23}} = 0.5 \tag{24}$$

$$log\left(\frac{W_{tx}}{W_{t18}}\right)_f = 4.79\,log(18+1) - 4.79\,log(L_x + L_2) + 4.33\,log(L_2) + \frac{G_t}{\beta_x} - \frac{G_t}{\beta_{18}}$$

$$= 4.79\,log(18+1) - 4.79\,log(15+1) + 4.33\,log(1) + \frac{(-0.2)}{0.457} - \frac{(-0.2)}{0.5} = 0.32 \tag{25}$$

$$EALF_{single} = \frac{1}{10^{0.32}} = 0.478 \tag{26}$$

The combined weight on the tandem axle is 60 kip.

$$G_t = log\left(\frac{4.2 - 2.5}{4.2 - 1.5}\right) = -0.2 \tag{27}$$

$$\beta_x = 0.4 + \frac{0.081(60+2)^{3.23}}{(5+1)^{5.19}2^{3.23}} = 0.886 \tag{28}$$

$$\beta_{18} = 0.4 + \frac{0.081(18+1)^{3.23}}{(5+1)^{5.19}1^{3.23}} = 0.5 \tag{29}$$

$$
\begin{aligned}
log\left(\frac{W_{tx}}{W_{t18}}\right)_f &= 4.79 \, log\,(18+1) - 4.79 \, log\,(L_x + L_2) + 4.33 \, log\,(L_2) + \frac{G_t}{\beta_x} - \frac{G_t}{\beta_{18}} \\
&= 4.79 \, log\,(18+1) - 4.79 \, log\,(60+2) + 4.33 \, log\,(2) + \frac{(-0.2)}{0.886} - \frac{(-0.2)}{0.5} = -0.982
\end{aligned}
\tag{30}
$$

$$EALF_{tandem} = \frac{1}{10^{-0.982}} = 9.59 \tag{31}$$

Now, total EALF for the Class 5 vehicle shown in Figure 4-21(c) is determined by adding Eq. (26) and (31), which is 0.478+9.59 = 10.06.

Similarly, for axle configurations shown in Figure 4-21(b) and (d), the EALFs are 14.4 and 2.99, respectively. These values clearly show that different axle configurations and their associated loads can lead to a significantly different EALF for the same amount of GVW. The inability to distribute the loads through the appropriate configuration of axles and tires can lead to higher values of EALF, which will subsequently cause a higher amount of damage to the pavement.

4.4 Thickness Comparison

As mentioned earlier, the EALF determined from the WIM analysis was used to determine the AC layer and slab thickness for the flexible and rigid pavement, respectively. In this section, the thickness determined using the EALF from the WIM data will be compared with the thickness determined using the FDOT-adopted design EALF for both the flexible and rigid pavement, respectively.

First, the average EALF was determined for each functional class of pavements to determine the thickness. It was obtained from the frequency of truck traffic and EALFs observed at the WIM stations located at various functional classes of pavements in the different years considered for the analysis. The overall average EALF by functional class is shown in Figure 4-22. It is important to note that EALFs shown in Figure 4-22 were obtained from all the traffic, including both legal and overweight vehicles passing through a WIM station.
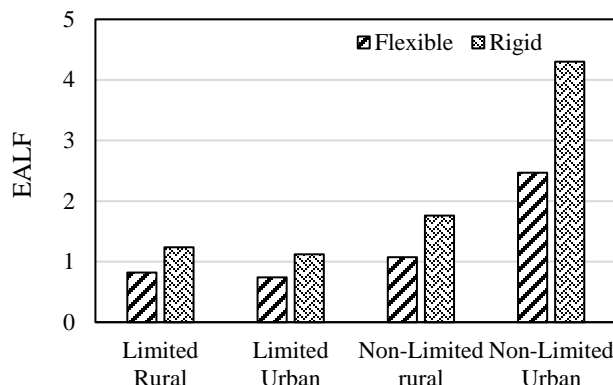
Figure 4-22: Average EALF by functional classes of pavements

4.4.1 Flexible Pavement

Figure 4-23 shows the thickness differences in flexible pavements determined using Eq. (14) for various functional class pavements with different resilient modulus (M_R) and lane factors. Figure 4-23 (a) and (b) show an inverse relation between the thickness differences and M_R for limited rural and limited urban flexible pavements. It means that when the resilient modulus of the subgrade layers is lower, AC thickness determined using FDOT design EALF will result in a relatively higher thickness compared to the EALF from WIM.

Figure 4-23(a) shows that when the resilient modulus of the subgrade is 4.0 ksi, FDOT's design EALF value produces overdesign in AC thickness by around 0.5 inches regardless of the lane factor. With an M_R of 32.0 ksi, the overdesign amount reduces to around 0.32 inch. Similarly, FDOT's design EALF also yields an overdesign in AC thickness for limited flexible urban pavements. The AC thickness overdesign ranges between 0.25 to 0.39 inches for the considered range of M_R.

Although AC thickness overdesign was observed for the limited rural and limited urban flexible pavements, underdesign was observed in the non-limited functional classes of pavements. From WIM analysis, EALFs for the non-limited rural and non-limited urban flexible pavements were found to be 1.07 and 2.47, respectively. These values are higher than the FDOT-adopted design EALFs of 0.96 and 0.89. The respective increments of 11% and 177% in the non-limited rural and non-limited urban EALF between the WIM and FDOT adopted values result in the underdesign of AC thickness, as shown in Figure 4-23 (c) and (d). Due to the lower difference between the FDOT and WIM EALF, the underdesign in AC thickness approximately ranges between 0.05-0.1 inches. Similarly, a higher difference between the FDOT and WIM EALF results in significant underdesign of around 1.5 to 1 inch for non-limited urban flexible pavements. Like limited pavements, non-limited pavement thickness variations are also inversely related to resilient modulus, M_R. Figure 4-23 also shows that thickness differences increase with a higher lane factor for a particular M_R. However, that difference is minimal or insignificant in terms of practical engineering considerations.
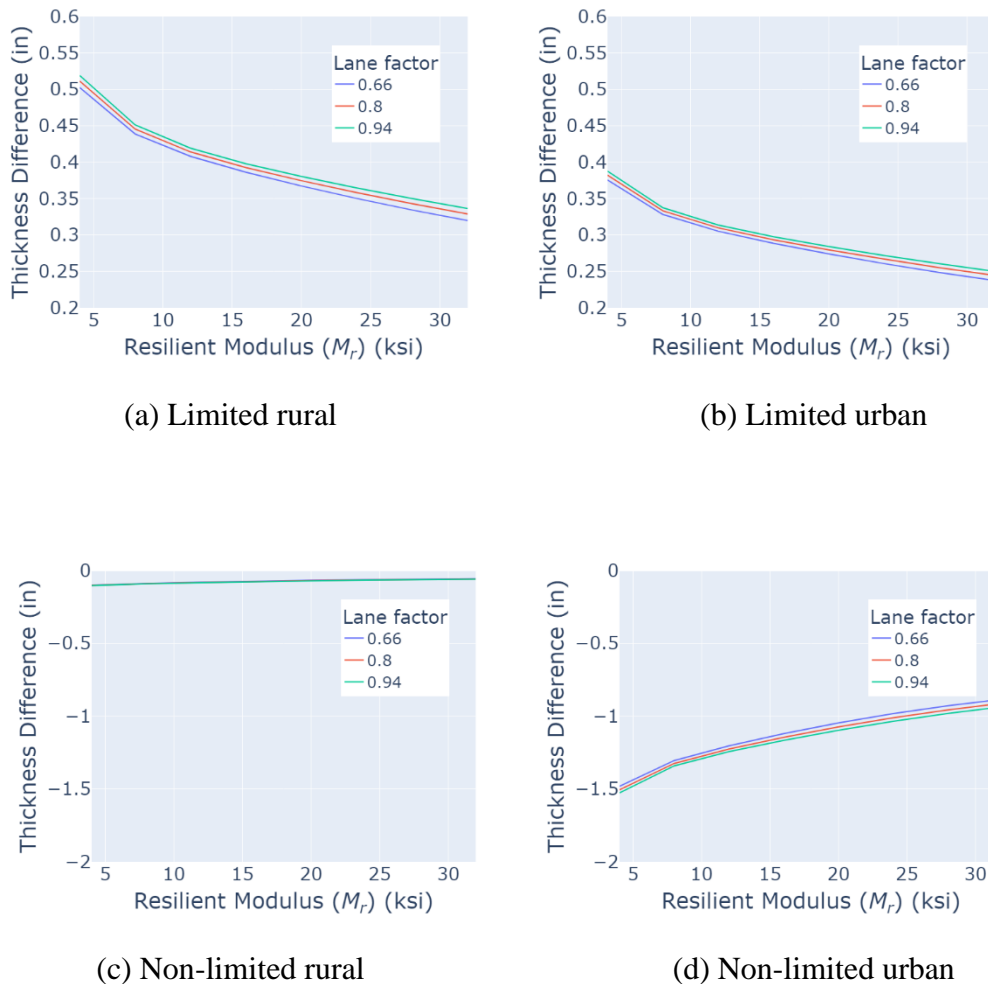
(a) Limited rural

(b) Limited urban

(c) Non-limited rural

(d) Non-limited urban

Figure 4-23: Thickness difference in AC layer

4.4.2 Rigid Pavement

Like flexible pavements in the previous section, Figure 4-24 shows the differences in slab thicknesses in rigid pavements determined using Eq. (16) for various functional classes of pavements. These slab thickness differences were determined for a range of modulus of subgrade reaction (k) and lane factors. Overall, Figure 4-24 shows a different trend compared to flexible pavement. Differences in slab thicknesses in rigid pavements were found to be relatively invariant of the changes in the modulus of subgrade reaction regardless of the pavement function class. In addition, the effect of lane factor was found to have a minimal effect in the thickness differences.

Figure 4-24 (a) and (b) show that FDOT's design EALF produces a higher slab thickness compared to the slab thickness determined using the WIM-calculated EALF for both limited rural and limited urban rigid pavements. For limited rural and limited urban rigid pavements, FDOT adopted EALF for design are 1.6 and 1.27, respectively. From the WIM data analysis, the corresponding functional classes of rigid pavements had EALFs of 1.21 and 1.12, respectively. Thus, the EALFs from FDOT design to WIM produces an overdesign of 0.54 in and 0.24 in for the limited rural and limited urban rigid pavements, respectively.

Unlike limited rural and limited urban pavements, FDOT adopted EALF produces an underdesign of slab thickness compared to the EALF from WIM for non-limited rural and non-limited urban pavements. FDOT adopted EALF for design of non-limited rural and non-limited urban pavements are 1.35 and 1.22, respectively. From the WIM data analysis, the corresponding functional classes of rigid pavements had EALFs of 1.66 and 3.52, respectively. Thus, the EALFs from FDOT design to WIM produces an underdesign of around 0.33 in and 1.8 in for the non-limited rural and non-limited urban rigid pavements, respectively.

(a) Limited rural

(b) Limited urban

(c) Non-limited rural

(d) Non-limited urban
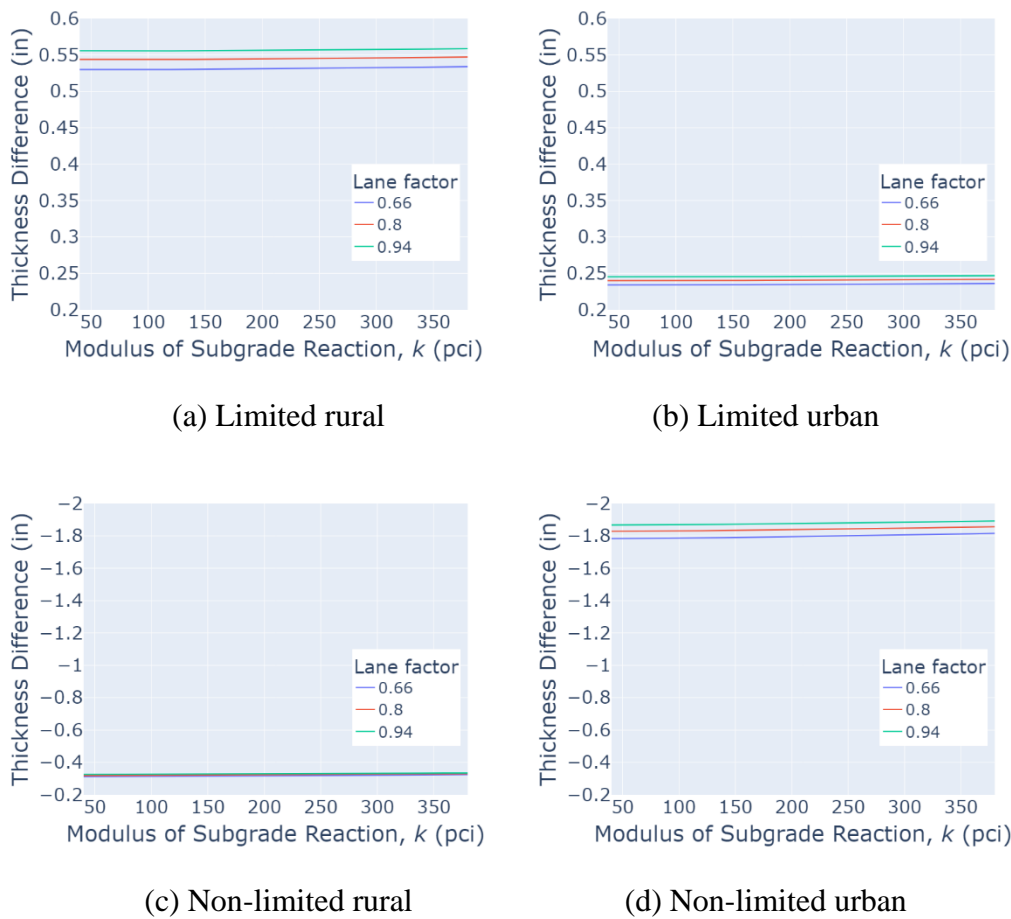
Figure 4-24: Difference in slab thickness for different modulus of subgrade reaction

Figure 4-25 shows the differences in thickness for various concrete modulus of elasticity in different functional classes of rigid pavements. According to FDOT's 2006 rigid pavement design manual, the concrete modulus should be 4,000 ksi while designing the rigid pavement slab thickness using the AASHTO 1993 equation. Literature search and data collected from FDOT also showed that the modulus of elasticity of concrete for Florida mixes varies between 3,000 ksi and 5,000 ksi (Tia et al., 2012). Thus, this study performed a sensitivity analysis by varying the modulus of elasticity of concrete to study its effect on the slab thickness variation.

Figure 4-25 shows that the differences in slab thickness determined using FDOT EALF and WIM EALF remain almost the same regardless of the concrete modulus of elasticity.

(a) Limited rural   (b) Limited urban

(c) Non-limited rural   (d) Non-limited urban
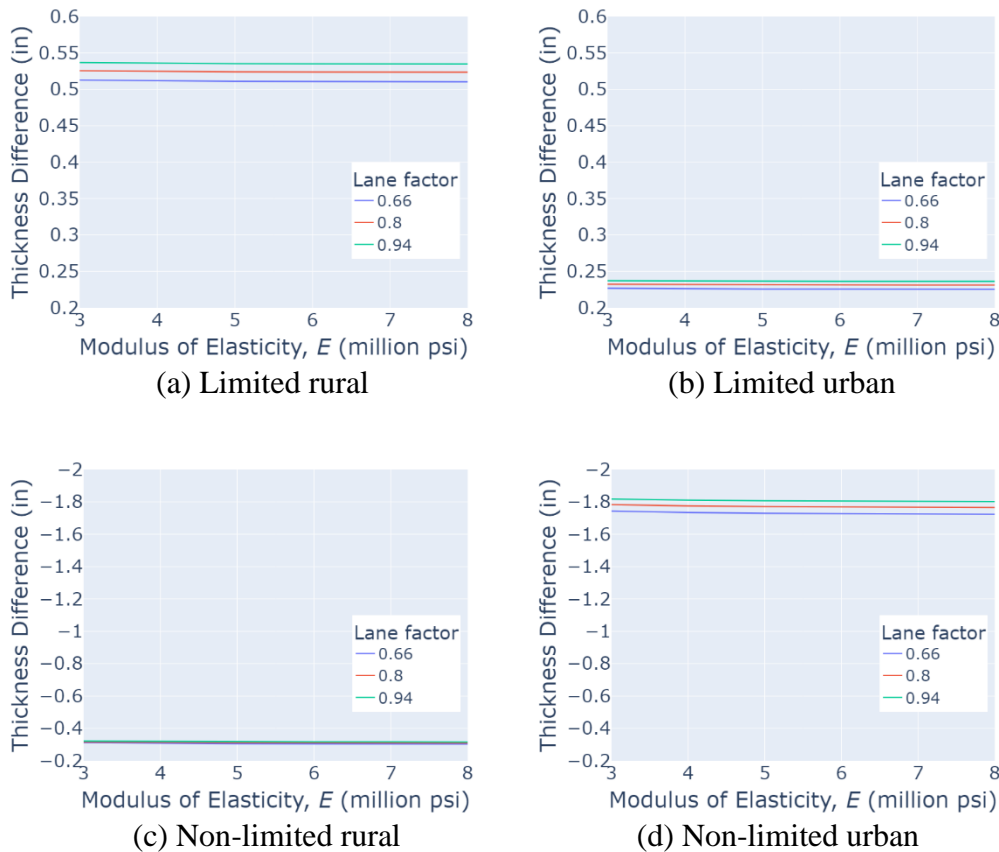
Figure 4-25: Difference in slab thickness for different concrete modulus

Along with the modulus of subgrade reaction and concrete modulus of elasticity, the effect of the modulus of rupture of concrete on designing the slab thickness was also studied. Based on the data from FDOT, the range of modulus of concrete rupture was from 450 psi to 600 psi (Tia et al., 2012). Figure 4-26 (a) and (b) show the overdesign of slab thickness for limited rural and limited urban functional classes of pavements for the considered range of modulus of rupture of concrete. For limited rural rigid pavements, the slab thickness overdesign was 0.56-0.64 in, and for limited urban, the value was around 0.25 in.

Underdesign of slab thickness was observed for the non-limited rural and non-limited urban rigid pavements, as shown in Figure 4-26 (c) and (d). The amount of underdesign of slab thickness varied between 0.34 in to 0.37 in, and 1.9 in to 2.2 in for non-limited rural and non-limited urban pavements, respectively.
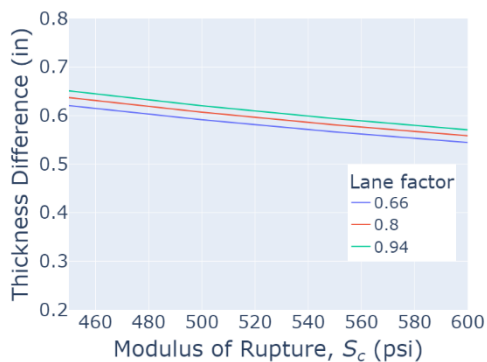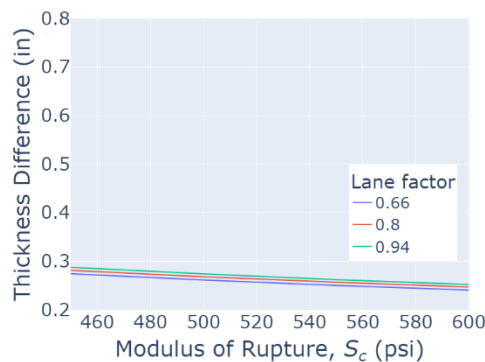
(a) Limited rural

(b) Limited urban

(c) Non-limited rural
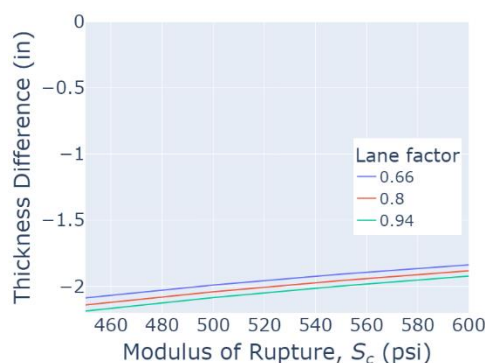
(d) Non-limited urban

Figure 4-26: Difference in slab thickness for different concrete modulus of rupture

Figure 4-24, Figure 4-25, and Figure 4-26 show that variation in modulus of rupture yields the highest difference in slab thickness determined from Eq. (16) while other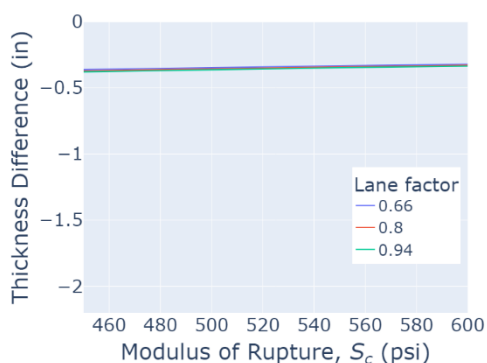 factors, such as concrete modulus and modulus of subgrade reaction, are kept constant. For this reason, only modulus of rupture was considered for further sensitivity analysis of rigid pavements.

4.5 Scenario-based EALF and Thickness Comparison

In this section, EALFs and surface layer thickness was determined based on different scenarios. Figure 4-27(a) shows the percentages of legal and overweight vehicles passing through the functional classes of pavements, and Figure 4-27(b) shows the frequency of total truck traffic, both legal and overweight vehicles, from 2011-2022 in the entire state of Florida. For limited rural and limited urban pavements, the overweight percentages were found to be less than 10%, while non-limited rural and non-limited urban pavements have overweight vehicle percentages of around 10%-15%. In addition, Figure 4-27(b) shows that in recent years, the frequency of truck traffic has increased on an average by 50% compared to the truck frequency observed in 2018. Thus, two scenario-based studies were conducted:

- Analysis with Legal weight vehicles only
- Analysis with Legal weight and twice the overweight vehicles

It is important to mention that the number of overweight trucks was increased by a factor of 2 to demonstrate the impact of overweight vehicles on the design of the surface course.

(a) Percentage of legal and overweight vehicles   (b) Total Traffic
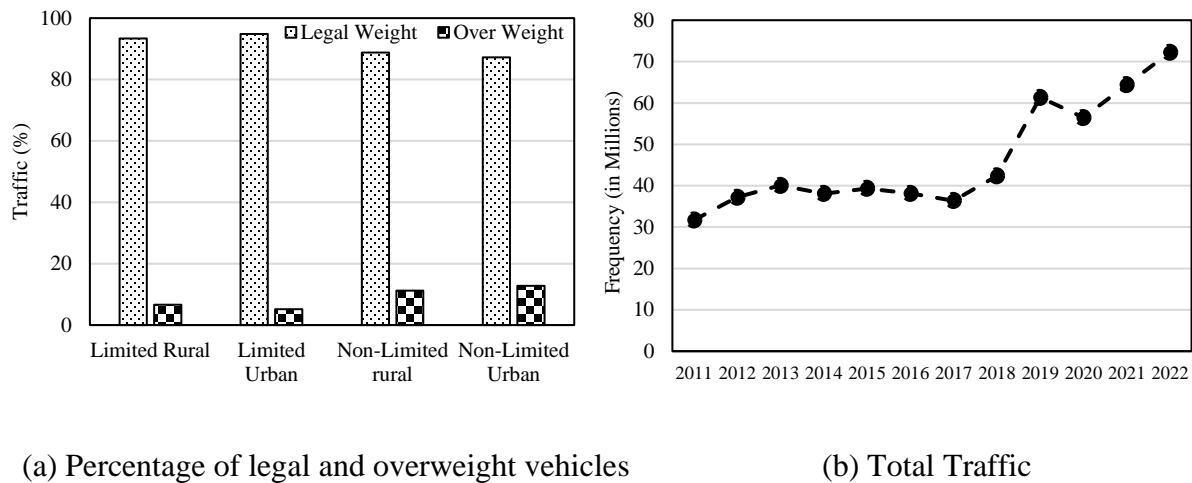
Figure 4-27: Distribution of traffic

4.5.1 Flexible Pavements with Legal Weight Only

Figure 4-28 shows the AC layer thickness differences observed for the legal weight vehicles in different functional classes of pavements. As mentioned earlier, these differences were obtained by determining the AC layer thickness using the EALF from FDOT-adopted design value and WIM data. For all the four functional classes of pavements considered in this study, FDOT's design EALFs resulted in higher AC layer thickness compared to the EALF from WIM data. This is expected as the EALFs from the legal weight vehicles are lower compared to the design EALFs. The EALFs for FDOT's design vary between 0.89 to 1.05, while the EALFs from legal weight-only WIM data range between 0.54 to 0.65. Except for non-limited urban, the range of AC thickness overdesign varied from 0.6 in to 1.0 in for all the functional classes of pavements. For non-limited urban, the AC thickness overdesign amount varied between 0.35 in to 0.65 in.

(a) Limited rural

(b) Limited urban

(c) Non-limited rural

(d) Non-limited urban
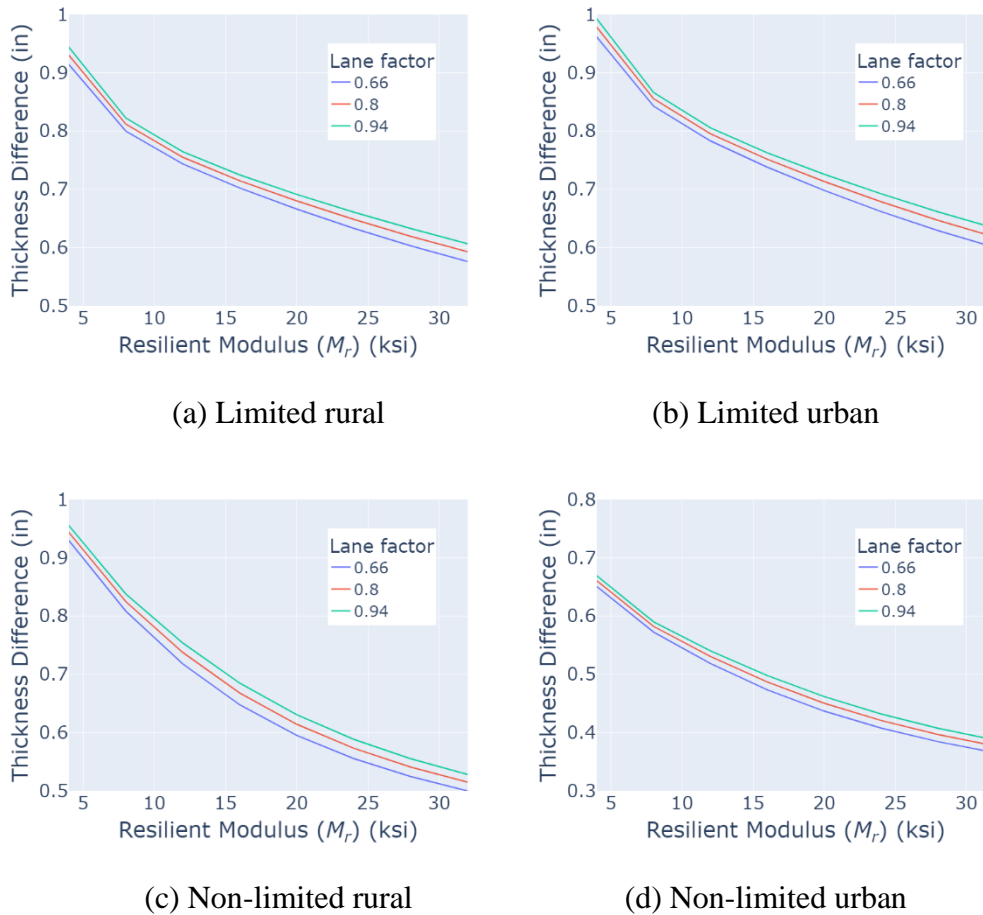
Figure 4-28: Thickness difference in AC layer for legal weight vehicles only

4.5.2   Rigid Pavements with Legal Weight Only

Figure 4-29 shows the slab thickness differences observed for the legal weight vehicles in different functional classes of rigid pavements. Similar to flexible pavements, FDOT-adopted EALFs resulted in higher slab thickness compared to the EALF from WIM data for all four functional classes of pavements. These overdesigns have been attributed to the lower EALFs from the legal weight vehicles compared to the FDOT's design EALFs. The EALFs from the FDOT design vary between 1.22 to 1.60, while the EALFs from legal weight-only WIM data range between 0.77 to 0.94.

(a) Limited rural

(b) Limited urban

(c) Non-limited rural

(d) Non-limited urban

Figure 4-29: Slab thickness differences in rigid pavement for legal weights only

4.5.3 Flexible Pavements with Legal Weight and Twice the Overweight

Figure 4-30 shows the AC layer thickness variation for various functional classes of pavements when the overweight vehicles were increased by a factor of 2. Only the number of overweight trucks was increased, but the amount of legal traffic was kept the same. Compared to the legal weight-only traffic in Figure 4-28(a), increasing the number of overweight vehicles by a factor of 2 increased the EALF from 0.65 to 0.95, around a 50% increment. Despite increasing the number of overweight vehicles, FDOT-adopted EALF still produced an overdesign for limited rural flexible pavements. The thickness overdesign amount varied between 0.1 in to 0.2 in for the considered M_R values, as shown in Figure 4-30(a). Almost similar design thickness was observed between the FDOT-adopted EALF and EALF from WIM analysis for the limited urban flexible pavements after doubling the overweight frequency, as shown in Figure 4-30(b). Figures 4-30(c) and (d) show that doubling the frequency resulted in the underdesign of AC thickness for both the non-limited rural and non-limited urban flexible pavements. For non-limited rural pavements, FDOT-adopted EALF resulted in the underdesign of AC thickness by around 0.4 in to 0.65 in, while the thickness underdesign ranges between 1.5 in to 2.5 in for non-limited urban pavement. The higher amount of underdesign for non-limited urban pavements is attributed to the fact that doubling the overweight vehicles resulted in an EALF of 3.21, which is almost 260% more than the FDOT-adopted design EALF of 0.89.

(a) Limited rural

(b) Limited urban
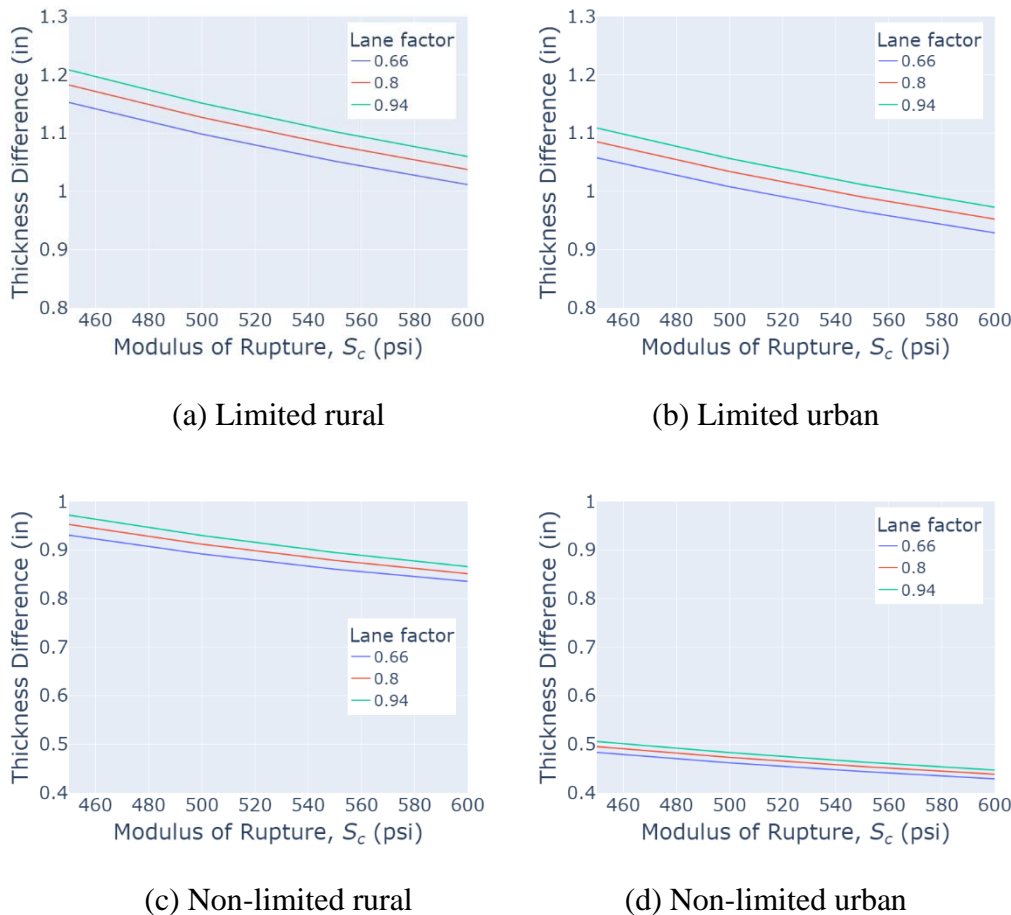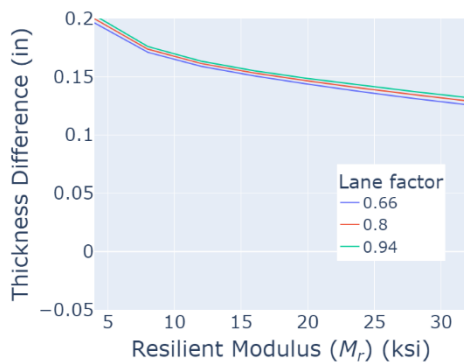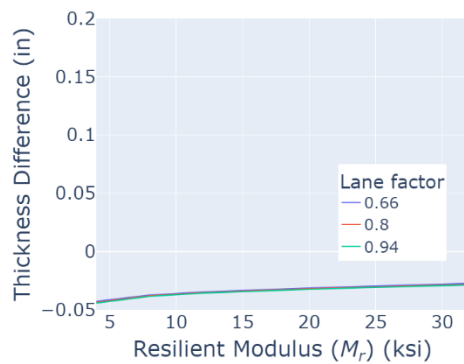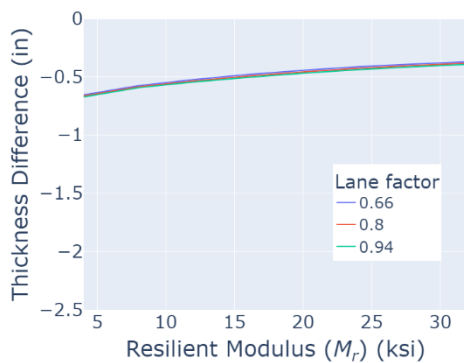

(c) Non-limited rural

(d) Non-limited urban

Figure 4-30: Thickness difference in AC layer for legal weight and twice the overweight

4.5.4   *Rigid Pavements with Legal Weight and Twice the Overweight*

Similar to flexible pavements, FDOT adopted EALF produced an overdesign of slab thickness for limited rural rigid pavements despite doubling the number of overweight vehicles. The amount of overdesign in slab thickness was observed to be around 0.2 in for the considered S_c values, as shown in Figure 4-31(a). Unlike limited urban flexible pavements, Figure 4-31(b) shows that around 0.25 in to 0.3 in underdesign was observed for limited urban rigid pavements when FDOT adopted EALF was used for the design. Figure 4-31(c) and (d) show that doubling the frequency resulted in the under design of slab thickness for both the non-limited rural and non-limited urban flexible pavements. FDOT adopted EALF results in the underdesign of slab thickness of around 1 in, and 2.8 in to 3.2 in for non-limited rural and non-limited urban rigid pavements, respectively. The higher amount of underdesign for non-limited urban pavements is attributed to the fact that doubling the overweight vehicles results in an EALF of 6.92, which is almost 470% more than the FDOT's design EALF of 1.22.
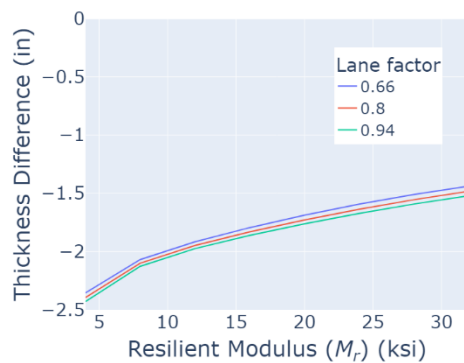
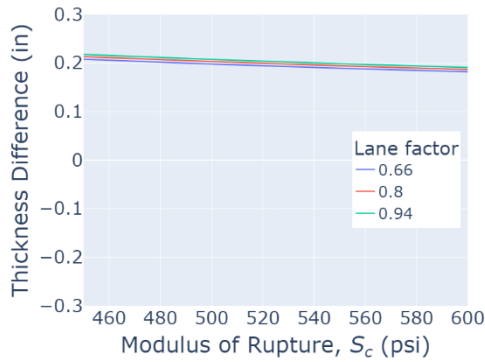(a) Limited rural

(b) Limited urban
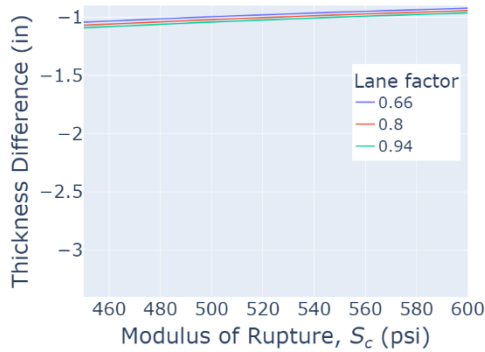
(c) Non-limited rural
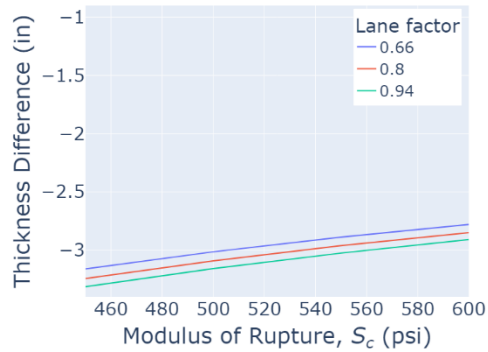
(d) Non-limited urban
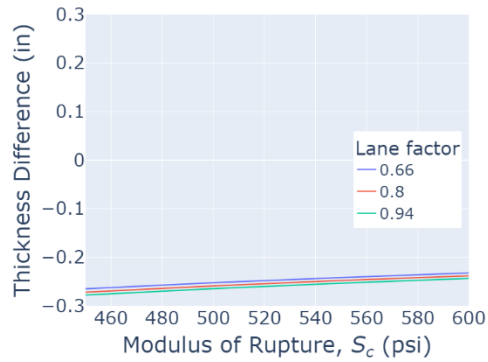
Figure 4-31: Slab thickness differences for legal weights and twice the overweight

Table 4-5 provides a summary of the EALFs based on the actual WIM data and various scenarios considered in this report. It also includes FDOT design EALFs for comparison.

Table 4-5: Summary of EALF for various conditions

Functional Class	Pavement Type	FDOT EALF Design	Average EALF WIM		
			All Traffic	Legal Weight Traffic	Legal Weight Traffic + Twice Over-Weight Traffic
Limited Rural	Flexible	1.05	0.81	0.65	0.95
	Rigid	1.6	1.21	0.94	1.46
Limited Urban	Flexible	0.9	0.74	0.54	0.92
	Rigid	1.27	1.12	0.77	1.43
Non-Limited Rural	Flexible	0.96	1.02	0.54	1.41
	Rigid	1.35	1.66	0.77	2.39
Non-Limited Urban	Flexible	0.89	2.04	0.6	3.21
	Rigid	1.22	3.52	0.93	5.66

Table 4-6 shows the implication of variations observed in the EALFs compared to the FDOT adopted design values. It summarizes the thickness differences observed between the FDOT-adopted EALF and various scenario-based EALFs discussed in this study. The positive value in Table 4-6 indicates an overdesign of thickness according to the FDOT design method, while a negative value denotes an under design.

Table 4-6: Summary of thickness differences

Functional Class	Pavement Type	Thickness Difference (in)			
		All Traffic	Legal Weight Traffic	Over Weigt Traffic	Legal Weight Traffic + Twice Overweight Traffic
Limited Rural	Flexible	0.32-0.5	0.65 to 0.95	-1.9 to -1	0.1 to 0.2
	Rigid	0.54	1	-2.15 to -1.9	0.2
Limited Urban	Flexible	0.25 to 0.38	0.65 to 1.0	-2.6 to -1.4	On Par
	Rigid	0.24	1	-3.1 to -2.75	-0.27 to -0.24
Non-Limited Rural	Flexible	-0.05 to -0.1	0.5 to 0.9	-2.6 to -1.3	-0.4 to -0.65
	Rigid	-0.33	0.85-0.95	-3 to -2.8	-0.95 to -1.05
Non-Limited Urban	Flexible	-1.5 to -1	0.35 to 0.65	-4.65 to -2.55	-1.5 to -2.4
	Rigid	-1.8	0.45-0.5	-5.4 to -4.85	-2.8 to -3.2

negative value denotes underdesign

Along with the observed legal weight vehicles, an underdesign of limited rural and limited urban functional classes of pavement is observed if the amount of OW vehicles becomes certain times higher than the currently observed values, as shown in Table 4-7.

Table 4-7: Multiplier of OW Vehicles to Reach Underdesign in Limited Functional Pavements

Functional Class	OW to Underdesign	
	Flexible Pavement	Rigid Pavement
Limited Rural	2.85	2.75
Limited Urban	2	1.5

Besides thickness difference, WIM data can also be used to determine the reduction in pavement life based on the ESAL. Using the EALF (E_{18}) from WIM data and FDOT, the difference in ESAL can be determined using Eq. (32).

$$\Delta ESAL = \sum_{i=1}^{design\ life} (total\ truck\ count \times D_F \times L_F \times E_{18}^{FDOT})$$

$$- \sum_{i=1}^{design\ life} (total\ truck\ count \times D_F \times L_F \times E_{18}^{WIM}) \tag{32}$$

$$= \sum_{i=1}^{design\ life} [total\ truck\ count \times D_F \times L_F \times (E_{18}^{FDOT} - E_{18}^{WIM})]$$

In Eq. (32), D_F is the directional distribution factor, taken to be 1, L_F is the lane factor. A range of L_F was considered, 0.66-0.94. In this study, the total truck count was obtained directly from the WIM data. However, they can also be obtained using Annual Average Daily Traffic (AADT) and percent of heavy trucks in 24-hour period (T_{24}), i.e., $total\ truck\ count = AADT \times T_{24} \times 365$.

Now, the $\Delta ESAL$ can be translated to change in pavement life based on the number of ESAL experienced by the pavement in a single year. This is done by dividing Eq. (32) with average ESAL from WIM, as shown in Eq. (33).

$$\Delta pavement\ life = \frac{\Delta ESAL}{ESAL^{WIM}/design\ life}$$

$$= \frac{\sum_{i=1}^{design\ life}[total\ truck\ count \times D_F \times L_F \times (E_{18}^{FDOT} - E_{18}^{WIM})]}{\left(\sum_{i=1}^{design\ life}(total\ truck\ count \times D_F \times L_F \times E_{18}^{WIM})\right)/design\ life} \tag{33}$$

For example, 271419 trucks pass through the non-limited rural pavements yearly. This average number was obtained from the WIM data analysis. The design life of the pavement is taken to be 20 years. The EALF of non-limited rural flexible pavement from FDOT and WIM were 0.96 and 1.02, respectively. Thus, from Eq. (33), the reduction in the life of non-limited rural flexible pavement due to the difference in FDOT adopted EALF and WIM calculated EALF is found to be 1.2 years.

$$\Delta pavement\ life = \frac{[271419 \times 1 \times 0.66 \times (0.96 - 1.02) \times 20]}{271419 \times 1 \times 0.66 \times 1.02 \times 20/20} = -1.2\ years \tag{34}$$

As observed before with the thickness difference analysis, lane factor has a negligible effect on the reduction in pavement life. Although a lane factor of 0.66 was used in the above example, changing it to 0.94 does not have any significant impact on the pavement life reduction.

Following the same steps, the change in pavement life for other functional classes of pavements are shown in Table 4-8.

Table 4-8: Summary of change in pavement life

Functional Class	Pavement Type	Change in Pavement Life (years)
Limited Rural	Flexible	5.9
	Rigid	6.4
Limited Urban	Flexible	4.3
	Rigid	2.7
Non-Limited Rural	Flexible	-1.2
	Rigid	-3.7
Non-Limited Urban	Flexible	-11.3
	Rigid	-13

negative value denotes pavement life reduction

5   IMPACT ON PAVEMENT

As the name suggests, super heavy loads (SHLs) are special types of loads that are heavier than regular truck loads. The vehicles that carry such loads are also typically longer and wider than regular trucks. Therefore, SHLs generally require special trailers with non-standard axle and tire configurations. For highway agencies that are responsible for maintaining a roadway network, it is important to identify the impact of SHL movement on the pavement by determining the pavement response at critical locations. However, simulation of the actual movement of the SHLs through pavement is computationally expensive and time consuming. Thus, a methodology will be proposed in this study for analyzing the impact of SHL movement on the adequacy and stability of the pavement structure. The proposed methodology will be demonstrated with an example of a SHL passing through a flexible pavement. The considered SHL has two platform trailers. The length (L) and width (B) of each platform trailer are 123.0 ft. and 20.0 ft., respectively. The dimension and size of the sample SHL used in this study were obtained from the research team's internal database. More information on the SHL will be provided later in the subsequent sections.

5.1   Objective

The primary objective of this task is to develop a methodology to evaluate the structural capacity of the pavement layers subjected to SHL movement. Specifically, this chapter will perform the following:

(a) Determination of the nucleus or representative unit of the SHL for response analysis
(b) Evaluate the potential for distresses in the AC layer
(c) Evaluate the bearing capacity and localized failure in the subgrade

5.2   Nucleus of SHL

SHL loads are generally comprised of nonstandard axle and tire configurations and include a significantly larger number of tires compared to some standard highway trucks. As such, it is not efficient nor practical to consider all the tires included in the SHL for pavement damage analysis. Therefore, a methodology was developed to identify the critical SHL tires that can be grouped together for the analysis, which can also be regarded as the minimum block of loads that need to be considered for pavement response under the SHL (Nabizadeh et al., 2019). This group or block of axles is referred to as the "nucleus" of the SHL.

A representative pavement structure is required to demonstrate the determination of the nucleus of a SHL, which is shown in Figure 5-1.
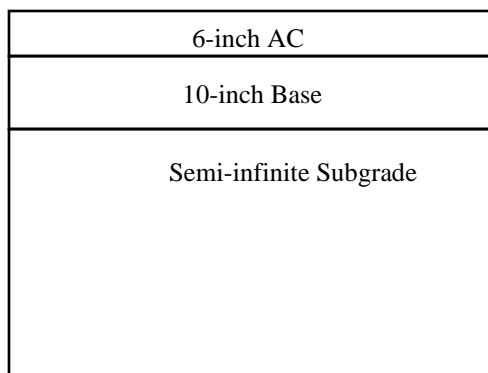
6-inch AC
10-inch Base
Semi-infinite Subgrade

Figure 5-1: A typical pavement section

Table 5-1 shows the typical modulus values assumed for the pavement section shown in Figure 5-1.

Table 5-1: Modulus of the pavement layers

Layer	Modulus (psi)
AC	350,000
Base	80,000
Subgrade	20,000

In general, the asphalt modulus is related to temperature. It is also related to frequency. During the SHL movement, the AC layer will have a certain temperature. It is assumed that the 350,000 psi is the modulus of the AC layer at the time of the SHL movement at the corresponding temperature and speed (frequency). It is recommended that multiple FWD tests be conducted closer to the day of the movement of the SHL. Among these tests, the modulus of the pavement layers should be determined based on the test that closely matches the environmental condition expected during the day of SHL movement. This will ensure an accurate representation of the pavement modulus and associated responses. However, conservative estimation can be made by reducing the FWD obtained AC modulus based on engineering judgement in case of higher degree of uncertainty.

In pavement analysis and design, it is important to determine the contact area between the tire and the pavement. Although in reality, the entire axle load is distributed over many tires (e.g., dual tires, tandem axle, etc.), it is not very convenient nor computationally efficient to consider all of the different tires, especially for an SHL with a large number of tires. As such, it is more convenient to consider a "representative" single load that may result in similar results as those from a large number of very closely spaced tires. The area of the representative single load is dependent on contact pressure, and generally, it is taken to be the tire pressure (Huang, 2004). Eq. (35) shows the contact radius, r, of the representative tire load.

$$r = \sqrt{\frac{nA_c}{\pi}} \tag{35}$$

where A_c is the tire contact area of each tire included in the analysis, p is the tire pressure, n is the number of tires, e.g., for dual tire, $n=2$.

As an example, consider the following configuration of a superheavy load (SHL) shown in Figure Figure 5-2:

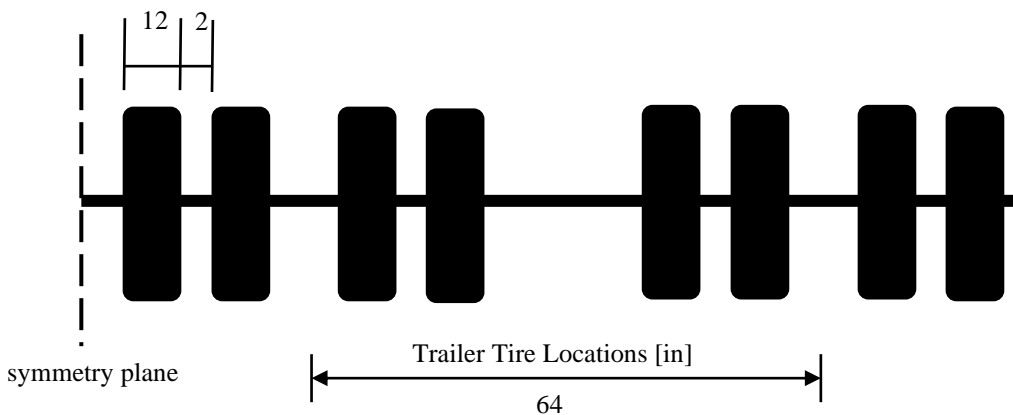**Figure 5-2: Schematic showing the dimensions in a one-half of an axle (not drawn to scale)**

Gross vehicle weight of the SHL = 4,660,000 lbs
number of trailers = 2
Gross weight of each platform trailer = 2,080,000 lbs
number of axles in each platform trailer = 26
number of tires in each axle = 16
weight on each tire = 5000 lbs
pressure on each tire = 100 psi

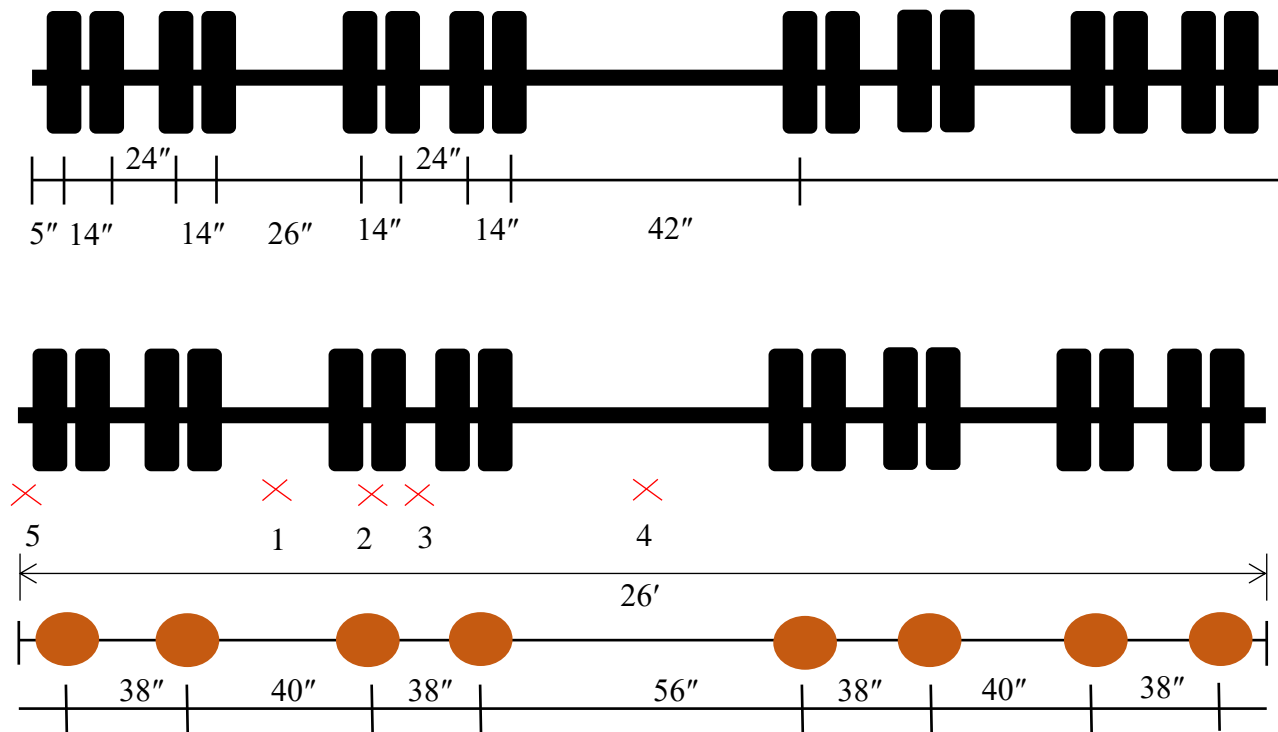The dual tires are represented by a circle as shown in Figure 5-3.

Figure 5-3: Dual tires in an axle represented with equivalent circles (not drawn to scale)

The contact radius for the dual tire is determined as shown in Eq. (44):

$$r = \sqrt{\frac{2 \times A_c}{\pi}} = \sqrt{\frac{2 \times \frac{5000}{100}}{\pi}} = 5.64 \; in \tag{44}$$

The red crosses shown in Figure 5-3 show the possible locations where the pavement response could be evaluated for determination of the nucleus based on the tire configuration in the transverse direction. For the SHL analysis, the pavement response corresponding to the critical distresses in each marked location need to be determined. In this study, bottom-up fatigue cracking and rutting in the AC layer and failure of subgrade were assumed to be the critical distress. Thus, strain at the bottom of the AC layer and stress & strain at the top of the subgrade layer need to be determined.

The process for determining the nucleus is demonstrated for Locations 1 and 2 in Figure 3.

5.2.1   Location 1

First, a single axle with tires on both sides of Location 1 was considered for the calculation of pavement response using layer elastic analysis (LEA). The computer program JULEA was used for response calculation at the centerline of each dual tire load at the critical locations. Various load configurations considered for nucleus determination for Location 1 are shown in Figure 5-4, with the loads colored in blue representing those that are being considered for the nucleus analysis.

As an example, Figure 5-4(a) shows that only the two loads directly adjacent to Location 1 are being considered for the nucleus analysis.
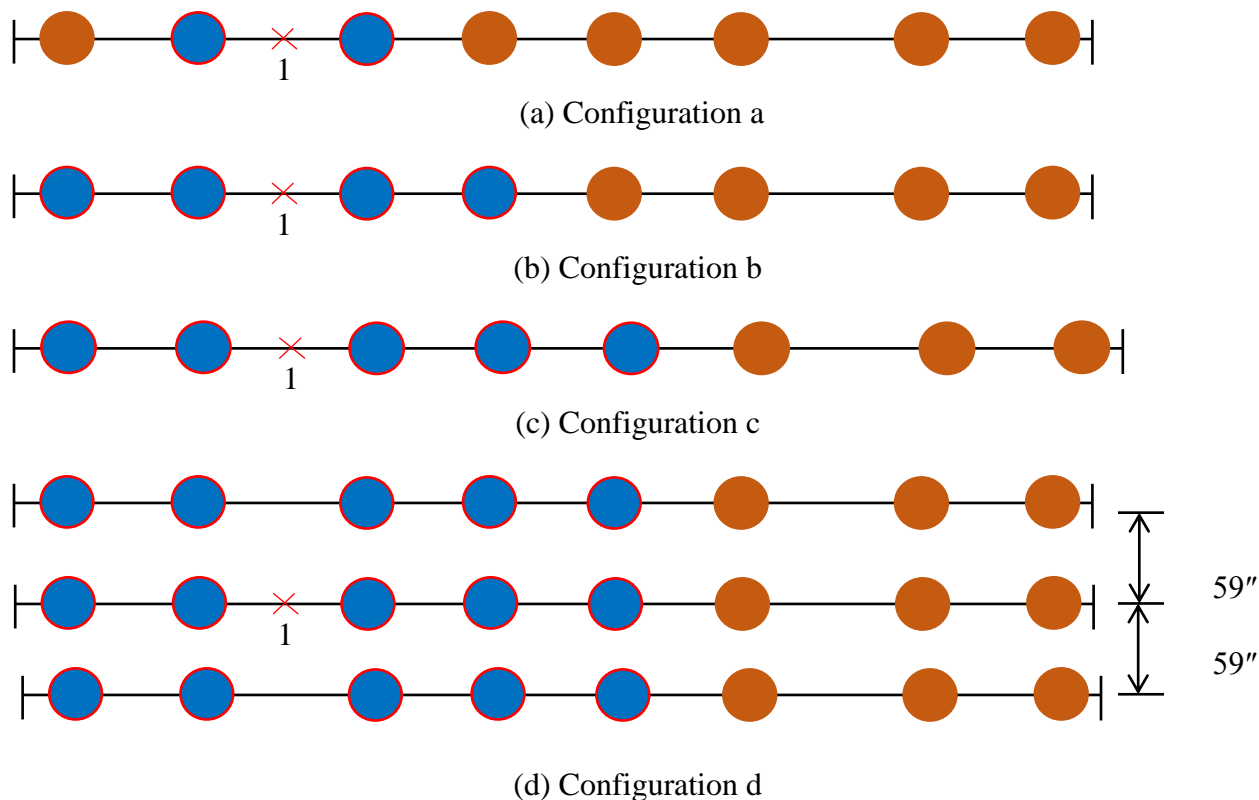

(a) Configuration a

(b) Configuration b

(c) Configuration c

(d) Configuration d

Figure 5-4: Different configurations considered for nucleus determination for Location 1

Table 5-2 shows the pavement responses for various Configurations shown in Figure 5-4. For each configuration, pavement responses were obtained at the critical locations under each load. The maximum responses obtained at each critical locations are reported in Table 5-2. From this table, it can be observed that the stress and strain variations at the bottom of AC, mid-depth of AC and at the top of the subgrade are less than 5.0% between configurations b and c. In addition, Table 5-2 also shows that the maximum strain at the mid-depth and bottom of AC, and the maximum stress on top of the subgrade occur in two different configurations. For this particular response location, the loads considered in Configuration b and Configuration d should become the nucleus of the platform trailer for the analysis of fatigue in AC and rutting, respectively.

However, as shown in Figure 5-3, the pavement responses associated with other potentially critical locations need to be investigated to find the most representative nucleus for the SHL analysis.

Table 5-2: Pavement responses for Location 1

Configuration No.	Number of Axle	Number of Representative Loads	Horizontal Tensile Strain at AC Bottom (µε)	Vertical Compressive Strain at Mid-Depth of AC (µε)	Stress at Top of SG (psi)
a	1	2	174.4	158.8	7.4
b	1	4	176.6	158.9	7.9
c	1	5	176.4	159.8	7.9
d	3	15	169.3	160.7	8.3

5.2.2 *Location 2*

Similar to Location 1, various load configurations were considered to identify the location of the nucleus for Location 2, as shown in Figure 5-5. The pavement responses obtained for these different configurations are provided in Table 5-3.
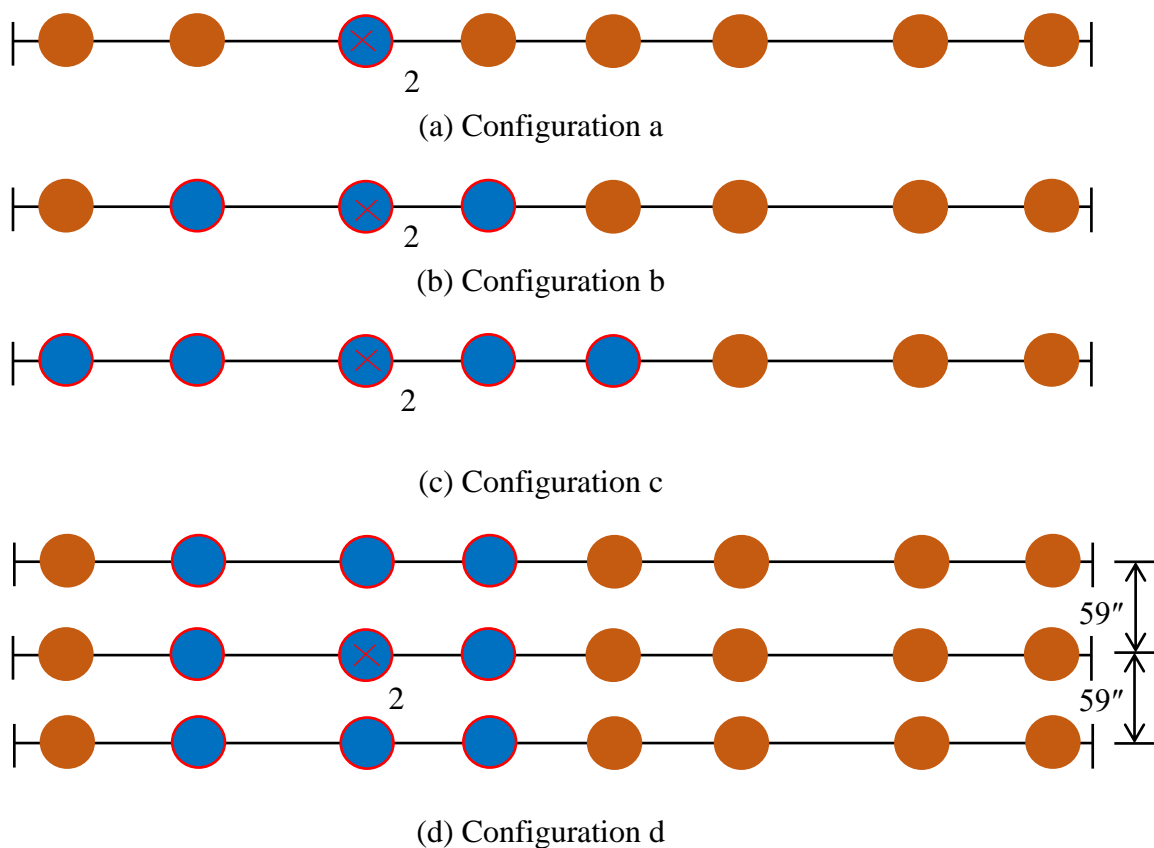

(a) Configuration a

(b) Configuration b

(c) Configuration c

(d) Configuration d

Figure 5-5: Different configurations considered for nucleus determination for Location 2

(e) Configuration e

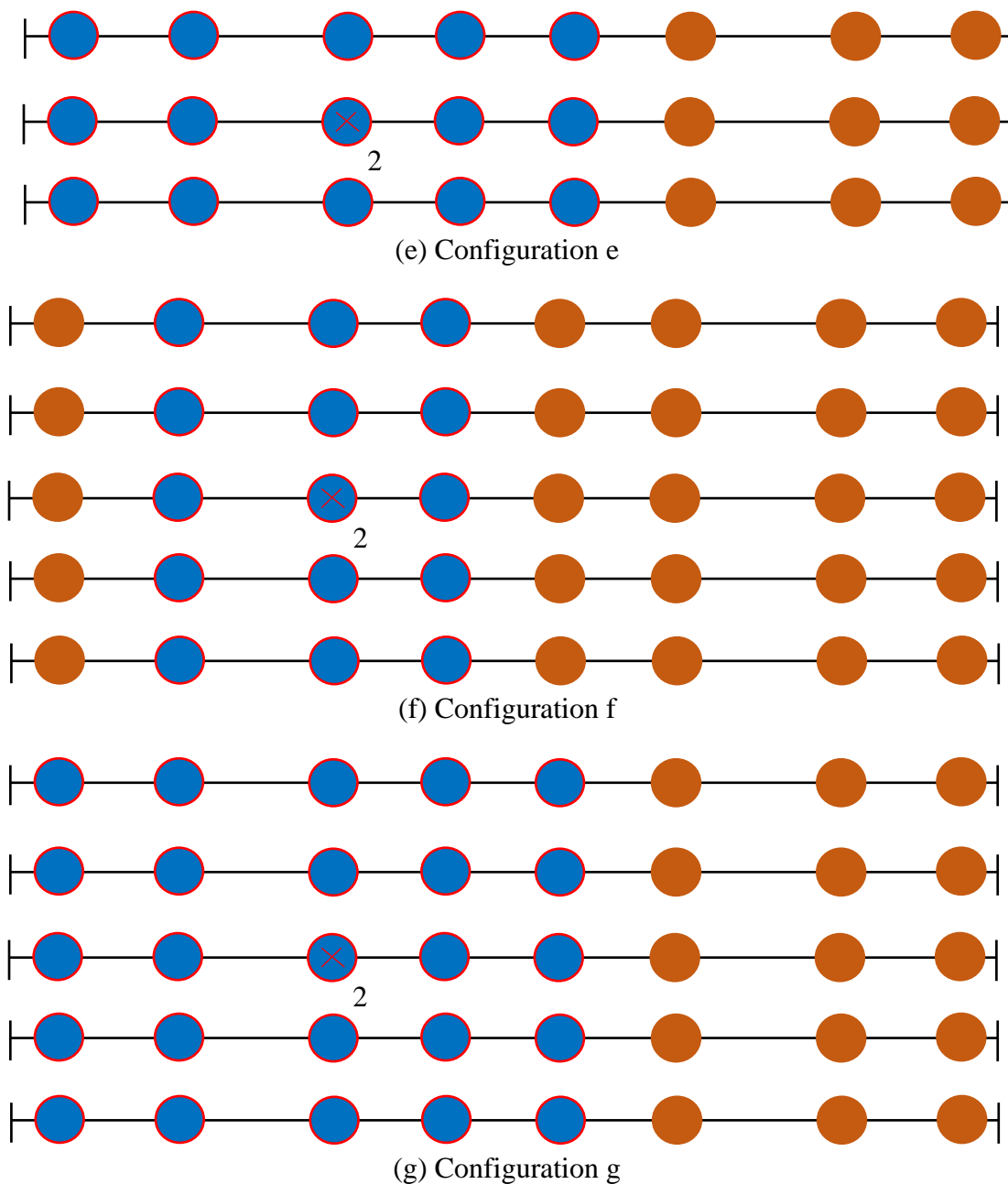

(f) Configuration f

(g) Configuration g

Figure 5-5: Different configurations considered for nucleus determination for Location 2

Table 5-3 shows that the strain at the bottom of AC under Configuration a, in which only a single representative load was considered, was found to be 172.5 $\mu\varepsilon$. The table also shows that when two additional loads were added in the transverse direction (one on each side), the strain at the bottom of AC was increased to 176.8 $\mu\varepsilon$ (See Configuration b). On the other hand, when two additional loads were added (i.e., Configuration c, shown in Figure 5(c)), the tensile strain at the bottom of the AC did not increase significantly. Moreover, a tensile strain value of 176.8 $\mu\varepsilon$ (obtained for Configuration b with 3 representative loads) at the bottom of AC was very close to the maximum tensile strain obtained for Location 1 with 4 or 5 loads. In addition, this strain value was not lower

than any horizontal tensile strain values observed in Location 1. Thus, Configuration b of Location 2 was considered to be the nucleus of the SHL for bottom-up fatigue cracking and rutting analysis.

Similarly, the stress at the top of the subgrade layer was found to be 8.3 psi for Configuration d. Adding extra loads in the longitudinal direction of travel did not cause any significant changes in the subgrade responses. Furthermore, a stress value of 8.3 psi at the top of the subgrade in Configuration d of Location 2 (with 9 representative loads) was equivalent to that of Location 1 with more number of tires considered. Therefore, Configuration d of Location 2 was considered as the nucleus of the SHL for the analysis of rutting.

Between two successive locations, if the critical response for a particular distress did not vary by more than 1%, then the response with a lower number of axles and representative load combination was taken to be the nucleus for practical purposes. This was done because although adding more tires and axles outside the nucleus might increase the response, no practical significance would have been observed in the calculated distresses if the gain in response was below a certain threshold, which was chosen to be 1% in this study.

Table 5-3: Pavement responses for Location 2

Configuration No.	Number of Axle	Number of Representative Loads	Horizontal Tensile Strain at AC Bottom ($\mu\varepsilon$)	Vertical Compressive Strain at Mid-Depth of AC ($\mu\varepsilon$)	Stress at Top of SG (psi)
a	1	1	172.5	159	6.9
b	1	3	176.8	158.8	7.9
c	1	5	176.5	159.8	7.9
d	3	9	173.4	160.7	8.3
e	3	15	172.6	160.1	8.3
f	5	15	173.5	160.3	8.3
g	5	25	172.8	160.7	8.3

Figure 5-6, Figure 5-7 and Figure 5-8 show the various configurations considered for the identification of the possible location of SHL nucleus for Location 3, 4 and 5. Table 5-4, Table 5-5 and Table 5-6 show the associated maximum pavement responses for Figure 5-6, Figure 5-7 and Figure 5-8, respectively.
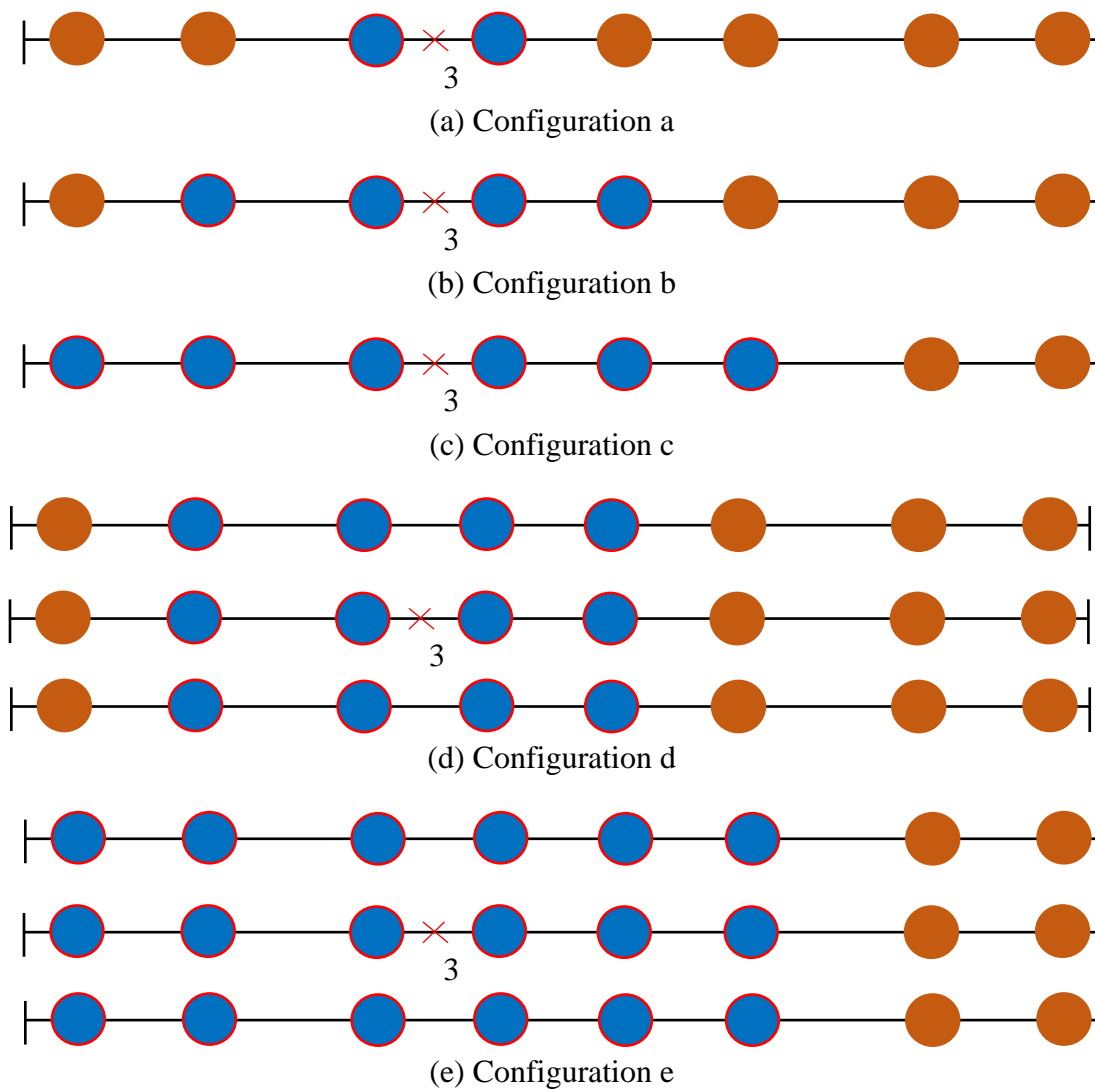
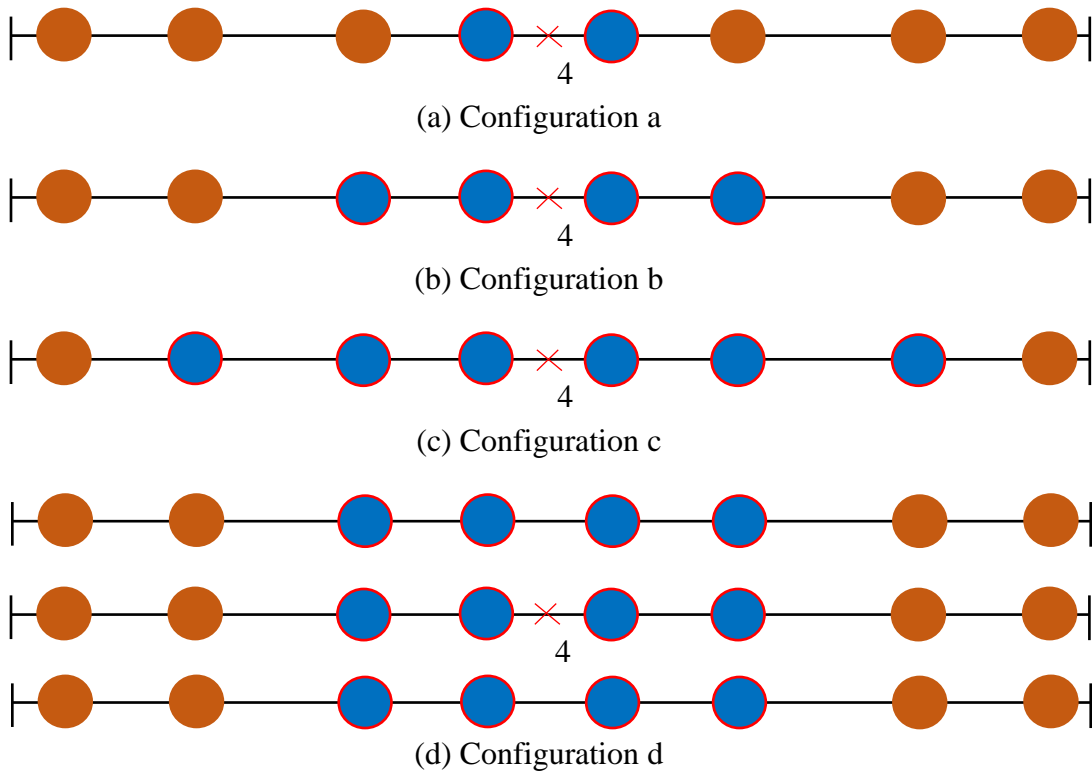**Figure 5-6: Different configurations considered for nucleus determination for Location 3**

Figure 5-7: Different configurations considered for nucleus determination for Location 4
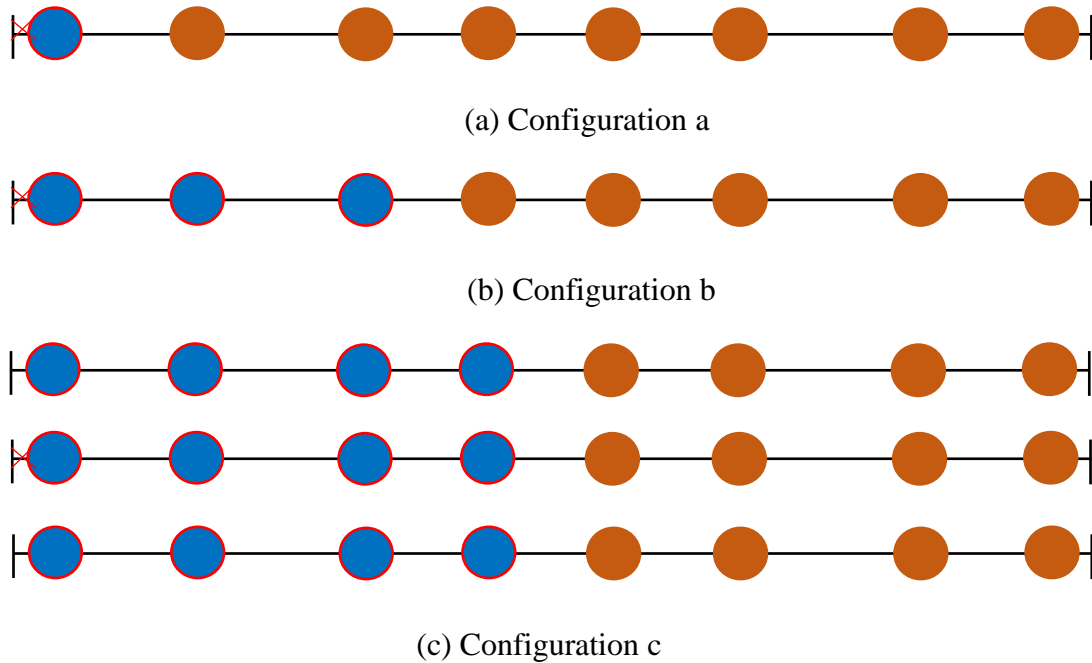

Figure 5-8: Different configurations considered for nucleus determination for Location 5

Table 5-4, Table 5-5 and Table 5-6 show that pavement responses determined for possible nucleus Locations of 3, 4 and 5 are not any higher than the responses observed for Location 2. Thus, the two nuclei found for Location 2 is the nuclei of the SHL considered in this study.

Table 5-4: Pavement responses for Location 3

Configuration No.	Number of Axle	Number of Representative Loads	Horizontal Tensile Strain at AC Bottom (με)	Vertical Compressive Strain at Mid-Depth of AC (με)	Stress at Top of SG (psi)
a	1	2	174.8	158.6	7.4
b	1	4	175	159.8	7.6
c	1	6	176.4	159.2	7.9
d	3	12	171.6	160.5	7.9
e	3	18	172.4	160.8	8.3

Table 5-5: Pavement responses for Location 4

Configuration No.	Number of Axle	Number of Representative Loads	Horizontal Tensile Strain at AC Bottom (με)	Vertical Compressive Strain at Mid-Depth of AC (με)	Stress at Top of SG (psi)
a	1	2	172.8	159.7	7.04
b	1	4	174.9	158.9	7.6
c	1	6	176.7	159.1	8.0
d	3	12	171.7	160.4	7.9

Table 5-6: Pavement responses for Location 5

Configuration No.	Number of Axle	Number of Representative Loads	Horizontal Tensile Strain at AC Bottom (με)	Vertical Compressive Strain at Mid-Depth of AC (με)	Stress at Top of SG (psi)
a	1	2	174.8	158.6	7.5
b	1	3	176.8	158.8	7.9
c	3	12	173	159.9	8.3

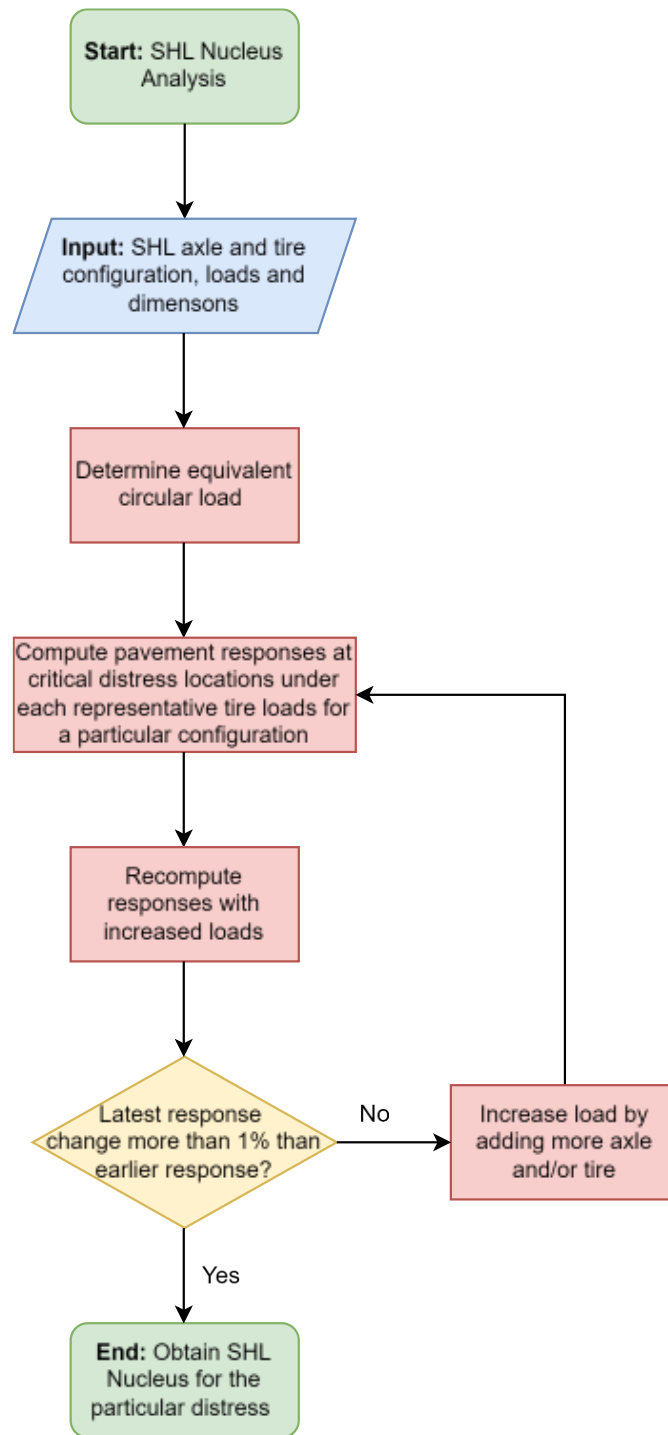The flowchart for SHL nucleus analysis is shown in Figure 5-9.

Figure 5-9: Flowchart for SHL nucleus analysis

The required parameters and the assumed values for SHL nucleus analysis are shown in Table 5-7.

Table 5-7: Parameters and assumed values for SHL analysis

SHL Nucleus Analysis Parameters	Assumed Values
Gross Vehicle Weight	4,660,000.00 lbs
Number of Trailers	2
Number of Axles	52
Number of Tires in Each Axle	16
Weight on Each Tire	5000 lbs
Tire Pressure	100 psi
Axle and Tire Spacing	From Schematic of SHL
AC Thickness	6 inch
Base Thickness	10 inch
Number of lifts in AC	2
AC Modulus	350000 psi
Base Modulus	80000 psi
Subgrade Modulus	20000 psi

5.3   Distresses in AC

In this study, the following distresses were considered to evaluate the impact of SHL movement through flexible pavements:

(a) Fatigue cracking
(b) Rutting

5.3.1   Fatigue Cracking

In this study, the Equivalent Single Axle Load (ESAL) was determined based on the repetitions of the nucleus load for the SHL using Eq. (37) to (49). ESAL is determined using Equivalent Axle Load Factor (EALF), which is a measure to calculate the damage caused to a pavement due to the passing of a non-standard axle compared to the damage caused by a standard axle. The standard axle is considered to be an 18-kip (80-kN) single axle load. The concept of ESAL is generally used in the empirical methods of pavement design, such as the one used by FDOT for flexible pavements.

$$log\left(\frac{W_{tx}}{W_{t18}}\right)_f = 4.79\,log(18+1) - 4.79\,log(L_x + L_2) + 4.33\,log(L_2) + \frac{G_t}{\beta_x} - \frac{G_t}{\beta_{18}} \tag{37}$$

$$G_t = log\left(\frac{4.2 - p_t}{4.2 - 1.5}\right) \tag{38}$$

$$\beta_x = 0.4 + \frac{0.081(L_x + L_2)^{3.23}}{(SN + 1)^{5.19}L_2^{3.23}} \tag{39}$$

$$EALF = \frac{W_{t18}}{W_{tx}} \tag{40}$$

$$ESAL = n_{nucleus} \times EALF \tag{41}$$

where, W_{tx} = number of x load applications at the end of time t
W_{t18} = number of 18-kip (80-kN) load applications at the end of time t
L_x = load in the nucleus axle (in kip)
L_2 = axle code: 1- single axle, 2-tandem axles, 3-tridem axles
SN = structural number of the pavement, taken as 5
p_t = terminal condition when pavement is considered, taken as 2.5
$\beta_{18} = \beta_x$ when L_x is equal to 18 and L_2 equals to 1
$n_{nucleus}$ = repetitions of the nucleus of the SHL

There are 16 tires in the SHL axle, and each tire has a load of 5-kip. Thus, the total load in the SHL axle, L_x, is 80-kip. As the nucleus determined for fatigue cracking had a single axle, the value of L_2 was taken to be 1. Using the structural number (SN) and terminal serviceability index (p_t) in Eq. (38) and (39), the following values G_t and β_x can be obtained as shown in (42) and (43).

$$G_t = \log\left(\frac{4.2 - 2.5}{4.2 - 1.5}\right) = -0.2 \tag{42}$$

$$\beta_x = 0.4 + \frac{0.081(80 + 1)^{3.23}}{(5 + 1)^{5.19}1^{3.23}} = 11.22 \tag{43}$$

$$\beta_{18} = 0.4 + \frac{0.081(18 + 1)^{3.23}}{(5 + 1)^{5.19}1^{3.23}} = 0.5 \tag{44}$$

Inserting the values of G_t, β_x and β_{18} in Eq. (37), the following value of logarithm of EALF can be obtained:

$$log\left(\frac{W_{tx}}{W_{t18}}\right)_f = 4.79\,log(18 + 1) - 4.79\,log(80 + 1) + 4.33\,log(1) + \frac{(-0.2)}{11.22} - \frac{(-0.2)}{0.5} = -2.63 \tag{45}$$

From Eq. (40), the EALF can be determined as

$$EALF = \frac{1}{10^{-2.63}} = 429.08 \tag{46}$$

As shown before, each individual axle comprises the nucleus of the SHL for fatigue damage. There are 52 axles for the SHL considered in this study. Thus, the nucleus is repeated 52 times. Therefore, from Eq. (41), the corresponding ESAL is determined to be:

$$ESAL = 52 \times 429.08 = 22312 \tag{47}$$

Therefore, using the steps outlined above, it was found that a single pass of the SHL platform trailer is equivalent to around 22,312 passes of single axle 18-kip load.

Using 18-kip single axle load with dual tires as the standard axle, layer elastic analysis was conducted to find the strain at the bottom of AC. The standard axle load is shown in Figure 5-10.
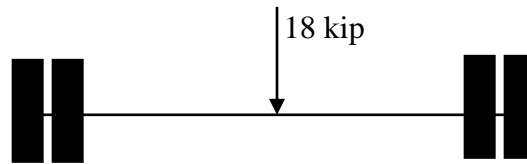

Figure 5-10: Standard 18-kip single axle with dual tires

From Eq. (35), the contact radius of the dual tires, shown in Figure 5-10, was determined to be 5.35 inch. Similar to the SHL tire, a contact pressure of 100 psi was used for the 18-kip single axle dual tires. For a load of 9,000 lbs and contact area of 90 in², the strain at the bottom of AC was determined to be 164.7 $\mu\varepsilon$.

Now, using the strain (ε_t) at the bottom of AC and modulus of the AC layer (E_{AC}), the allowable number of load repetitions for fatigue cracking (N_f) can be determined using the relation developed by the Asphalt Institute, as shown in Eq. (48)

$$N_f = 0.0796\varepsilon_t^{-3.291}E_{AC}^{-0.854} \tag{48}$$

Assuming that the equivalent number of single axle passes for the SHL can be estimated by the ESAL calculated previously, the fatigue damage due to a single pass of the SHL can be estimated using the following equation.

$$Damage\ (\%) = 100 \times \frac{ESAL}{N_f} \tag{49}$$

The strain at the bottom of the AC layer under an 18-kip single axle was found to be 164.7 $\mu\varepsilon$. Thus, using AC modulus of 350,000 psi and Eq. (48), the fatigue life N_f was determined to be 4,141,335. Therefore, fatigue damage in the AC layer for a single pass of the SHL platform trailer is calculated to be 0.54% using Eq. (49).

5.3.2 Rutting

In this study, rutting in the AC layer due to passing of the SHL is determined using the equations adopted by Mechanistic-Empirical Pavement Design Guide (MEPDG) (AASHTO, 2010). Rutting in AC layer can be determined using Eq. (50) to (53)

$$\Delta_{p(AC)} = \beta_{1r} k_z \varepsilon_{r(AC)} 10^{k_{1r}} n^{k_{2r}\beta_{2r}} T^{k_{3r}\beta_{3r}} \tag{50}$$

$$k_z = (C_1 + C_2 D) \times 0.328196^D \tag{51}$$

$$C_1 = -0.1039 \times H_{AC}^2 + 2.4868 \times H_{AC} - 17.342 \tag{52}$$

$$C_2 = 0.0172 \times H_{AC}^2 - 1.7331 \times H_{AC} + 27.428 \tag{53}$$

where,
$\Delta_{p(AC)}$ = plastic strain accumulated in AC layer
T = pavement temperature
D = depth below the surface
H_{AC} = thickness of the AC layer
k_{1r}, k_{2r}, k_{3r} = global field calibration parameters with the value of k_{1r}, k_{2r}, and k_{3r} taken to be -3.35412, 0.4791, and 1.5606, respectively.
β_{1r}, β_{2r}, β_{3r} = mixture specific calibration parameters, taken to be 1
n is the number of loads repetitions

The AC rutting calibration coefficients used in this study were obtained from the recalibration of MEPDG project, NCHRP 1-40D (Darter et al., 2006; Robbins et al., 2017). As mentioned previously, the thickness of the AC layer was taken to be 6 inches. It was also assumed the AC layer is constructed in two lifts, with mid depth temperatures of these two lifts being 90° and 85°F, respectively.

Using the thickness of the AC layer, and Eq. (52) and (53), the values of C_1 and C_2 are calculated to be -2.864 and 11.817.

For the top 3.0-in. AC lift, $D = 1.5$ in. for the mid-depth. At this depth, a passing of an 18-kip single axle load with dual tires causes a vertical strain of 105.7 $\mu\varepsilon$. Similar to the fatigue analysis, it was assumed that the equivalent number of single axle passes for the SHL can be estimated using the ESAL concept. However, unlike fatigue, the number of axles in SHL nucleus was three for rutting. Thus, the total axle load, L_x, was 192 kip (80×3=240 kip), and SHL nucleus was repeated 52/3 =17.33 times for a single pass. Using the axle code $L_2 = 3$, along with the updated L_x and SHL repetitions, the ESAL was calculated to be 12,328 from Eq. (37) to (41). Therefore, a single pass of an SHL platform trailer is equivalent to 12,328 passes of an 18-kip single axle for rutting. Using Eq. (50), the accumulated rut at mid-depth of the first lift of the AC layer was determined to be 0.018 inch. For the second lift of AC, the value of D was 4.5 inch. At this depth, passing of a single axle 18-kip load causes vertical strain of 186 $\mu\varepsilon$. Using Eq. (50), the accumulated rut at mid-depth

of the second lift of the AC layer was determined to be 0.004 inch. Therefore, the total rut in the AC layer due to the passing of the SHL platform trailer is found to be $\Delta_{p(AC)} = (0.018 + 0.004)$ inch = 0.022 inch.

5.4 Failure of Subgrade

Subgrade is the weakest layer of the flexible pavement structure. The following failure modes were considered for the subgrade failure due to the movement of the SHL:

(a) Ultimate bearing capacity failure
(b) Localized shear failure

5.4.1 Ultimate Bearing Capacity of Subgrade Soil

With the nonconventional axle and tire loadings and configurations, the vertical stress distribution below the pavement surface under a superheavy vehicle will lead to higher and overlapping stress distributions as compared to normal live load models and applied stresses. These stresses can result in a critical limit state condition of instantaneous global bearing failure or localized serviceability failure in the subgrade.

The first step in the analysis is to determine the soil shear properties and parameters that would be used to assess the subgrade capacity against global bearing capacity and localized shear failures. For global bearing capacity failure, the shear strength parameters (friction angle, ϕ, and cohesion, c) of the subgrade layers are required. These parameters can be determined either from laboratory testing or estimated using geotechnical subsurface information. Nabizadeh et al. (2019) recommends the usage of multiple levels of FWD load to determine the shear strength parameters of the soil. Although their approach utilizes convenient nondestructive testing to determine the shear strength parameters of the subgrade, it has some shortcomings. In this study, the shear strength properties of the subgrade soils can be determined based on soil samples and the corresponding typical shear strength parameters based on their classification. If the soil samples cannot be determined, then design or historical data should be used to identify the subgrade soil type and subsequently the shear strength parameters.

In this study, Meyerhof's equation was used to determine the ultimate bearing capacity of the subgrade soil, as shown in Eq. (54)

$$q_u = c' N_c F_{cs} F_{cd} F_{ci} + q N_q F_{qs} F_{qd} F_{qi} + \frac{1}{2} \gamma B N_\gamma F_{\gamma s} F_{\gamma d} F_{\gamma i} \tag{54}$$

where, c' = cohesion of soil, q = effective stress at the bottom of the foundation, γ = unit weight of the soil, B = width of foundation, $F_{cs}, F_{qs}, F_{\gamma s}$ = shape factors, $F_{cd}, F_{qd}, F_{\gamma d}$ = depth factors, $F_{ci}, F_{qi}, F_{\gamma i}$ = load inclination factors, N_c, N_q, N_γ = bearing capacity factors.

As mentioned previously, the SHL considered for demonstration has two platform trailers. The length (L) and width (B) of each platform trailer were 123.0 ft. and 20.0 ft., respectively. The stress on the top of subgrade is needed to determine the ultimate bearing capacity of the subgrade soil. For the analysis, the load and area of one trailer was used. The loads on one platform trailer are 2,080,000 lbs. Dividing

this weight with the length and width of the platform trailer provide the average stress on the subgrade soil for ultimate bearing capacity analysis, which is 5.9 psi. Subgrade stress determined from nucleus analysis, shown in Table 5-3, will be used for the element level localized shear failure, which will be discussed in the next section.

Based on a soil report from Collier County, FL, subgrade is taken to be comprised of silty sand (Ardaman & Associates, Inc., 2019). For bearing capacity analysis on a silty sand, a typical value of ϕ 30° with no cohesion ($c = 0$) is considered in this study.

Based on the unit weights of the pavement layers, shown in Figure 5-11, the value of effective stress (q) at top of the subgrade is determined as $q = (6/12)\times145+(10/12)\times130 = 180.83$ lb/ft^2
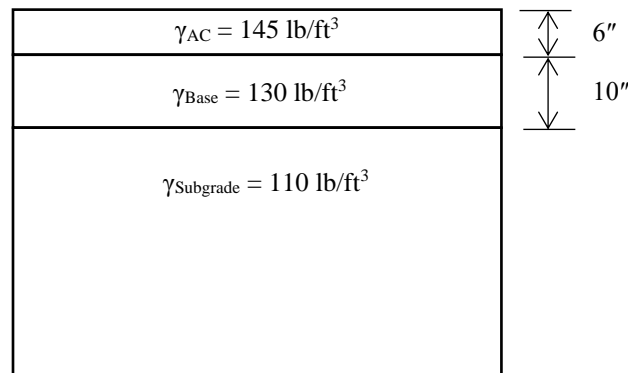

Figure 5-11: Unit weights of different pavement layers

For the case considered, the depth of foundation or subgrade soil was $D_f = 1.33'$ (16 inch). Therefore, the ratio of D_f/B becomes

$$\frac{D_f}{B} = \frac{1.33}{20} = 0.067 < 1 \tag{55}$$

The bearing capacity factors can be either determined using chart or the Eqs. (56) and (58)

$$N_q = \tan^2\left(45 + \frac{\emptyset}{2}\right)e^{\pi\tan\emptyset} = \tan^2\left(45 + \frac{30}{2}\right)e^{\pi\tan 30°} = 18.4 \tag{56}$$

$$N_c = \left(N_q - 1\right)\cot\emptyset = (18.4 - 1)\cot 30° = 30.139 \tag{57}$$

$$N_\gamma = 2\left(N_q + 1\right)\tan\emptyset = 2(18.4 + 1)\tan 30° = 22.4 \tag{58}$$

The shape and depth factors can be determined using Eqs. (59) and (64)

$$F_{qs} = 1 + \left(\frac{B}{L}\right)\tan\emptyset = 1 + \left(\frac{20}{123}\right)\tan 30° = 1.09 \tag{59}$$

$$F_{qd} = 1 + 2\tan\emptyset\,(1 - \sin\emptyset)^2\left(\frac{D_f}{B}\right) = 1 + 2\tan 30°\,(1 - \sin 30°)^2\left(\frac{1.33}{20}\right) = 1.019 \qquad (60)$$

$$F_{cd} = F_{qd} - \frac{1 - F_{qd}}{N_c\tan\emptyset} = 1.019 - \frac{1 - 1.019}{30.139\times\tan 30°} = 1.02 \qquad (61)$$

$$F_{\gamma s} = 1 - 0.4\left(\frac{B}{L}\right) = 1 - 0.4\left(\frac{20}{123}\right) = 0.935 \qquad (62)$$

$$F_{\gamma d} = 1 \qquad (63)$$

$$F_{cs} = 1 + \left(\frac{B}{L}\right)\left(\frac{N_q}{N_c}\right) = 1 + \left(\frac{20}{123}\right)\left(\frac{18.4}{30.139}\right) = 1.099 \qquad (64)$$

All the inclination factors are one, as the applied load does not have any angle with the vertical direction. The equations for shape and depth factors for other soil types or geometric conditions can be obtained elsewhere (Nabizadeh et al., 2019).

Plugging all the factors, the value of ultimate load per unit area (q_u) can be determined, as shown in Eq. (65).

$$q_u = \frac{0\times 30.13\times 1.099\times 1.02\times 1 + 180.83\times 18.4\times 1.09\times 1.019 + \frac{1}{2}\times 110\times 20\times 22.4\times 0.935\times 1}{144} \qquad (65)$$
$$= 185.7\ \text{psi}$$

Generally, a Factor of Safety (FS) of three is used for the ultimate bearing capacity of soils (Das & Sivakugan, 2018). Therefore, the allowable load per unit area (q_{allow}) can be estimated using Eq. (66).

$$q_{allow} = \frac{q_u}{FS} = \frac{185.7}{3} = 61.9\ \text{psi} \qquad (66)$$

As, $q_{allow} > 5.9$ psi, the movement of the SHL will not cause any failure in the subgrade due to exceedance of the ultimate bearing capacity. The above calculation of bearing capacity was conducted for a single soil type, silty sand. For different types of soil, only the cohesion (c) and angle of internal friction (φ) will change. The analysis steps outlined in the study will remain the same. Ultimate bearing capacity of subgrade soil for various combinations of soil properties, i.e., cohesion (c) and angle and internal friction (φ), is shown in Table 5-8.

Table 5-8: Variation of allowable bearing capacity with different soil properties

Cohesion (c)	Angle of Internal Friction (φ)	Allowable Ultimate Bearing Capacity (psi)	Applied Stress from SHL (psi)	Satisfactory
15	0	4.36	5.9	No
30	0	8.31	5.9	Yes
0	15	8.1	5.9	Yes
15	15	16.7	5.9	Yes
30	15	25.35	5.9	Yes
0	30	61.9	5.9	Yes
15	30	86.43	5.9	Yes
30	30	110.9	5.9	Yes

Along with the ultimate bearing capacity failure, another critical mode of failure can be the slope instability at the edge of the pavement. Unlike a flat surface, the foundation on the edge of a slope has asymmetric shearing surfaces on both sides of the foundation. This asymmetry at the edge of the slope can provide reduced shearing resistance and lead to bearing capacity failure due to the loads from SHL. To avoid any potential issues regarding the bearing capacity, SHLs should use controlled traffic to keep them away from the sloped edge of the pavement.

5.4.2   Service Limit State and Localized Shear Failure

In addition to the ultimate limit state evaluation through the bearing capacity analysis, service limit state can be a major concern for super heavy loads. This limit state includes a localized shear failure analysis and deflection-based analysis. Localized shear failure can occur in regions where the stresses exceed the yield limit, leading to local instability and excessive deformations. Multiple yield criteria can be found in the literature including the Mohr-Coulomb criterion and the Drucker-Prager yield criterion. Implementing these models and analyses require some involved shear parameters characterization in the lab and using typical parameters from soil classification can be misleading. A general description of the Drucker-Prager yield criterion is described in the following subsection.

5.4.2.1   Drucker-Prager Yield Criterion

In 1952, Drucker and Prager extended the concept of metal plasticity to geomaterials (Drucker & Prager, 1952). Similar to von Mises approximation of the Tresca criterion for metals, Drucker-Prager represents a smooth approximation of the Mohr-Coulomb failure surface in three dimensions. The mathematical representation of the Drucker-Prager failure surface is shown in Eq. (67)

$$f(\sigma_{oct}, \tau_{oct}) = \frac{3}{\sqrt{2}}|\tau_{oct}| - \alpha\sigma_{oct} - \beta = 0 \tag{67}$$

where, τ_{oct} is the octahedral shear stress, σ_{oct} is the octahedral normal stress, and α and β are the material constants, and they are functions of the cohesion (c) and angle of internal friction (ϕ) of the soil. In the octahedral plane, Drucker-Prager yield criterion can be represented using Figure 5-12.
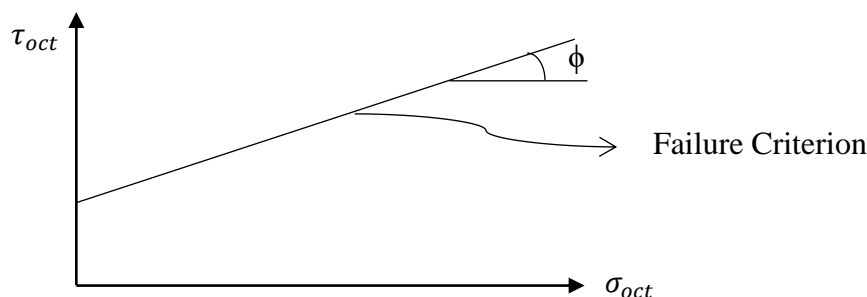

Figure 5-12: Drucker-Prager failure criterion plotted on octahedral plane.

In octahedral plane, the Drucker-Prager yield criterion is a straight line. Factor of safety can be defined as the ratio between the applied stress and octahedral stress at failure. Factor of safety is a measure of how far the state of stress of an element is situated on the octahedral plane from the failure surface.

Past studies have also adopted the Drucker-Prager yield criterion for identifying the localized shear failure in the subgrade soil (Nabizadeh et al., 2019) Stress on the critical element is used to determine the capacity of the subgrade soil against the localized shear failure. The critical element can be idealized as an elemental block of soil where the stress may first exceed the capacity upon loading beyond a threshold limit. In this study, the critical element is taken to be the subgrade nucleus located at the top of the subgrade to be on the conservative side.

It is important to note that localized shear failure is different from local shear failure under ultimate limit states. Local shear failure typically occurs under excessive load in loose soil. The failure surface in local shear cannot reach the surface; rather, it is confined within OC and OA, as shown in Figure 5-13. Local shear failure is not typically a concern for subgrade soil, as it is compacted with a relative density of more than 95%. Vesic showed that for a relative density of more than 70% and $D_f/B < 1$, general shear failure is typically the governing mode of failure (Vesic, 1973; Das & Sivakugan, 2018).
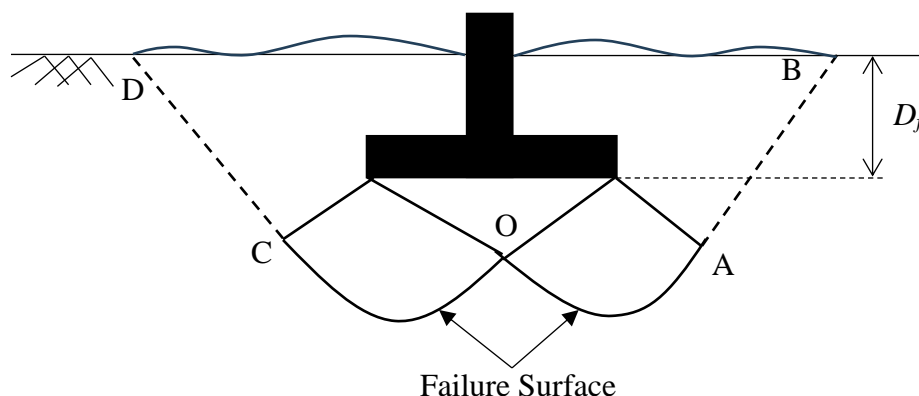

Figure 5-13: Local shear failure of soil

On the contrary, localized shear failure does not necessarily involve a full failure surface, but an individual element reaches the critical yield state. The following steps, adopted by Nabizadeh et al.

(2019), can be followed to determine the localized shear failure in the subgrade soil according to the Drucker-Prager yield criterion:

1. The principal stresses at the top of the subgrade due to nucleus of SHL should be determined from the layer elastic analysis.
2. The value of cohesion (c) and angle of internal friction (ϕ) of the subgrade soil should be determined from the soil sample collected from the field or from design data.
3. Using the principal stresses, two stress invariants, octahedral normal stress (σ_{oct}) and octahedral shear stress (τ_{oct}) is calculated using Eq. (68) and (69).

$$\sigma_{oct} = \frac{1}{3}(\sigma_1 + \sigma_2 + \sigma_3) \tag{68}$$

$$\tau_{oct} = \frac{1}{3}\sqrt{(\sigma_1 - \sigma_2)^2 + (\sigma_2 - \sigma_3)^2 + (\sigma_3 - \sigma_1)^2} \tag{69}$$

4. After the stress invariants are determined, the Factors of Safety (FOS) against local shear failure is determined using Eq. (70)

$$FOS = \frac{\alpha\sigma_{oct} + \beta}{\frac{3}{\sqrt{2}}|\tau_{oct}|} \tag{70}$$

where, α and β are function of cohesion and angle of internal friction. They are determined using Eq. (71) and (72)

$$\alpha = \frac{6\sin\phi}{3 - \sin\phi} \tag{71}$$

$$\beta = \frac{6c\cos\phi}{3 - \sin\phi} \tag{72}$$

A FOS of 2 is generally accepted for the localized shear failure.

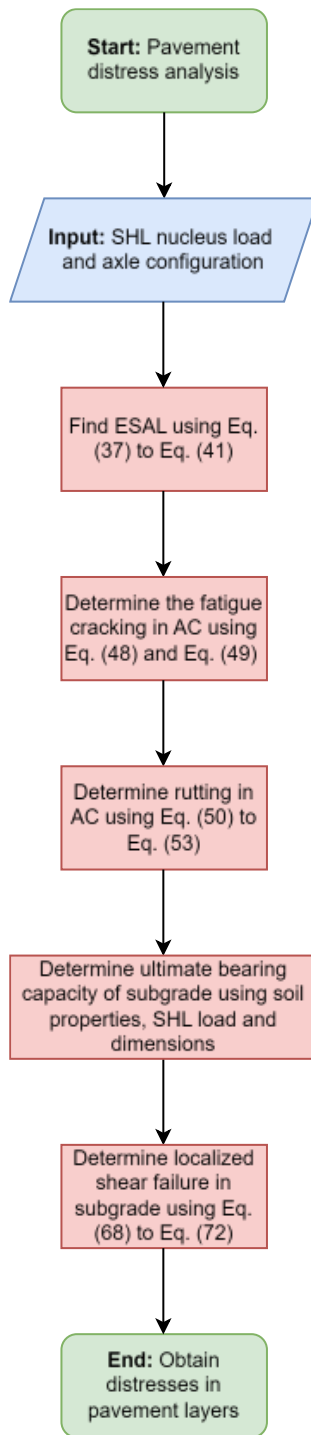The flowchart for pavement distress analysis is shown in Figure 5-14.

Figure 5-14: Flowchart for pavement distress analysis

The required parameters and the assumed values for pavement distress analysis is shown in Table 5-9.

Table 5-9: Parameters and assumed values for distress analysis

Performance Evaluation Parameters	Assumed Values
Standard Axle	18000 lbs
Axle Type	1
Terminal serviceability index	2.5
Structural Number (SN)	5
Repetitions of SHL Nucleus	52
Strain at AC bottom -for fatigue cracking	Obtained from SHL nucleus
Strain at mid-depth of AC lifts -for AC rutting	Obtained from SHL nucleus
k_{1r}	3.35412
k_{2r}	0.4791
k_{3r}	1.5606
β_{1r}	1
β_{2r}	1
β_{3r}	1
Soil Type	Obtain from field test (in this study assumed silty sand)
Cohesion of subgrade soil (c)	0
Angle of internal friction (φ)	30°

6 CONCLUSIONS AND RECOMMENDATIONS

This report analyzed the WIM data from 2011-2022 for various stations around the state of Florida. Depending on the functional class of pavement where the WIM stations are located, the analyzed data were grouped into four categories: limited rural, limited urban, non-limited rural, and non-limited urban. Along with the comparative analysis between the FDOT-adopted design EALF and EALF from WIM, this report also performed a sensitivity analysis to quantify the impact of EALF variations in the design thickness of the surface course. In addition, this report also outlines the necessary steps required to evaluate the impact of SHL movement on pavement life. Based on the analysis results, the following conclusions and recommendations are provided:

- Both the WIM and FOX data indicated that both the truck volume and the weight of the trucks are generally increasing in the State of Florida. More specifically, based on the sites that had data for the 5-year period between 2015 and 2019, it was found that Florida's limited access highways experienced an average of 18 percent increase in total truck volume (from 37M to 44M), a relatively negligible 3 percent reduction in average GVW (from 42 kip to 41 kip), and a significant 108 percent increase in OW truck volume (from 1.1M to 2.3M). Although the actual amount of traffic on non-limited highways is far less than the limited highways, the trends observed from non-limited highways were more severe. Based on the sites with 5-year data, the non-limited access roadways showed an average of 66 percent increase in total truck volume (from 5.1M to 8.4M), 29 percent increase in average GVW (from 35 kip to 45 kip), and 301 percent increase in OW truck volume (from 196K to 786K).
- For some WIM stations, high EALFs were observed for both the legal weight and overweight vehicles. These higher EALFs were almost always observed in the year 2021. The higher EALFs may have resulted from the trucks carrying more weight in 2021, possibly due to the ease of COVID-era restrictions and shortage of labor.
- FDOT-adopted design EALFs are adequate for limited rural and limited urban functional classes of pavements, except for limited urban rigid pavements. All limited functional classes of pavements produced overdesign, or at least on-par design, even after increasing the overweight frequency by 2.
- FDOT-adopted design EALFs consistently produced underdesign of surface layer thickness compared to the EALF calculated from the WIM data for non-limited functional pavements. This underdesign is more prominent in the non-limited urban pavements, especially with the increase in overweight vehicles. Increasing the overweight truck traffic by a factor of two resulted in a 470% increment in the EALF compared to the FDOT-adopted design value.
- According to practical engineering considerations, lane factors were found to have a minimal or insignificant impact on the thickness of the surface layer in both flexible and rigid pavements.
- It is recommended that FDOT consider updating the EALF values used for the design of non-limited pavements. In addition, FDOT may conduct a field study to identify the deterioration rate of the non-limited pavements. If the non-limited pavements are found to deteriorate at a faster rate than anticipated, then FDOT may need to adopt the EALFs calculated from the WIM data for pavement design. FDOT's current practice of pavement design, i.e., the AASHTO 1993 method for flexible pavement and mechanistic-empirical

(ME) method for rigid pavement, does not need to be changed; rather, an updated set of EALFs could be used for non-limited pavements that may address the issue of underdesign. For instance, the ESAL or $W18$ obtained from Eq. (13) using the updated EALF could be used with Eq. (12) to determine the SN, and subsequently the thicknesses, of the layers according to the AASHTO 1993 flexible pavement design method used by FDOT.

- Along with the nucleus analysis, detailed examples of the distress analysis, such as fatigue cracking and rutting in the AC layer, ultimate bearing capacity, and localized shear failure in the subgrade, were provided to determine the impact of SHL movement. The methodology presented does not require any backcalculation or iteration. Although layer elastic analysis was used in this study, the presented methodology can be combined with other analysis methods as well, such as viscoelastic analysis.

REFERENCES

AASHTO. (2010). *Mechanistic-Empirical Pavement Design Guide, Interim Edition: A Manual of Practice.* Washington, D.C.: American Association of State Highway and Transportation Officials (AASHTO).

Ali, H., Nowak, A.S., Stallings, J. M., Chmielewski, J., Stawska, S., Babu, A. R., and Haddadi, F. (2020) *Impact of Heavy Trucks and Permitted Overweight Loads on Highways and Bridges Now and in the Future versus Permit Fees, Truck Registration Fees, and Fuel Taxes.* Tallahassee, FL: Florida Department of Transportation.

Al-Qadi, I. L., and Wang, H. (2009). *Pavement Damage Due to Different Tire and Loading Configurations on Secondary Roads* (No. 008IY01). West Lafayette, IN: NEXTRANS.

Ardaman & Associates, Inc. (2019). *Subsurface Soil Exploration and Geotechnical Engineering Evaluation Proposed Naples Beach Restoration and Water Quality Improvement Project.* Naples, FL: Collier County.

Banerjee, A., Prozzi, J. A., and Buddhavarapu, P. (2013). Framework for Determining Load Equivalencies with DARWin-ME. *Transportation Research Record: Journal of the Transportation Research Board*, *2368*(1), 24-35.

Banerjee, A., Prozzi, J. P., and Prozzi, J. A. (2012). Evaluating the Effect of Natural Gas Developments on Highways: Texas Case Study. *Transportation Research Record: Journal of the Transportation Research Board*, *2282*(1), 49-56.

Big Truck Guide. (2016). Explaining the Difference between Divisible and Indivisible Loads, https://www.bigtruckguide.com/explaining-the-difference-between-divisible-and-indivisible-loads/, last accessed June 28, 2021.

CPCS, Perkins Motor Transport, Inc., and Portscape, Inc. (2016). *NCHRP Report 830: Multi-State, Multimodal, Oversize/Overweight Transportation* (NCHRP Project No. 08-97). Washington, D.C.: National Cooperative Highway Research Program, Transportation Research Board, National Research Council.

Darter, M., Mallela, J., Titus-Glover, L., Rao, C., Larson, G., Gotlif, A., Von Quintus, H., Khazanovich, L., Witczak, M., El-Basyouny, M., El-Badawy, S., Zborowski, A., and Zapata, C. (2006). *Changes to the Mechanistic-Empirical Pavement Design Guide Software Through Version 0.900* (NCHRP Research Results Digest 308). Washington, D.C.: Transportation Research Board.

Das, B. M., and Sivakugan, N. (2018). *Principles of Foundation Engineering.* Cengage learning.

Dey, K., Putman, B.J., Chowdhury, M., and Bhavsar, P. (2015). *Quantification of Accelerated Pavement Serviceability Reduction Due to Overweight Truck Traffic.* 94th Annual Meeting of Transportation Research Board, Washington, D.C.

Drucker, D. C., and Prager, W. (1952). Soil mechanics and plastic analysis or limit design. *Quarterly of applied mathematics, 10*(2), 157-165.

Dunning, A., Dey, K. C., and Chowdhury, M. (2016). *Review of State DOTs Policies for Overweight Truck Fees and Relevant Stakeholders' Perspectives*, Journal of Infrastructure Systems, *22*(3), 05016002.

FDOT Pavement Design Section. (2024). *Flexible Pavement Design Manual*. Tallahassee, FL: Florida Department of Transportation.

FDOT. (2018) *Truck Empty Backhaul*, https://fdotwww.blob.core.windows.net/sitefinity/docs/default-source/statistics/docs/truck-empty-back-haul-final-report-2018.pdf?sfvrsn=8efaa9c_0, last accessed June 28, 2021.

FDOT Pavement Design Section. (2022). *Rigid Pavement Design Manual*. Tallahassee, FL: Florida Department of Transportation.

FHWA. (2021). *Oversize/Overweight Load Permits*, https://ops.fhwa.dot.gov/freight/sw/permit_report/index.htm, last accessed June 28, 2021.

FHWA. (2019). *Compilation of Existing State Truck Size and Weight Limit Laws*, https://ops.fhwa.dot.gov/freight/policy/rpt_congress/truck_sw_laws/app_a.htm, last accessed July 29, 2024.

Florida Senate. (2020). *The 2020 Florida Statutes.*

Hajj, E.Y., Batioja-Alvarez, D.D., and Siddharthan, R.V. (2017). *Mechanistic-Based Pavement Damage and Associated Cost from Overweight Vehicles in Nevada* (Report No. 609-13-803). Carson City, NV: Nevada Department of Transportation.

Hajj, E.Y., Siddharthan, R.V., Nabizadeh, H., Elfass, S., Nimeri, M., Kazemi, S. Batioja-Alvarez, D.D., and Piratheepan, M. (2018). *Analysis Procedures for Evaluating Superheavy Load Movement on Flexible Pavements, Volume I: Final Report* (Report No. FHWA-HRT-18-049). Washington, D.C.: Federal Highway Administration.

Huang, Y. H. (2004). *Pavement analysis and design* (*2nd Edition*). New Jersey: Pearson Prentice Hall Upper Saddle River.

Khanal, S., Olidis, C., and Hein, D.K. (2016). *Modelling Pavement Response to Superheavy Load Movement*. 2016 Conference of the Transportation Association of Canada, Toronto, ON.

Nabizadeh, H., Hajj, E., Siddharthan, R., Nimeri, M., Elfass, S., & Piratheepan, M. (2019). *Analysis Procedures for Evaluating Superheavy Load Movement on Flexible Pavements, Volume V: Appendix D, Estimation of Subgrade Shear Strength Parameters Using Falling Weight Deflectometer* (Report No. FHWA-HRT-18-053). Washington, D.C.: Federal Highway Administration.

Papagiannakis, A.T. (2015). *NCHRP Synthesis 476: Practices for Permitting Superheavy Load Movements on Highway Pavements*. Washington, D.C.: National Cooperative Highway Research Program, Transportation Research Board, National Research Council.

Robbins, M. M., Rodezno, C., Tran, N., and Timm, D. (2017). *Pavement ME design–A summary of local calibration efforts for flexible pavements* (NCAT Report 17-07). Auburn, AL: National Center for Asphalt Technology.

Tran, N., Robbins, M. M., Timm, D. H., Willis, R., & Rodezno, C. (2015). *Refined limiting strain criteria and approximate ranges of maximum thicknesses for designing long-life asphalt pavements* (NCAT Report 15-05R). Auburn, AL: National Center for Asphalt Technology.

Sadeghi, J. M. and Fathali, M. (2007). *Deterioration Analysis of Flexible Pavements under Overweight Vehicles*. Journal of Transportation Engineering, *133*(11), 625-633.

Sebaaly, P., Siddharthan, R., and Huft, D. (2003). *Impact of Heavy Vehicles on Low-Volume Roads*. Transportation Research Record: Journal of the Transportation Research Board, *1819*(1), 228-235.

Titi, H. H., Coley, N., Latifi, V., and Matar, M. (2014). *Characterization of Overweight Permitted Truck Routes and Loads in Wisconsin*. Transportation Research Record: Journal of the Transportation Research Board, *2411*(1), 72-81.

Tia, M., Verdugo, D., and Kwon, O. (2012). *Evaluation of long-life concrete pavement practices for Use in Florida* (No. 00093785). Tampa, FL: University of South Florida.

Tjan, A., and Fung, C. (2005). *Determination of Equivalent Axle Load Factor of Trailer with Multiple Axles on Flexible Pavement Structures*. Journal of the Eastern Asia Society for Transportation Studies, *6*, 1194-1206.

Vesic, A. S. (1973). Analysis of ultimate loads of shallow foundations. *Journal of the Soil Mechanics and Foundations Division, 99*(1), 45-73.

Wu, D., Zhao, J., Liu, H., and Yuan, C. (2019). The Assessment of Damage to Texas Highways due to Oversize and Overweight Loads Considering Climatic Factors. *International Journal of Pavement Engineering*, *20*(7), 853-865.

APPENDIX A: FHWA VEHICLE CLASSES

Class 1 Motorcycles		**Class 7** Four or more axle, single unit	
Class 2 Passenger cars			
		Class 8 Four or less axle, single trailer	
Class 3 Four tire, single unit			
		Class 9 5-Axle tractor semitrailer	
Class 4 Buses		**Class 10** Six or more axle, single trailer	
		Class 11 Five or less axle, multi trailer	
Class 5 Two axle, six tire, single unit		**Class 12** Six axle, multi-trailer	
		Class 13 Seven or more axle, multi-trailer	
Class 6 Three axle, single unit			

APPENDIX B: SUMMARY TABLES FOR WIM AND FOX DATA

District	ID	SITE	County	County Section	Milepost	Roadway	Avg. Traffic		Trends			
							Avg. Truck Traffic per Year (× 1,000)	OW Truck Traffic per Year (× 1,000)	Total Traffic	Truck Count	Avg. Truck Weight	OW Truck Count
1	W50	9950	Collier	3175000	61.558	I-75	2224	40	17%	17%	-12%	-22%
	W51	9951	Polk	16320000	17.789	I-4 / SR-400	3063	184	10%	12%	12%	771%
	F1	I-75 NB Exit 158	Charlotte	1075000	9.754	I-75	157	46	150%	150%	182%	28291%
2	W02	9902	Madison	35090000	24.61	I-10	2102	64	5%	5%	0%	13%
	W04	9904	Alachua	26260000	4.927	I-75 / SR-93	3093	52	138%	144%	-7%	-17%
	W05	9905	Duval	72280000	2.77	I-95	2473	88	15%	15%	-11%	69%
	W14	9914	Duval	72001000	23.567	I-295 / SR-9A	3499	91	19%	18%	-6%	-30%
	W23	9923	Nassau	74160000	5.571	I-95 / SR-9	3642	370	78%	77%	4%	631%
	W36	9936	Columbia	29170000	17.17	I-10 / SR-8	1559	100	29%	28%	-3%	158%
	W56	9956	Hamilton	32100000	19.696	I-75	3678	228	73%	69%	3%	115%
	F2	I-75 SB MM 451 White Springs	Hamilton	32100000	9	I-75	92	42	-75%	-67%	-46%	-88%
	F3	I-95 SB MM 377 Yulee	Nassau	74160000	8	I-95	152	8	155%	150%	-41%	-5%
3	W49	9949	Escambia	48260000	8.7	I-10 / SR-8	1834	87	28%	27%	-6%	123%
	W58	9958	Walton	60002000	19.186	I-10 / SR-8	1204	126	154%	163%	6%	251%
	F4	I-10 EB Exit 152 Grand Ridge	Jackson	53002000	25.2	I-10	10	3	304%	283%	-4%	465%
	F5	I-10 EB Pensacola MM2	Escambia	48260000	1.77	I-10	69	24	109%	109%	18%	292%
	F6	I-10 WB Exit 158	Jackson	53002000	31.22	I-10	14	0	-85%	-85%	253%	-5%
4	W13	9913	St. Lucie	94470000	2.933	SR-91 (TP)	1563	145	30%	30%	6%	313%
	W33	9933	Broward	86472000	4.258	SR-869 (TP)	1702	80	69%	41%	20%	384%
	W52	9952	Palm Beach	93220000	42.741	I-95	2087	39	-24%	-2%	-8%	43%
	F7	I-95 NB Indiantown Rd	Palm Beach	93220000	44.1	I-95	39	11	89%	69%	-22%	63%
	F8	I-95 SB Becker Rd	St. Lucie	94001000	0.095	I-95	9	0	268%	107%	-1%	79%
	F9	I-95 SB MM 113	Martin	89095000	22.1	I-95	33	0	286%	181%	1%	194%

District	ID	SITE	County	County Section	Milepost	Roadway	Avg. Traffic		Trends			
							Avg. Truck Traffic per Year (× 1,000)	OW Truck Traffic per Year (× 1,000)	Total Traffic	Truck Count	Avg. Truck Weight	OW Truck Count
5	W06	9906	Volusia	79110000	4.678	I-4 / SR-400	1617	31	60%	60%	-6%	138%
	W19	9919	Brevard	70220000	39.08	I-95	2859	93	-36%	-36%	14%	-38%
	W20	9920	Sumter	18130000	17.589	I-75	1366	65	-63%	-63%	-12%	-83%
	W31	9931	Sumter	18470000	3.379	SR-91 (TP)	2329	111	18%	20%	-4%	-63%
	W60	9960	Orange	75002000	29.641	SR-482	732	49	115%	174%	3%	198%
	W61	9961	Osceola	92471000	33.446	SR-91 (TP)	362	10	-71%	-71%	-1%	-72%
	F10	I-95 SB Palm Coast	Flagler	73001000	8	I-95	60	2	139%	50%	9%	-19%
6	W34	9934	Miami-Dade	87471000	36.09	SR-821 (TP)	2135	46	-84%	-85%	3%	-87%
7	W53	9953	Hillsborough	10075000	19.073	I-75	1845	120	192%	182%	-3%	117%
	W55	9955	Hillsborough	10320000	13.076	I-275	986	51	-4%	-5%	-11%	-32%
	W62	9962	Hills-borough	10190000	23.689	I-4	2839	8	291%	306%	1%	376%

District	ID	SITE	County	County Section	Milepost	Road-way	Avg. Traffic		Trends			
							Avg. Truck Traffic per Year (× 1,000)	OW Truck Traffic per Year (× 1,000)	Total Traffic	Truck Count	Avg. Truck Weight	OW Truck Count
1	W18	9918	Hendry	7030000	10.618	US-27 / SR-80	680	46	3%	1%	-2%	43%
	W27	9927	Polk	16100000	0.816	SR-546	303	3	10%	10%	-13%	-60%
	W48	9948	Polk	16170000	17.539	US-27 / SR-25	860	46	10%	10%	-100%	-24%
	F11	US-27 SB Hendry	Hendry	7030000	10.195	US-27	399	175	88%	97%	-3%	83%
2	W09	9909	Levy	34010000	3.184	US-19 / SR-500	233	12	86%	66%	-38%	32%
	W63	9963	Bradford	28010000	0.06	US-301	1040	43	98%	98%	4%	254%
	F12	US-90 EB Madison	Madison	35010000	20.965	US-90	27	16	2%	-1%	1%	-4%
3	W07	9907	Bay	46040000	22.531	US-231 / SR-75	331	14	49%	46%	-11%	96%
	W16	9916	Escambia	48040000	9.399	US-29 / SR-95	301	11	-12%	-12%	22%	730%
	W40	9940	Gadsden	50080000	13.079	SR-267	73	5	65%	60%	-14%	82%
	W43	9943	Jackson	53020000	12.386	US-90 / SR-10	115	11	34%	34%	2%	151%
	W57	9957	Jackson	53060000	5.205	SR-77	59	6	7%	7%	6%	27%
	W59	9959	Walton	60060000	21.435	US-331	78	3	95%	96%	-3%	51%
	F13	SR-77 SB Panama City	Bay	46060000	11	SR-77	76	32	126%	107%	12%	269%
	F14	US-231 SB Welcome Center	Jackson	53050000	17.7	US-231	42	22	104%	106%	0%	114%
	F15	US-27 SB Gadsden	Gadsden	50040000	3.442	US-27	19	14	335%	242%	11%	351%
	F16	Gadsden CR-12B (Deactivated)	Gadsden	NA	NA	CR-12B	2	0	81%	-67%	99%	-36%
5	W25	9925	Volusia	79060000	6.903	SR-600	211	3	41%	41%	1%	73%
	W29	9929	Volusia	79010000	11.126	SR-546	60	0	59%	57%	3%	177%
	F17	CR-475 EB Wildwood	Sumter	NA	NA	CR-475	6	2	49%	87%	1%	69%
	F18	CR-484 SB Wildwood	Marion	NA	NA	CR-484	40	4	51%	51%	-80%	-81%
	F19	SR-40 EB Marion	Marion	36080000	31.7	SR-40	31	23	93%	93%	-1%	80%
	F20	US-1 NB Palm Coast	Flagler	73010000	18.2	US-1	63	10	130%	317%	-29%	149%
	F21	US-1 SB Palm Coast	Flagler	73010000	18.2	US-1	106	21	291%	340%	4%	208%
6	W47	9947	Miami-Dade	87090000	8.1	US-27 / SR-25	1512	42	10%	6%	2%	67%
7	F22	US-92 EB Seffner	Hills-borough	10030000	11.253	US-92	32	2	18%	18%	-5%	-6%